The hydrology of northern boreal lakes in the Taiga Shield and Plains, Northwest Territories and the importance of catchment characteristics in mediating responses to climate

Josef A. Viscek, BSc, MBA

Earth Science

Submitted in partial fulfillment of the requirements for the degree of

Master of Science

Faculty of Mathematics & Science, Brock University
St. Catharines, Ontario

ABSTRACT

Freshwater lakes are prominent features across northern boreal regions and are sensitive to changing climate conditions. This study, spanning the 2017-18 ice-free seasons, broadens our understanding of how variable climate and landscape conditions influence subarctic lake hydrology in the North Slave Region near Yellowknife, Northwest Territories (NT), Canada. We studied 20 lakes located within the Taiga Shield and Taiga Plains ecozones through an integrated approach, utilizing water isotope tracers (δ^2H and $\delta^{18}O$), lake level changes, local meteorological conditions and remotely sensed catchment data. Lake water isotope data were obtained twice during the ice-free season (May and August) and evaporation/inflow (E/I) ratios were calculated to identify the relative importance of catchment hydrological controls. Hydrological data were compared to measured and modelled catchment characteristics, including relative lake/catchment size, slope, land cover and recent wildfire burn area. Overall, precipitation was a major driver of seasonal and interannual lake hydrological change, while evaporation was a major driver of summer water loss. Relative catchment size (lake area to catchment area (LA/CA)) was found to be an important driver of lake hydrology, however, this relationship is complicated by storage deficits associated with variable meteorological conditions. During wet conditions (e.g., freshet and periods of high rainfall), lakes with larger catchments (low LA/CA) had more positive water balances than lakes with high LA/CA. Under drier conditions, lake catchment size and associated fill-and-spill hydrological connectivity was reduced. Lake basins with high LA/CA (particularly those with shallower depth and greater surface area) were more prone to evaporative water loss. Lake hydrological conditions were less influenced by catchment land cover compositions, including burn area. Findings presented here highlight important drivers of lake water balances in subarctic boreal regions, which are sensitive to ongoing changes in climate. This study is part

of a broader research project funded and supported by NWT *Cumulative Impact Monitoring Program (CIMP)*, which is using a multi-proxy, paleo-ecological approach to determine long-term (i.e., 2,000 years) records of hydrology, drought, fire and water quality to inform future policy planning.

ACKNOWLEDGMENTS

I would like to thank my thesis Supervisor, Dr. Kevin Turner (Brock University), for taking me on as a graduate student and giving me the opportunity to contribute to the Yellowknife research project. A thank you is also extended to fellow thesis committee members, Dr. Michael Pisaric (Brock University) as well as Ms. Shawne Kokelj (Hydrologist, Government of Northwest Territories), whose local NT expertise was integral to the project's success. Also, to Dr. Francine McCarthy (Graduate Program Director) and the Brock University Department of Earth Sciences. Thank you, also, to Dr. Daniel Peters (University of Victoria) for serving as the thesis external examiner, and to Dr. Cheryl McCormick for serving as the thesis defence Chair.

Thank you to the Government of Northwest Territories, *Cumulative Impact Monitoring Program (CIMP)* for project funding and support. This research was completed under a Northwest Territories Scientific Research Licence (Licence No. 15989), as issued to Dr. Michael Pisaric by the Aurora Research Institute–Aurora College. Additional financial support for the project was provided by the Northern Scientific Training Program (NSTP), Natural Science and Engineering Research Council of Canada (NSERC) and the Natural Resources Canada Polar Continental Shelf Program's (PCSP).

A warm thanks is extended to my friends and colleagues from Brock University and the Water and Environment Lab (WEL), including Rebecca Gunter, Danny Hughes, Paul Michael Pilkington, Scott Cocker, Emily Ham, Jessica Zugic and Martina Tepavcevic; and especially Caitlin Garner, Dana Harris and Brent Thorne for your assistance and project support.

Also, thank you to the additional supporters and contributors who helped make this research project possible: Dr. Katrina Moser (CIMP research project coordinator, University of Western Ontario) and lab team; Dr. Jean-Philippe Martin (project support, Brock University);

Dr. Kyung-Hee Kim and Dr. Vincenzo De Luca's biological sciences laboratory (laboratory support, Brock University); Dimitre Iankoulov (project support, Brock University); Dr. Steve Kokelj and Dr. Kumari Karunaratne (local project support, NWT Geological Survey); Michael Gilday (Canadian Olympian, project field assistant); Mike Palmer ("MP2", local project support); Mike Palmer ("MP3", project field assistant); Colin Avey and the NWT Centre for Geomatics (GIS data support); Dr. Mingsheng Ma (University of Alberta – Biogeochemical Analytical Service Laboratory (BASL)) for water isotope analyses; and Taiga Environmental Laboratory (Yellowknife) for water chemistry analyses. Further, a special thank you is extended to James Telford, Dr. Brent Wolfe and the Wilfrid Laurier University lab group for their assistance and laboratory support, as well as the University of Waterloo-Environmental Isotope Laboratory (UW-EIL). Also, to Aurora Jenny's Bed & Breakfast and Great Slave Helicopters (Yellowknife) for your service and gracious hospitality.

Last but not least, thank you to my family for your love and support.

TABLE OF CONTENTS

LIST OF FIGURES

LIST OF TABLES

LIST OF ACRONYMS

‰	Per Mille (Parts Per Thousand)
δ^2H	Hydrogen 2/1 isotopic concentration
δ^{18}O	Oxygen 18/16 isotopic concentration
CIMP	Cumulative Impact Monitoring Program
DEM	Digital Elevation Model
ECCC	Environment and Climate Change Canada
GMWL	Global Meteoric Water Line
GNWT	Government of Northwest Territories
IMB	Isotope Mass Balance
LA/CA	Lake Surface Area to Catchment Area Ratio
LA/LD	Lake Surface Area to Lake Centre Depth Ratio
LMWL	Local Meteoric Water Line
masl	Metres Above Sea Level
Met Station	Meteorological Station
NT	Northwest Territories
OLI	Operational Land Imager
PCA	Principal Component Analysis
USGS	United States Geological Survey
VSMOW	Vienna Standard Mean Ocean Water

CHAPTER ONE

INTRODUCTION

1.1 Introduction

Northern boreal (Taiga) lakes are prominent features throughout Arctic and subarctic regions which provide important habitat for abundant plant and wildlife species, and are integral for maintaining the culture and lifestyle of local communities. In the Taiga Shield and Plains ecozones within the northern Great Slave Lake region (North Slave Region) of the Northwest Territories (NT), these interconnected lakes, wetlands and watercourses serve as significant stores of water within the landscape and are important components of regional hydrological cycles. At this time, it has been well documented that Arctic and subarctic landscapes are sensitive to changes in climate and are undergoing considerable ecosystem change (Pientz et al., 2004; Smol et al., 2005; Schindler and Smol, 2006; Prowse et al., 2009; Carroll et al., 2011; Larsen et al., 2014). As highlighted in *Canada's Changing Climate Report* (Bush and Lemmen, 2019), NT is warming about three times the global rate. These conditions have resulted in increasing permafrost thaw, greater erosion of coastlines and rivers, changing ice conditions and longer ice-free seasons, changes to water quality and quantity, as well as alteration to wildlife habitat and migration (Bush and Lemmen, 2019). Hydrological changes to lakes across northern regions can be expected to be complex and highly variable according to interannual climate and geomorphological conditions (Turner, 2014; Gibson, 2019; Spence, 2019).

Climate models also indicate that with increasing atmospheric temperatures, greater thunderstorm frequency and intensity in northern regions is likely to increase the potential for lightning-ignited wildfires (Price and Rind, 1994; Kochtubajda et al., 2006; Veraverbeke et al., 2017). Severe drought-like conditions (subsequent years of below-average precipitation) near

Yellowknife, NT during 2013-2015 negatively impacted hydropower production and led to the most intense wildfire season in twenty years during 2014 (Darwent, 2016; GNWT, 2016). The current body of research suggests that the hydrological responses of northern aquatic ecosystems to catchment fire may be highly variable (Robinne et al., 2020; Figure 1.1).

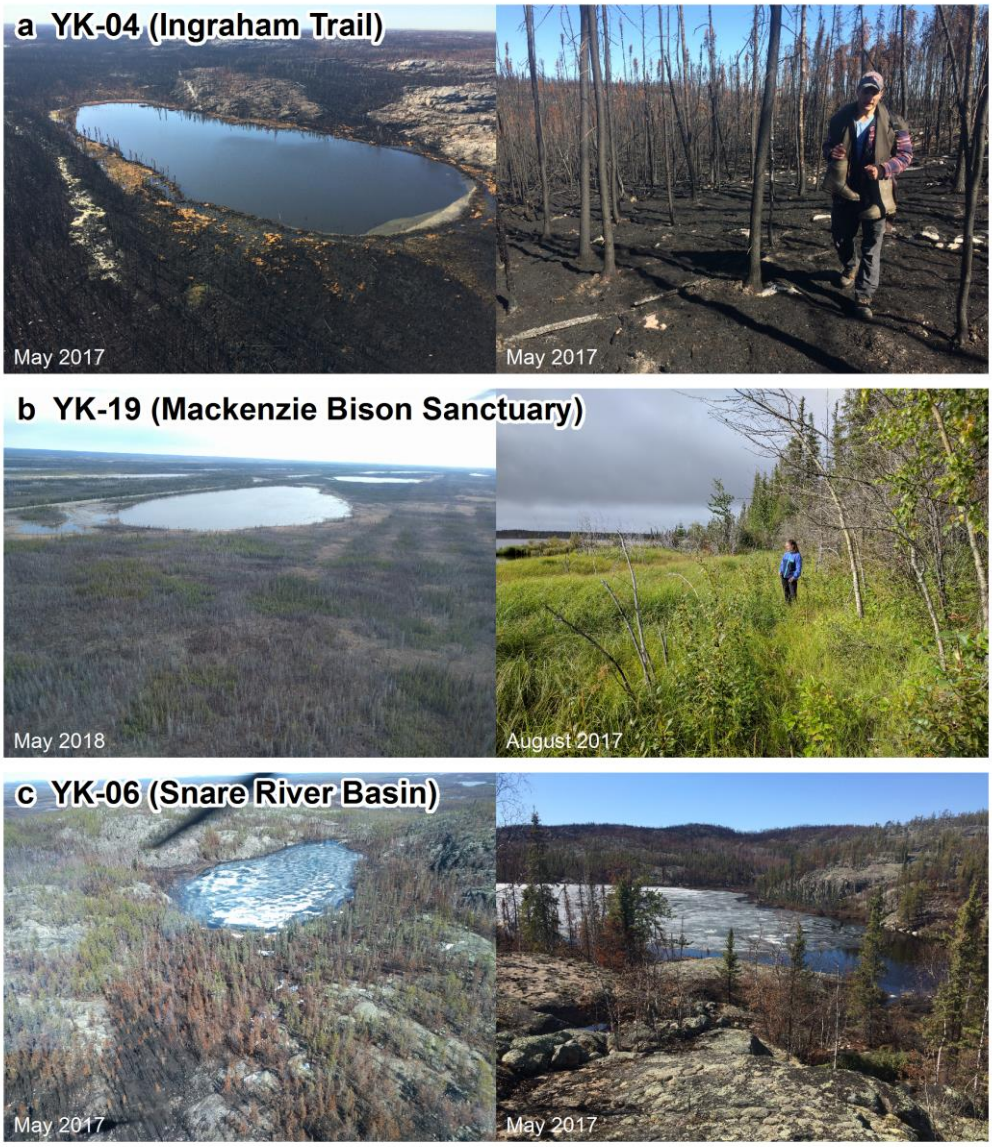

Figure 1.1 – Aerial and ground photographs showing various examples of study lake catchments burned by wildfire within the North Slave Region, NT, including (a) study lake YK-04 (near Ingraham Trail), 100% burn during 2016; (b) study lake YK-19 (within Mackenzie Bison Sanctuary), 100% burn during 2014; and (c) study lake YK-06 (within Snare River Basin), 100% burn during 2016. As the vegetation in the photographs suggests, burn severity and regeneration may vary (photographs by J.Viscek).

In shallow-soiled Shield lake environments where permafrost development is limited, hydrological connectivity plays an increasingly important role in watershed dynamics. As has been previously shown in studies at the Pocket Lake and Baker Creek catchments near Yellowknife, NT since 1991, seasonal and interannual hydrological variation are common in northern boreal regions (Gibson, 2019). Identifying multi-year periods of drier and low flow conditions is very important for interpreting the hydrological processes of regional watersheds (Gibson, 2019), as catchment connectivity is largely influenced by seasonal meteorological conditions. Hydrological connectivity will vary depending on seasonal timing of precipitation, the intensity of rainfall events, catchment physigography and storage deficits (Bracken and Croke, 2007; Spence et al., 2019). In these chain-of-lakes Shield systems, lakes may predominantly function as individuals rather than as part of a greater catchment or perennial watercourse (Spence et al., 2019). Particularly under drier conditions, as catchment water bodies become increasingly disconnected during the ice-free season the influence from evaporation will be greater (Gibson and Reid, 2014). Studies suggest that high evaporation rates and storage deficit dynamics may reduce downstream flow under typical summer conditions (Spence et al., 2019). The studies at Pocket Lake and Baker Creek represent the longest regional record of their kind in NT that have utilized isotopic as well as conventional hydrological study methods. However, these studies may be expanded across a broader scale to develop a more thorough understanding of regional hydrological patterns.

Techniques utilizing water isotope tracers are highly useful for evaluating water balance interactions across vast hydrological systems (Burgman et al., 1987; Rozanski et al., 1993; Edwards et al., 2004; Turner et al., 2010 and 2014; Gibson and Reid, 2014, MacDonald et al., 2017). These studies utilize comparison of hydrogen (δ^2H; deuterium) and oxygen ($\delta^{18}O$) isotope

compositions to characterize lake and river hydrological conditions. Water isotopes are quite useful in areas with strong seasonal temperature gradients, such as northern regions. Analyses are based on the relative concentration of lighter versus heavier water molecules under varying seasonal meteorlogical conditions. Global atmospheric moisture patterns are primarily driven by the evaporation of warm, well-mixed ocean water (of known isotopic composition) near the equator (Edwards et al., 2004). During poleward migration of major air masses, progressive rain-out of mass and heavy isotopes occurs according to an understood linear relationship known as the Global Meteoric Water Line (GMWL). Essentially, lake water isotope data provide an indication of the relative hydrological influence of snowmelt (lower isotopic composition), rainfall (higher isotopic composition) and evaporation (leading to more enriched isotopic composition conditions) in aquatic systems. These isotope data compliment traditional hydrometric research methods which rely on field measurements and installed gauges, but may be more easily employed across wider regions. In cold regions like NT, lake isotope compositions are seasonally influenced by surges of inflow during spring snowmelt, followed by relatively short, arid summers with high evaporation rates (Gibson and Reid, 2014). Historical (1943-2018) precipitation data from Yellowknife suggest mean levels of approximately 142 mm of rainfall (May-September), as well as 122 mm of winter snowfall (October-April; ECCC, 2018). The lake isotope compositions provide quantitative information about relative input water contributions (e.g., snowmelt, rain and permafrost thaw) as well as the relative influence of evaporation, typically expressed as an evaporation-to-inflow ratio (*E/I*; MacDonald et al., 2017). Advancing studies of northern hydrological processes must increasingly look to couple water isotope tracer data with other novel and less expensive/field-intensive approaches. Combining quantitative water isotope analyses with remote sensing catchment modelling has been

demonstrated to be highly informative for hydrological characterization of northern lakes (Turner et al., 2014).

Landscape characteristics, such as catchment size, morphology and land cover play an important role in lake water balance. Catchments that are more densely forested are likely to provide a windbreak for deposited snow, promoting snowpack and resulting in enhanced spring runoff to lakes (Essery and Pomeroy, 2004; Bouchard et al., 2013; Turner et al., 2014). Within the Shield landscape of the North Slave Region, lakes are marked by differing limnological characteristics, such as area, depth and organic content (Van Den Berghe et al., 2018). Lakes with greater catchment size relative to lake area have been shown to convey water downstream more effectively (Spence et al., 2019). Catchments with more numerous and larger upstream lakes are more likely to transmit and maintain downstream flow (Spence et al., 2019). When water levels are high, flow from larger storage basins within a catchment can enhance and sustain streamflow to lower basins for a greater duration. Conversely, during drought, upstream catchment flow is supressed as water body levels increasingly fail to rise above outlet elevation thresholds (Spence et al., 2019).

Ongoing and future hydrological studies within subarctic boreal regions should continue to investigate the relationships among climate, catchment characteristics and lake water balances. The integration of conventional hydrological analyses with modern remote sensing techniques will be increasingly important for the long-term monitoring of these complex relations across vast northern landscapes. Such studies will be integral in anticipating future hydrological responses under variable climate scenarios.

1.2 Objectives

This study builds on previous northern boreal hydrological studies through the investigation of 20 study lake catchments within the North Slave Region of NT. The study presents a two-year water isotope dataset for 2017-18, including bi-annual (i.e., May and August) sampling during the ice-free season to capture seasonal and interannual lake water balance responses. Lake isotope records were evaluated in conjunction with in-situ water level data, catchment physical characteristics and local meteorological data. The timing of the study presented an opportunity to evaluate lake catchments and hydrological responses during average (2017) and above-average (2018) ice-free season rainfall conditions. This period represented a time of general hydrological recovery in the region following relatively drier conditions between 2013-16.

The specific objectives of this study were to 1) identify the seasonal and interannual lake hydrological conditions of 20 study lakes across the Taiga Shield and Plains ecozones of the North Slave Region; 2) identify the relative importance of catchment characteristics (e.g., physiography, land cover and burn area) in determining lake hydrological responses; and 3) determine the effectiveness of our integrated approach for elucidating the complex relations among climate, catchment and lakes. We hypothesize that lake hydrology will be variable among sites and depend strongly on precipitation, catchment connectivity and land cover properties.

The findings of this research program enhance our knowledge of how warming northern climate and associated landscape changes and disturbance are influencing lake hydrology in subarctic boreal regions. The work is part of a broader research project funded and supported by NWT *Cumulative Impact Monitoring Program (CIMP)*, which is using a multi-proxy, paleo-

ecological approach to determine long-term (i.e., 2,000 years) records of drought, fire and water quality to inform future policy planning.

1.3 Thesis Format

This thesis paper follows the monograph format. Following this introductory chapter (Chapter One), Chapter Two provides an extensive literature review containing important background information relevant to the project. Chapter Three includes the main research paper which presents the key findings of this hydrological study. Chapter Four includes supplementary hydrological analyses of representative case study lakes. Chapter Five presents the conclusions of the study and future recommendations. Equations and calculations are provided in Appendix One; isotope raw data are provided in Appendix Two; and supplementary tables and figures are provided in Appendix Three.

REFERENCES

Bouchard, F., Turner, K.W., MacDonald, L.A., Deakin, C., White, H., Farquharson, N., et al. 2013. Vulnerability of shallow subarctic lakes to evaporate and desiccate when snowmelt runoff is low. *Geophys. Res. Lett*. 40(23), 6112-6117. Doi: 10.1002/2013GL058635.

Bracken, L.J. and Croke, J. 2007. The concept of hydrological connectivity and its contribution to understanding runoff-dominated geomorphic systems. *Hydrological Processes*. 21(13), 1749-63.

Burgman, J.O., Calles, B. and Westman, F. 1987. Conclusions from a ten year study of oxygen-18 in precipitation and runoff in Swedon. Symposium on Isotope Techniques in Water Resources Development. International Atomic Energy Agency, Vienna, 30 March-3 April 1987, IAEA-SM-299/107.

Bush, E. and Lemmen, D.S. 2019. Canada's changing climate report; Government of Canada, Ottawa, ON. 444 p.

Carroll, M.L., Townshend, J.R.G., DiMiceli, C.M., Loboda, T. and Sohlberg, R.A. 2011. Shrinking lakes of the Arctic: spatial relationships and trajectory of change. *Geophysical Research Letters*. 38, L20406, http://dx.doi.org/10.1029/2011GL049427.

Darwent, R., ed. 2016. Fire severest in the 2014 Northwest Territories fires. Nat. Resour. Can., Can. For. Serv., North. For. Cent., Edmonton, AB. *Insights*. No 4b.

Edwards, T.W.D., Wolfe, B.B., Gibson, J.J., Hammarlund, D. 2004. Use of water isotope tracers in high latitude hydrology and paleohydrology. In: Pienitz, R., Douglas, M.S.V., Smol, J.P. (Eds.), Long-Term Environmental Change in Arctic and Antarctic Lakes. Springer, Dordrecht, The Netherlands, pp. 187-207.

Environment and Climate Change Canada (ECCC). 2018. Historical data (hourly, daily, monthly). Yellowknife, Northwest Territories (station: Yellowknife A; climate identifier: 2204101). Retrieved between 2018 and 2019 from http://climate.weather.gc.ca/historical_data/search_historic_data_e.html.

Essery, R., Pomeroy, J. 2004. Vegetation and topographic control of wind-blown snow distributions in distributed and aggregated simulations for an arctic tundra basin. *Journal of Hydrometeorology*, Special Section 5, 735-744.

Gibson, J.J. and Reid, R. 2014. Water balance along a chain of tundra lakes: a 20-year isotopic perspective. *J. Hydrol*. 519, 2148-2164.

Gibson, J.J. 2019. Isotope-based evaporation and water balance studies at Pocket Lake and Baker Creek: 2019 update. Submitted to Shawne Kokelj, Government of Northwest Territories. InnoTech Alberta. December 31, 2019.

Government of Northwest Territories (GNWT). 2016. North Slave hydro system. Yellowknife, NT. 2 pp.

Government of Northwest Territories (GNWT) Centre for Geomatics. 2017. NWT Fire History (digital shapefile), 1965-2016. Obtained from http://www.geomatics.gov.nt.ca/dldsoptions.aspx on February 24, 2017.

Kochtubajda, B., Flannigan, M.D., Gyakum, J.R., Stewart, R.E., Logan, K.A., Nguyen, T.V. 2006. Lighting and fires in the Northwest Territories and responses to future climate change. *Arctic*. 59(2), 211-221.

Larsen, J.N., Anisimov, O.A., Constable, A., Hollowed, A.B., Maynard, N., Prestrud, P., et al. Polar Regions. In: Barros, V.R., Field, C.B., Dokken, D.J., Mastrandrea, M.D., Mach, K.J., Bilir, T.E., et al., editors. Climate change 2014: impacts, adaptation, and vulnerability part b: regional aspects contribution of working group II to the fifth assessment report of the Intergovernmental Panel on Climate Change. Cambridge, United Kingdom and New York, NY, USA. Cambridge University Press. 2014, p. 1567-1612.

MacDonald, L.A., Wolfe, B.B., Turner, K.W., Anderson, L., Arp, C.D., Birks, S.J., Bouchard, F., Edwards, T.W.D., Farquharson, N., Hall, R.I., McDonald, I., Narancic, B., Ouimet, C., Pienitz, R., Tondu, J. and White, H. 2017. A synthesis of thermokarst lake water balance in high-latitude regions of North America from isotope tracers. *Arctic Science*. 3, 118-149.

Pienitz, R., Douglas, M.S.V. and Smol, J.P. 2004. Long-term environmental change in Arctic and Antarctic lakes. Published by Springer. Dordrecht, The Netherlands. 272-275.

Price, C. and Rind, D. 1994. Possible implications of global climate change on global lightning distributions and frequencies. *Journal of Geophysical Research*. 99, 10823-10831.

Prowse, T.D., Furgal, C., Wrona, F.J. and Reist, J.D. 2009. Implications of climate change for northern Canada: freshwater, marine, and terrestrial ecosystems. *Ambrio*. 35, 282-289.

Robinne, F.-N., Hallema, D.W., Bladon, K.D. and Buttle, J.M. 2020. Wildfire impacts on hydrologic ecosystem services in North America high-latitude forests: A scoping review. *Journ. of Hydrol.* 581, 124360.

Rozanski, K., Araguás-Araguás, L. and Gonfiantini, R. 1993. Isotopic patterns in modern global precipitation. In: Swart, P.K., McKenzie, J., Lohmann, K.C. and Savin, S. (eds.), Climate change in continental isotopic records. *Geophysical Monograph*, 78, American Geophysical Union, Washington, 1-36.

Schindler, D.W. and Smol, J.P., 2006. Cumulative effects of climate warming and other human activities on freshwaters of Arctic and subarctic North America. *Ambrio*. 35, 160-168.

Smol, J.P., Wolfe, A.P., Birks, H.J.B., Douglas, M.S.V., Jones, V.J., Korhola, A., Pienitz, R., Ruhland, K., Sorvari, S., Antoniades, D., Brooks, S.J., Fallu, M.A., Hughes, M., Keatley,

B.E., Laing, T.E., Michelutti, N., Nazarova, L., Nyman, M., Paterson, A.M., Perren, B., Quinlan, R., Rautio, M., Saulinier-Talbot, E., Siitonen, S., Solovieva, N. and Weckstrom, J. 2005. Climate-driven regime shifts in the biological communities of Arctic lakes. *Proceedings of the National Academy of Sciences of the United States of America*. 102, 4397-4402.

Spence, C., Ali, G., Oswald, C.J. and Wellen, C. 2019. An application of the T-TEL assessment method to evaluate connectivity in a lake-dominated watershed after drought. *Journal of the American Water Resources Association*. 55(2), 1-16.

Turner, K.W., Wolfe, B.B., Edwards, T.W.D. 2010. Characterizing the role of hydrological processes on lake water balances in Old Crow Flats, Yukon Territory, Canada, using water isotope tracers. *Journal of Hydrology*. 386 (2010), 103-117.

Turner, K.W., Wolfe, B.W., Edwards, T.W.D., Lantz, T.C., Hall, R.I. and Larocque, G. 2014. Controls on water balance of shallow thermokarst lakes and their relations with catchment characteristics: a multi-year, landscape-scale assessment based on water isotope tracers and remote sensing in Old Crow Flats, Yukon (Canada). *Glob. Change Biol*. 20(5), 1585-1603. Doi: 10.1111/gcb.12465.

Van Den Berghe, M.D., Jamieson, H.E. and Palmer, M.J. 2018. Arsenic mobility and characterization in lakes impacted by gold ore roasting, Yellowknife, NWT, Canada. *Environmental Pollution.* 234, 630-641.

Veraverbeke, S., Rogers, B.M., Goulden, M.L. Jandt, R.R., Miller, C.E., Wiggins, E.B. and Randerson, J.T. 2017. Lightning as a major driver of recent large fire years in North American boreal forests. *Nature Climate Change*. 7(7), 529-534.

CHAPTER TWO

LITERATURE REVIEW

This chapter provides important background information necessary to contextualize the present study, including: background information about the North Slave Region of study, NT; an overview of hydrological changes detected across northern regions driven by variable climate; a summary of previous hydrological studies in the North Slave Region of study; and a summary of the conventional isotope mass balance (IMB) approaches used in this study in assessing lake hydrological conditions.

2.1 Background of North Slave Region, NT

2.1.1 Physiography

The landscape within the North Slave Region in central NT is slightly undulating and of relatively low relief compared to the Cordilleran mountainous region to the west (Pienitz et al., 2004). The region is underlain by Precambrian sedimentary bedrock in the south and granatic-gneissic bedrock in the north (Pienitz et al., 2004; Ecosystem Classification Group, 2008). At approximately 315 million hectares (ha) in size, the boreal (Taiga) forest is the largest band of uninterupted forest in Canada (Weber and Stocks, 1998). Spanning from Newfoundland to west of the Yukon Territory and into Alaska, the forest varies in latitudinal width and species composition. Overall, 47% of the immense Mackenzie River basin is situated within the NT. This drainage basin represents the largest source of freshwater for the Arctic Ocean in North America. The basin spans 1.8 million square kilometres (km^2), ranking it tenth largest in the world by drainage area (Kochtubajda et al., 2006). With an area > 28,500 km^2 and a maximum depth of 614 m, Great Slave Lake is a prominent and hydrologically-important feature in the region (Piper, 2018). The North Slave Region (focus of the current study) is characteristic of

both upland and lowland subarctic landscapes, complete with numerous interconnected lakes, wetlands and watercourses which ultimately drain to Great Slave Lake (Figures 2.1 and 2.2).

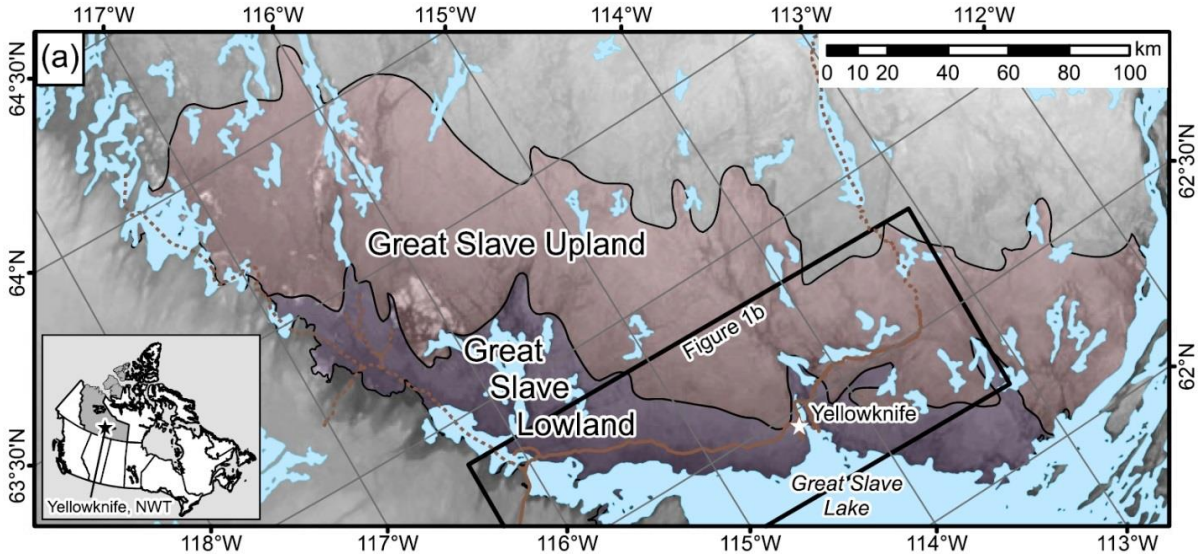

Figure 2.1 – Map illustrating the upland and lowland regions within the North Slave Region, NT (reproduced from Morse et al., 2016).

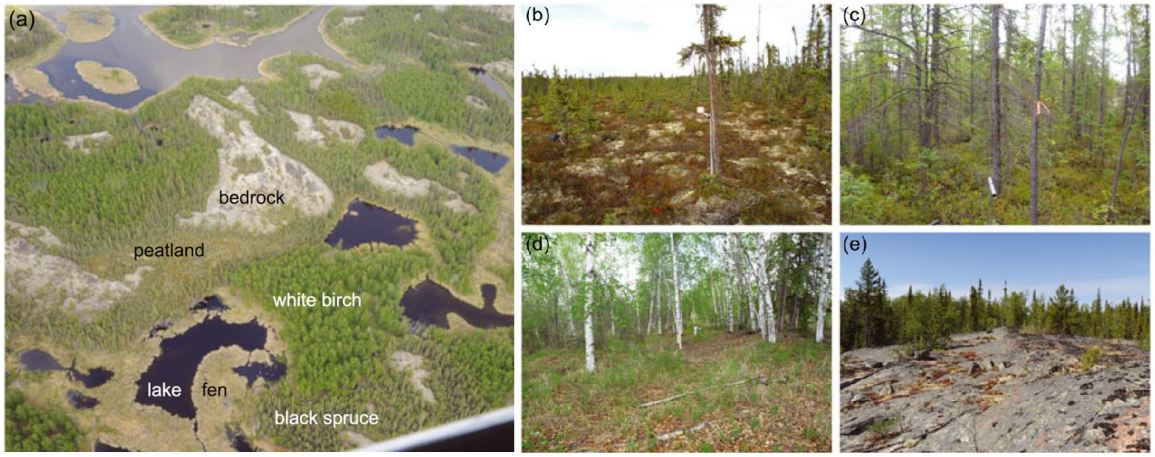

Figure 2.2 – Photographs of various surface conditions typical of the North Slave Region, NT: overview of mosaic of surface conditions, including (a) fens and lakes; (b) peatland; (c) black spruce forests; (d) white birch forests; and (e) bedrock (reproduced from Morse et al., 2016).

2.1.2 Climate

The climate in NT varies locally and regionally, but generally comprises short, warm summers and very cold winters (Weber and Stocks, 1998). The mean summer (July-August) temperature is 15.6 degrees Celsius (°C); and mean winter (October-April) temperature is -15.4

°C (Environment and Climate Change Canada (ECCC), 2018b). Climate in NT is influenced by a number of factors, including latitude, intensity of solar radiation, topography and the character of weather systems (Phillips, 1990). Large water bodies such as Great Slave Lake serve as a moderating influence on the local climate, resulting in longer relative growing seasons in the surrounding regions (Piper, 2018). There exists steep gradients in both climate and environment in these subarctic boreal regions (Pienitz et al., 2004). While solar radiation arrives at relatively low angles, limiting heat energy reaching the surface, this effect is offset by long summer days (Phillips, 1990). These patterns are largely the result of mixing of warm, moist Pacific air masses from the south with cold, dry Arctic air (i.e., Arctic Front) from the north (Bryson, 1966).

Long-term climate records for Yellowknife from the Yellowknife Airport meteorological station (met station) are available from 1943, as maintained by ECCC (2018a). Climate data from 1943-2018 indicate a general increasing trend in mean annual temperature ($R^2 = 0.30$ with $p = 0.11$); while total annual precipitation during this time period has been relatively steady ($R^2 = 0.07$ with $p < 0.05$; Figure 2.3). The historical data indicate broad cycles of both temperature and precipitation fluctuation since 1943.

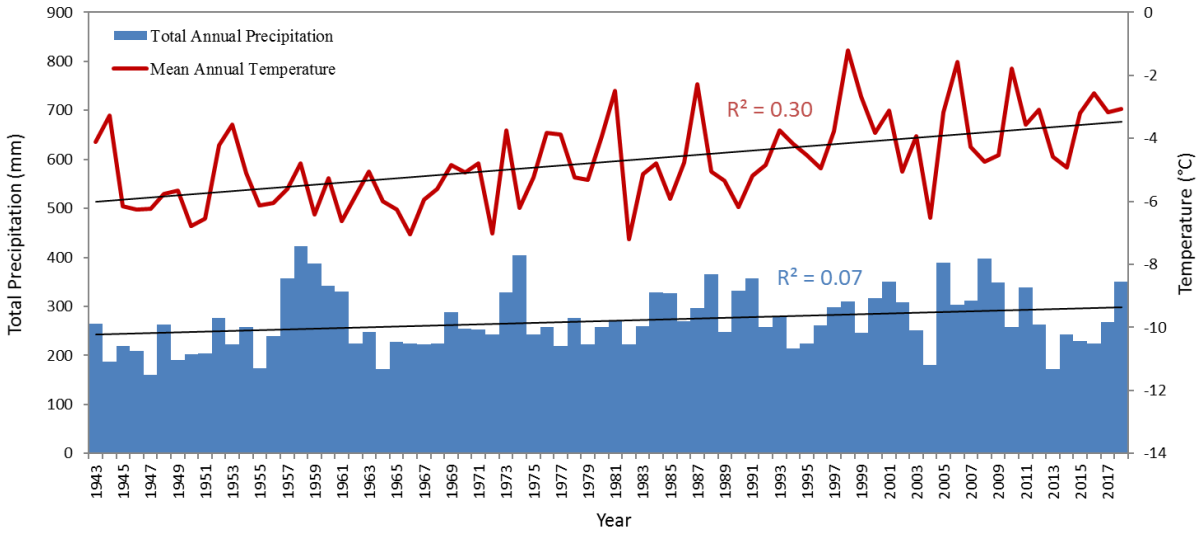

Figure 2.3 – Historical (1943-2018) total annual precipitation and mean annual temperature trend for Yellowknife. The mean annual temperature data indicate a general increasing trend across this time period (R^2= 0.30), while total annual precipitation data indicate no appreciable trend (R^2= 0.07; ECCC, 2018a).

During the years encompassing the present study (2017 and 2018), mean monthly temperatures were near average (ECCC, 2018a; Figure 2.4). Average winter snowfall fell during 2016-17 (122 mm of snow water equivalent), while below average snowfall fell during 2018 (80 mm of snow water equivalent; ECCC, 2018a). The 2017 ice-free season (May-September) saw average total rainfall (147 mm), while the 2018 ice-free season saw pronounced total rainfall (256 mm), with June and July 2018, in particular, experiencing well above average rainfall levels. Overall, 2018 saw the most seasonal rainfall in Yellowknife since 1943 when climate records were first maintained (ECCC, 2018a; Figure 2.4). The 2017-18 study period reflected a time of general hydrological recovery in the region following a relatively dry period during 2013-16.

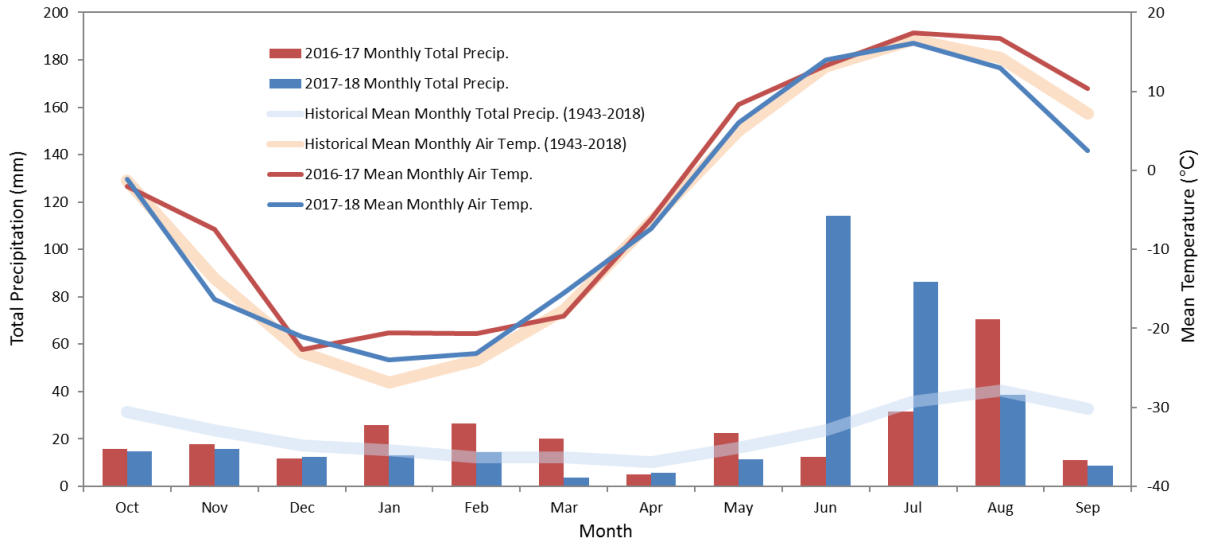

Figure 2.4 – Monthly total precipitation and mean air temperature for the 2017 and 2018 study years, respectively, with the 1943-2018 means highlighted (Yellowknife Airport met station; ECCC, 2018a). Mean monthly temperatures were near average during 2017 and 2018. Average winter snowfall fell during 2016-17 (122 mm of snow water equivalent), while below average snowfall fell during 2018 (80 mm of snow water equivalent). The 2017 ice-free season was indicative of relatively average conditions (May-September total rainfall = 147 mm). The 2018 ice-free season reflected particularly wet conditions (May-September total rainfall = 256 mm), with the most seasonal rainfall in Yellowknife since 1943 (when climate records were first maintained).

Recurring wind patterns also influence regional meteorological conditions and the onset of storm systems. Mean wind speed in Yellowknife is moderate at 12.8 kilometres per hour

(km/h); and the most frequent wind direction is from the east and south (ECCC, 2018b). Wind speed and direction patterns recorded in Yellowknife were similar during the 2017 and 2018 ice-free seasons (May-September), respectively (Figure 2.5). The predominant wind direction was generally from the south, with secondary influence from the east. From May-September during the years of study, the predominant wind speed range was 10-20 km/hr. Sustained wind gusts stronger than 30 km/hr were much less common (ECCC, 2018a).

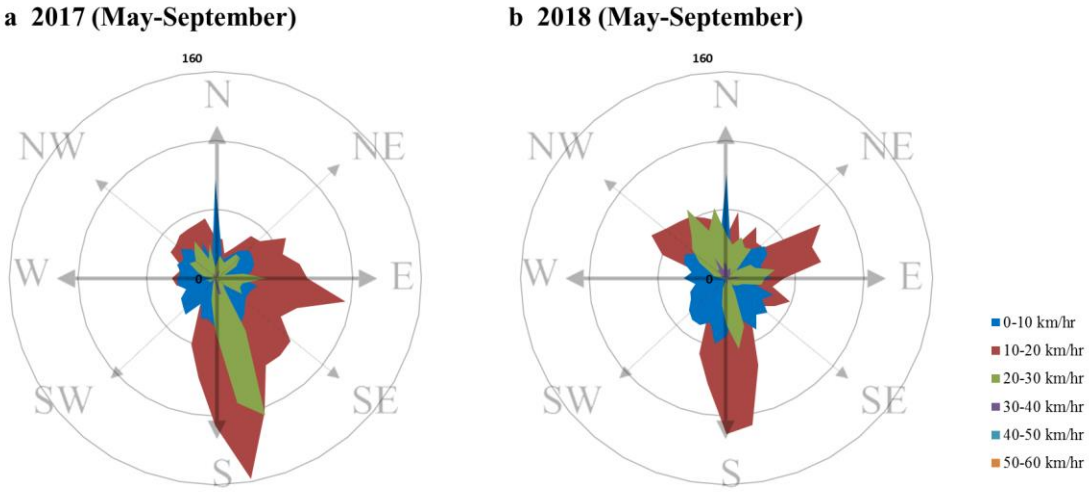

Figure 2.5 – Wind rose diagrams depicting wind speed and direction in Yellowknife during the ice-free season (May-September) for study years 2017 (a) and 2018 (b), respectively (ECCC, 2018a).

Overall, the environmental impacts associated with the general warming trend observed since the mid-twentieth century are not yet fully understood. In particular, it is still unclear how the many water bodies in the North Slave Region which are sensitive to climate are responding to increasing temperatures and lengthening of ice-free seasons.

2.1.3 General Ecology

The North Slave Region encompasses two terrestrial ecozones, including the Taiga Shield and Taiga Plains (Figure 2.6). These ecozones are further differentiated into the Taiga Shield High Boreal and Taiga Plains High Boreal ecoregions within the area of study, as described below.

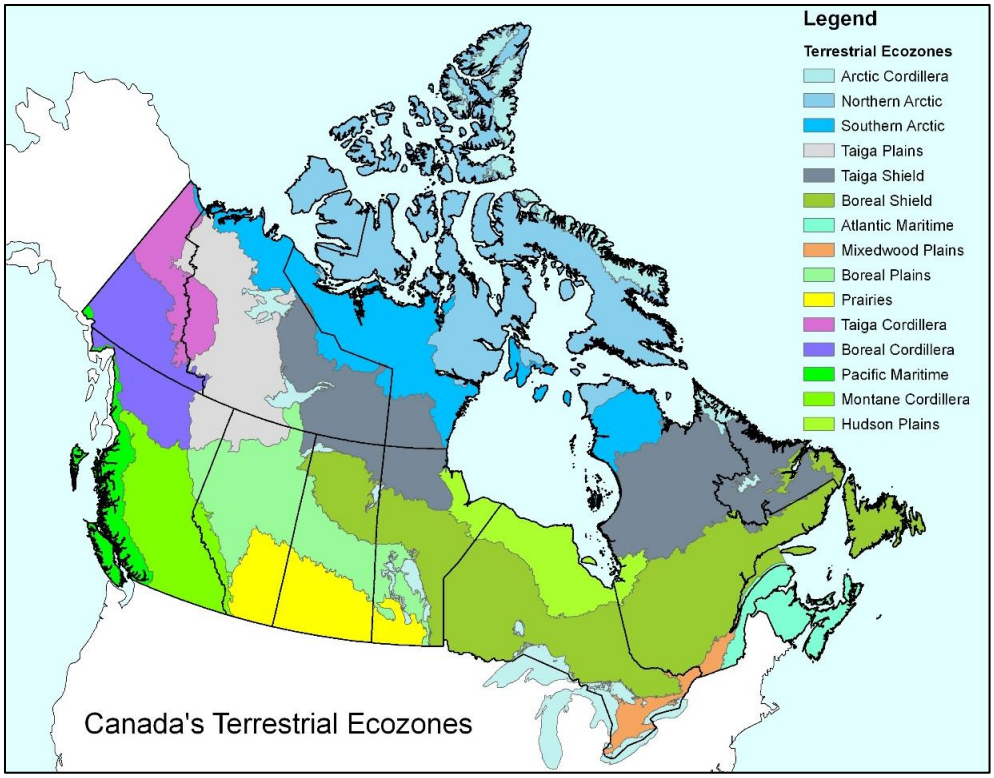

Figure 2.6 – Map illustrating the terrestrial ecozones of Canada, including the Taiga Shield and Taiga Plains ecozones in the North Slave Region of study (NRCAN, 2017).

Taiga Shield High Boreal Ecoregion

The Taiga Shield High Boreal ecoregion within the Taiga Shield ecozone lies on Precambrian sedimentary bedrock in the southern portions and vast swaths of glacier-carved, fractured granite in the north (Figure 2.7). Soils derived from scattered outwash and lacustrine deposits are generally shallow and coarse (Ecosystem Classification Group, 2008). The landscape is covered with numerous of lakes, ponds and wetlands, carved out during past glaciation. Large lakes occupy 30% of the area; and several large rivers drain south across the landscape into Great Slave Lake.

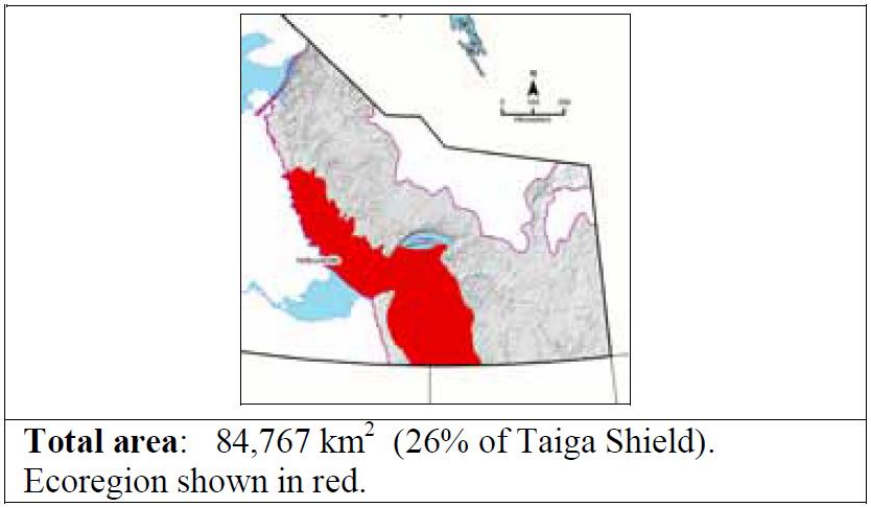

Figure 2.7 – Map illustrating the Taiga Shield High Boreal Ecoregion of NT (reproduced from Ecosystem Classification Group, 2008).

Common tree species in this ecoregion include scattered stands of black spruce, jack pine, white birch and trembling aspen, with regeneration on burn areas (Ecosystem Classification Group, 2008; Ecological Framework of Canada, 2019b). The forests are mixed with wetlands, bogs and bare outcrops dominated by lichens and shrubs. Within wet depressions and along lakeshores, small peat plateaus, shore fens and floating fens are common. Permafrost freeze/thaw is a major landscape influence in low-lying areas (Ecosystem Classification Group, 2008). The region experiences relatively frequent and large wildfire activity (Ecological Framework of Canada, 2019b).

Taiga Plains High Boreal Ecoregion

The Taiga Plains High Boreal ecoregion within the Taiga Plains covers the area west of Great Slave Lake and features broad extents of nearly level to gently rolling plains, subdued plateaus with intersecting large wetlands, muskeg, small lakes and stream channels (Figure 2.8; Ecological Framework of Canada, 2019a). Forest growth is generally poor in the region. Shallow, organic soils and peat plateaus are common, situated atop poorly drained, glacially-

deposited till and horizontal layers of sedimentary rock, namely limestone, shale, sandstone and conglomerates (Ecosystem Classification Group, 2007).

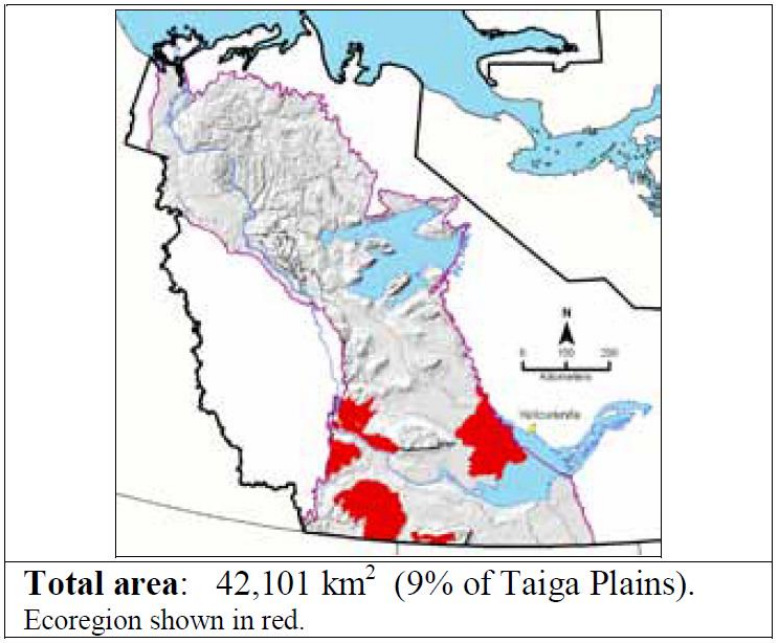

Figure 2.8 – Map illustrating the Taiga Plains High Boreal Ecoregion of NT (reproduced from Ecosystem Classification Group, 2007).

Low-growing, open black spruce forests, treed bogs, horizontal fens and peat plateaus dominate the landscape. Many frequently burned areas consist of extensive pure jack pine stands, with sparse bearberry and lichen understories common. Upland mixed-wood forests include white spruce, jack pine, tamarack, white birch and balsam poplar (Ecosystem Classification Group, 2007). Low-growing shrubs including willow and alder, as well as various sedges and mosses, are typical in this region (Ecological Framework of Canada, 2019a). Landscape features include surface water that accumulates as the active layer thaws. Since the region is relatively flat, hydrological changes can have a disproportionately large influence on the size of lakes (deMontigny, 2014). No major rivers exist in this ecoregion, which also experiences relatively frequent and large wildfire activity (Ecological Framework of Canada, 2019a). The 10,000 km^2 Mackenzie Bison Sanctuary is situated within the Taiga Plains. The sanctuary provides important

habitat for approximately 2,000 to 3,000 wood bison (*Bison bison athabascae)*, which is Canada's last genetically pure, disease-free herd (Larter et al., 2000). Bison help to maintain the structure, composition and stability of vegetation and wildlife (Gates et al., 2010).

2.1.4 Wildfire Disturbance

Throughout boreal forest regions, fires are an essential disturbance that help control insects and disease, as well as promote landscape and biological diversity (Ward and Mawdsley, 2000). Further beneficial impacts of fire include increasing soil nutrients and resetting successional pathways (Mustaphi and Pisaric, 2014). Negative impacts to fires may include danger to human life (e.g., air quality issues) and damage to infrastructure, in addition to threats to valuable commercial resources (Ward and Mawdsley, 2000). There still exists substantial gaps in the understanding of freshwater cycling processes, which limits predictive forecasting of flows and storage following climate and burn disturbances (Quinton et al., 2009). Hydrologic responses of northern aquatic ecosystems to fire are highly variable (Robinne et al., 2020) and may include changes in streamflow, water yields and freshet snowmelt input to lakes.

Severe drought conditions experienced in the region near Yellowknife, NT during 2013-2015 negatively impacted hydropower production, and led to the most intense wildfire season in twenty years during 2014 (Darwent, 2016; GNWT, 2016). In Canada, over the past 25-years, wildfires have burned an average of 2.3 million hectares (ha) annually (Figure 2.9). Depending on the extent of fire in any given year, fire management costs have ranged from $500 million to $1 billion (Natural Resouces Canada, 2019b). Climate models indicate that increasing atmospheric temperatures could increase the frequency and intensity of thunderstorms, which will increase the potential for lightning-ignited wildfires (Price and Rind, 1994; Kochtubajda et al., 2006; Veraverbeke et al., 2017). The standardization of studies and further use of geospatial

(remote sensing) technologies will help develop a firmer understanding of wildfire risks to water resources in northern forests (Robinne et al., 2020).

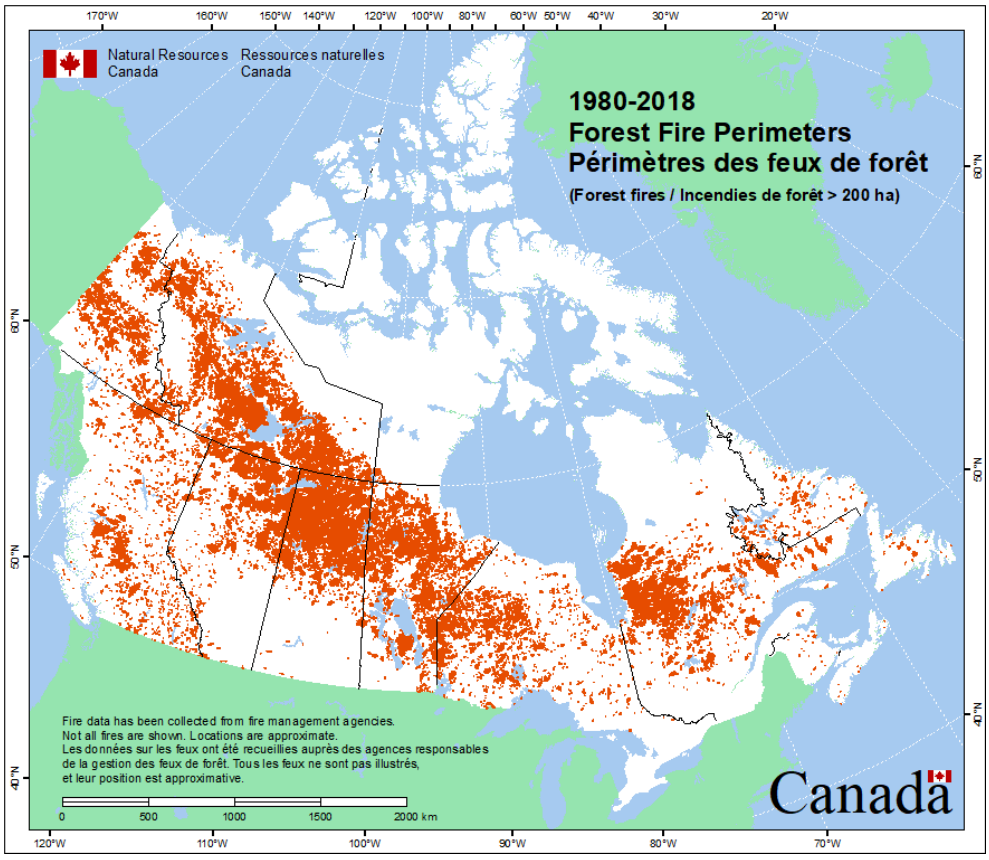

Figure 2.9 – Figure illustrating wildfire burn area from 1980-2018 (NRCAN, 2019a).

Fuel and Ignition

Fire occurence is ultimately linked to climate, with longer and warmer summer seasons conducive to increasing storm and lightning activity (Flannigan and Wotton, 2001; Kochtubajda et al., 2006). Veraverbeke et al. (2017) suggests that lightning ignitions have been increasing since 1975. Wildfire distrubances are expected to increase in the coming future under all forecasted emission scenarios (Flannigan et al., 2013). The two most important factors that influence fire in boreal forests are weather and climate (Flannigan and Wotton, 2001). While long-term climate conditions influence species distribution in a given region, short-term weather patterns affect temperature, humidity, precipitation, wind and fuel moisture, which ultimately

dictate the potential ignition and spread of fire (Flannigan and Wotton, 2001; Liu and Wimberly, 2015). The primary ignition source for boreal wildfires is lightning strikes from convective storm events during the summer season (Kochtubajda et al., 2006; Flannigan and Wotton, 2001). The number, distribution and size of wildfires can vary substantially during any given year (Kochtubajda et al., 2006). In NT, thunderstorms play an important role in the water and fire cycles of the boreal ecosystem (Kochtubajda et al., 2006).

Fine fuels will rapidly dry out during prolonged periods of minimal precipitation and low relative humidity, increasing the likelihood of fire ignition and dispersion, particularly with increasing wind (Whelan, 1995; Flannigan and Wotton, 2001). Dry forests (e.g., jack pine, birch) do not significantly differ from wetlands in total fuel load, with the greatest fuel loads typically located in wet spruce forests bordering wetlands (Thompson et al., 2017). Grass wetland burns are common and far-ranging in northern Canada during drought years (Thompson et al., 2017). The occurrence and intensity of fire is influenced by forest species type, age, and the timing since the last burn. More intense fires occur where more fuel is available and where fire has not occurred within a typical return period for a given area (Erni et al., 2018).

Local Factors and Topography

Landscape characteristics, particularly topography and vegetation fuel loading, are important factors in assessing suceptibility to fire (Mustaphi and Pisaric, 2013). Topography creates different microclimates with variable precipitation patterns that ultimately influence fuel load and supply, as well as vegetation type (Mustaphi and Pisaric, 2013). Topographic features including mountains, lakes and major rivers can act as natural firebreaks that suppress fire continuity. Fires tend to burn more effectively upgradient, as convective heat tends to dry out fuel ahead of it. Finally, slope aspect will influence fires. South-southeast facing slopes generally receive the most amount of sunlight, drying out fuel and increasing the likelihood of fire ignition

and spread (Gavin et al., 2006; Mustaphi and Pisaric, 2013). Vegetation species that are considered fire tolerators have thicker bark, and are more prone to understory ground fires (Pausas, 2015).

Wildfire Impacts on Water Chemistry

Recent studies have evaluated the effects of fire on water chemistry in northern regions with discontinuous permafrost. Results suggest that fire appears to amplify water chemistry differences of streams located in the Taiga Shield and Plains regions of NT, respectively (Tank et al., 2017). Streams situated in burned watersheds of the Taiga Plains region show a slight increase in turbidity, conductivity, alkalinity and pH, and slight decrease in metal concentrations; while streams in the Taiga Shield region show very little water chemistry variation in burned verus unburned watersheds (Tank et al., 2017). Overall, the effects of fire appear to be relatively modest compared to other watershed characteristics that dictate stream water chemistry (Tank et al., 2017). These results support the findings of Moser et al. (1998), who (as previously eluded to) found that surrounding vegetation and recent fire history had little influence on lake limnic properties. More research is required across a broader scale in the Yellowknife region to determine how catchment fires impact water chemistry within lake basins.

2.2 Hydrological Responses to Changing Climate in Northern Regions

2.2.1 Overview

Many recent studies have highlighted how Arctic and subarctic landscapes are sensitive to accelerating climate warming and are undergoing increasing ecosystem change (Pientz et al., 2004; Smol et al., 2005; Schindler and Smol, 2006; Prowse et al., 2009, Larsen et al., 2014). Intermittent changes in climate in the Canadian subarctic over the last several thousand years is thought to be influenced by Pacific Ocean climate variability and changes to the jet stream (Dalton et al., 2018). Hydrological changes to lakes across northern regions are complex and

highly variable according to local climate and geomorphological conditions. These changes are also projected to increasingly imapct aquatic biogeochmical processes and carbon dynamics, aquatic food web structure, biodiversity and wildlife habitat (Wrona et al., 2006).

Warming climate conditions may have dramatic impacts to northern permafrost regimes, which are integral hydrological processes that bind together the landscape (Figure 2.10). Permafrost may exist beneath ecotopes of all types, including peatland and forests; but is absent beneath bedrock outcrops, fens and lakes (Morse et al., 2016). Thawing permafrost can have implications for the integrity of human infrastructure in northern regions (e.g., northern roads, rail and transmission corridors and buildings). This is particularly true for permafrost landscapes rich in thermokarst lakes, which are the result of surface water accumulation as ice-rich ground subsides (Grosse and Jones, 2013).

Figure 2.10 – Map illustrating the extent of the major permafrost regions in the northern hemisphere (Ahlenius, 2007).

A number of recent studies have sought to characterize hydrological conditions and changes across northern regions, which are dominted by thermokarst lakes. Changes in Old Crow Flats, Yukon (Labrecque et al., 2009; Turner et al., 2010), Alaska (Yoshikawa and

Hinzman, 2003; Riordan et al., 2006) and Siberia (Smith et al., 2005; Karlson et al., 2012) indicate a decrease in lake abundance and size, driven by increasing susceptibility of thermokarst lakes to sudden drainage events from thawing permafrost (Frohn et al., 2005; Hinkel et al., 2007; Wolfe and Turner, 2008; Marsh et al., 2009; Pohl et al., 2009; Jones et al., 2011) as well as evaporation (Labrecque et al., 2009; Turner et al., 2010). In other regions of Alaska (Jorgenson and Shur, 2007), northern Quebec (Payette, 2004) and Siberia (Smith et al., 2005), thawing permafrost and lake perimeter breaching has resulted in temporary increases in water surface area. It is important to note that catchment characteristics, such as relative size, depth and land cover play an important role in lake water balance. Shallower thermokarst lakes, in particular, are expected to continue to display hydrological variability in response to climate warming (Roach et al., 2011; Wolfe et al., 2011; Jepsen et al., 2012, Bouchard et al., 2013). Catchments that are more densely forested are likely to provide a windbreak for deposited snow, promoting snowpack and resulting in enhanced spring runoff to lakes (Essery and Pomeroy, 2004; Bouchard et al., 2013; Turner et al., 2014). It is important to identify how catchment characteristics influence lake hydroecology elsewhere including the northern Canadian Shield in the North Slave Region of NT.

In addition to direct impacts of lake hydrology, enhanced permafrost thawing across Arctic and subarctic regions is expected to increase sediment, nutrient and carbon loadings to aquatic systems. Water chemistry impacts are expected to vary regionally depending on the extent of permafrost coverage. While nutrient and carbon enrichment from permafrost thawing will enhance cycling and productivity of aquatic systems, the status of these systems as major carbon sinks on the landscape is likely to change (Wrona et al., 2006; Kokelj et al., 2009). Many recent studies have attempted to evaluate these changes to water chemistry (e.g., clarity, nutrient

supply and nutrient cycling; MacDonald et al., 2012; Kokelj and Jorgenson, 2013) and aquatic biological communities in high-latitude lakes (Schindler and Smol, 2006; Carroll et al., 2011; Karlsson et al., 2011). For example, studies south of Great Slave Lake within the Peace-Athabasca Delta in northern Alberta utilized stable water isotope and chemistry analytical techniques to evaluate relationships among lake water balance and limnological conditions (Wolfe et al., 2006). This research determined that water balance varies depending on whether lakes are connected to the river drainage network (high input/low evaporaton influence) versus isolated (low input/high evaporation influence). Northern waterfowl and wildlife are likely to be impacted by these changes as well, which may include alteration to habitat and migration route suitability, and seasonal timing of migration route availability. It is expected that the magnitude, distribution and duration of the impacts and responses will vary depending on the system and location (Wrona et al., 2006; Kokelj and Jorgenson, 2013).

Overall, the changes to hydrological systems across Arctic and subarctic regions due to evolving climate conditions are complex and diverse. More research is required to improve our understanding of relations among lakes, catchment conditions and climate, in an effort to anticipate hydrological responses to changes at regional scales, especially within the North Slave Region.

2.2.2 Hydrological Responses in North Slave Region, NT

The upland Shield landscape of the North Slave Region generally encompasses high bedrock land cover with shallow soil conditions. As a result, extensive discontinuous permafrost is present beneath just 10-50% of the landscape (Heginbottom et al., 1995; Brown et al., 2002; Zhang et al., 2014; Morse et al., 2016). Studies suggest that most permfrost in this region exists in direct relation to the distribtuion of forested ecotopes, and that ecotopes with greater organic layer thickness and latent heat influence may be increasingly protected from degradation due to

climate warming (Shur and Jorgenson, 2007; Jorgenson et al., 2010; James et al., 2013; Zhang et al.; 2014, Morse et al., 2016). As climate warming persists, the overall extent of discontinuous permafrost in the North Slave Region will likely continue to be reduced to isolated, more ecosystem-protected peatland areas (i.e., just 2% of the landscape; Morse et al., 2016).

While some regions may experience drier ground conditions in response to warming conditions, other regions may be getting wetter. An examination of satellite imagery of the flat, low-lying Taiga Plains region of NT between 1986 and 2011 found that the proportion of water cover nearly doubled during this time period, from 5.7% to as high as 11% (Korosi et al., 2017). These landscape changes are complex and related to climate; however, the precise hydrological mechanisms for change are not yet fully understood. The increasing loss of sedge meadowlands (a preferred grazing habitat for bison) may be the cause of increasing bison movement and sightings beyond the Mackenzie Bison Sanctuary boundaries (Korosi et al., 2017). These critical interactions between climate, lake catchments and ecology underscore the need for further studies within the North Slave Region across a broader scale. It is becoming increasingly important to evaluate lake water balance alongside catchment physical characteristics such as hydrological connectivity and land cover. By developing a more robust understanding of these hydrological drivers, we will be better able to forecast changes to lakes under variable climate scenarios.

Previous studies at Pocket Lake and Baker Creek, NT

Hydrological studies at Pocket Lake and Baker Creek (Shield systems) near Yellowknife, NT since 1991 represent the longest regional record of their kind using isotopic as well as conventional hydrological study methods (Gibson, 2019; Figure 2.11). The information derived from these studies is highly useful for informing the present study and interpreting results. Reuslts show that seasonal and inter-annual hydrological variation are common in northern

boreal regions (Gibson, 2019). Identifying multi-year periods of drier and low flow conditions is very important for interpreting the hydrological processes of regional watersheds (Gibson, 2019), as catchment connectivity is largely influenced by seasonal meteorological conditions.

As previously shown at Baker Creek, the numerous, interconnected water bodies that make up a drainage network often have storage capacity thresholds defined by outlet surface elevations (Spence et al., 2019). As such, when respective lake water levels drop below these threshold elevations hydrological connectivity and downstream channel discharge is likely to be limited to the greater catchment (Spence, 2000). Lakes with a larger catchment relative to lake area will convey water downstream more effectively (Spence et al., 2019). Also, catchments with more numerous and larger upstream lakes are more likely to transmit and maintain downstream flow (Spence et al., 2019).

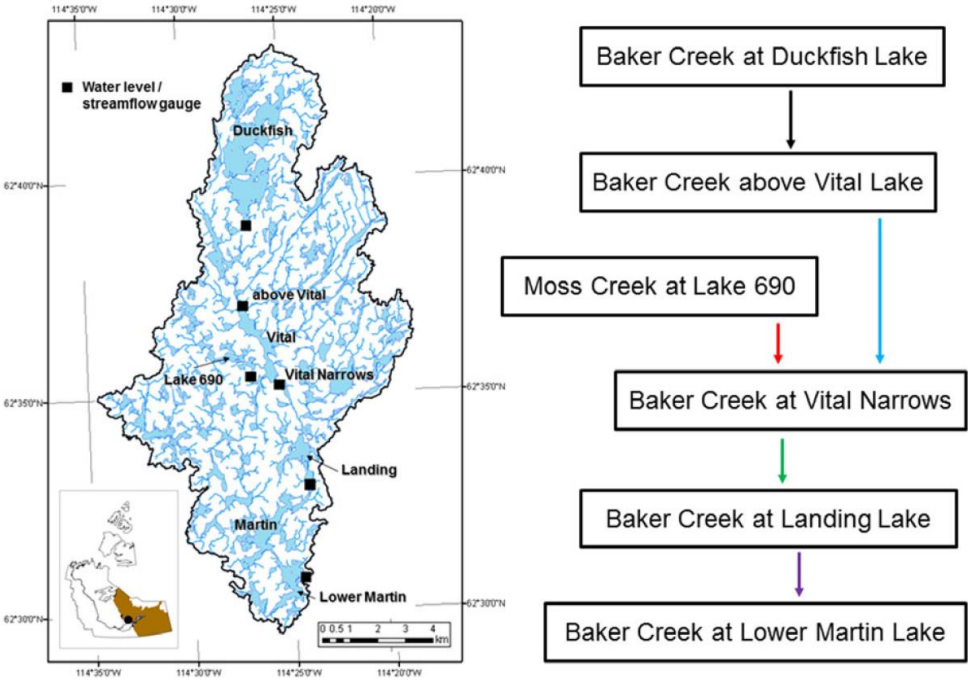

Figure 2.11 – Figure illustrating the Baker Creek watershed and previous study locations near Yellowknife, NT (reproduced from Spence et al., 2019).

When water levels are high, flow from larger storage basins within a catchment can enhance and sustain streamflow to lower basins for a greater duration (Spence et al., 2019). Conversely, during drought, upstream catchment flow is supressed as water body levels increasingly fail to rise above outlet elevation thresholds (Spence et al., 2019). Given that the Baker Creek watershed is comprised of a complex chain-of-lakes, effective drainage area will vary depending on disconnections between lakes along the chain (Spence et al., 2010).

Variation in catchment hydrological connectivity over time has been attributed to a number of factors, including seasonal timing of precipitation, storage deficits and the intensity of rainfall events (Bracken and Croke, 2007). Under drier conditions, the evaporation influence increases as the watershed becomes partially disconnected and respective lake areas along the chain increase (Gibson and Reid, 2014). It is speculated that the release of active layer storage to lakes within the watershed during dry years results in more of a buffering role relative to rainfall (Ombradovic and Sklash, 1986; Gibson and Reid, 2014). Overall, the Baker Creek watershed may be classified as an evaporative system, which is fairly representative of this forest-tundra transition region. The key processes driving lake hydrology are ultimately connectivity of the chain-of-lakes and the evolution of water balance within water bodies along the chain (Gibson and Reid, 2014). More research is required across a broader extent to fully understand the "fill-and-spill" mechanisms of Shield systems in the North Slave Region.

Lake Biogeochemical and Limnological Processes

Lake hydrology in the North Slave Region must be assessed in relation to associated biogeochemical and limnological processes, as hydrological connecitvity is linked to lake residency time (Spence et al., 2019). Lake connectivity has been shown to be a reasonable predictor of DOC concentrations in the Canadian Shield (Gergel et al., 1999; Spence et al., 2019). Studies of the Baker Creek watershed (introduced above) suggest that enhanced winter

streamflow from increasingly common late summer/fall rains result in higher wintertime loads of carbon and solutes (Spence et al., 2015). Under these enhanced, late-season streamflow conditions wth ample lake volumes, more water is transmitted over frozen, shallow (and highly conductive) soils. As biological activity under lake ice slows, net mineralization and nitrification rates increase (Spence et al., 2015).

Other regional water chemistry studies of freshwater lakes in NT reveal that underlying geology strongly influences limnic properties (Moser et al., 1998; Pientz et al., 1997). Shield lakes are likely to have higher concentrations of A1 and Fe, and lower pH, specific conductivity and proportion of ions (e.g., Ca, SO_4, Li, Mg and Na), relative to sinkhole (karst) and muskeg lakes (Moser et al., 1998). Compared to sinkhole lakes, muskeg lakes have higher concentratins of DOC and increasing productivity, with greater particulate organic carbon (POC), chlorophyll a, nitrogen (NH_3 and NO_2; Moser et al., 1998). These findings highlight the close relationship between catchment physiography, hydrological connectivity and limnological conditions which influence aquatic ecology in the North Slave Region.

2.2.3 Hydrological Responses to Wildfire

Previous studies across northern regions have sought to investigate the effects of wildfire on hydrological regimes. The annual number of published studies related to fire impacts in high-latitude forests has increased steadily in recent years. A recent scoping review of post-hydrologic effects of wildfire was completed by Robinne et al. (2020) and involved the screening of 2,935 peer-reviewed articles, with selection of 82 studies for dissemination. The cumulative conclusion of this review determined that the hydrologic response of northern riverine ecosystems to fire is highly variable. Annual streamflow and peakflows were found to increase post-fire in some studies (Pomeroy et al., 2012; Springer et al., 2015), with only water yields increasing in others (Eaton et al., 2010a; Mahat et al., 2015). A study on the Canadian Shield reported a two-year

increase in baseflows and annual yield after fire, even under drier conditions (Schindler et al., 1980). Similarly, a study on the boreal plains (Pelster et al., 2008) reported higher yields six years after fire. An increase in peakflows from snowmelt runoff was identified by Mahat et al. (2015), while several studies show the opposite response with snowmelt decoupled between burned and unburned areas (Burke et al., 2005; Eaton et al., 2010b; Owens et al., 2013).

In recent studies of burned sample plots in western North America (Alberta and British Columbia), evidence of increased snowfall accumulation and input to water bodies during spring melt has been shown (Burles and Boon, 2011; Pomeroy et al., 2012; Winkler et al., 2015). Burn areas result in more energy available for snowmelt (earlier freshet) and more rapid snowmelt (shorter freshet; Burles and Boon, 2011; Winkler et al., 2015), as well as a greater contribution of snowmelt to annual streamflow (Eaton et al., 2010a; Owens et al., 2013). The current body of research suggests that aquatic ecosystems are generally resilient to fire effects (e.g., concentration of total nitrogen and phosphorous, chlorophyll levels and abundance of waterfowl young) in both streams and lakes (Jalal et al., 2005; Kreutzweiser et al., 2012; Lewis et al., 2014). Differences in burn severity in northern boreal forests can result in considerable variability in survival, density, regrowth and distribution of residential biota, which can last decades or even centuries (Burton et al., 2008). The standardization of studies and further use of geospatial (remote sensing) technologies will help develop a firmer understanding of relations among wildfire and water resources in northern forests (Robinne et al., 2020).

2.3 Isotope Mass Balance Approaches in Studying Lake Hydrology

2.3.1 Summary

As previously described, water isotope tracers are effective in evaluating water balance interactions in hydrological systems (Gibson and Reid, 2014). These approaches may be further employed across a broader scale in studying lake hydrological changes within the North Slave

Region. Stable water isotopes including hydrogen (δ^2H; deuterium) and oxygen ($\delta^{18}O$), are highly informative of past and present hydrological conditions because of the well-understood physics of the isotopic partitioning processes in the global water cycle (Rozanski et al., 1993; Araguás et al., 2000; Edwards et al., 2004). This relatively inexpensive approach to water balance research typically requires a minimal sample amount (< 30 ml) from each site, making it an effective study solution. Water isotope data have shown to be particularly useful for characterizing hydrology and hydroclimatology in remote regions and at high latitudes (Brock et al., 2009; Burgman et al., 1987; Wolfe and Edwards, 1997; Gibson 2001 and 2002; Gibson and Edwards, 2002; Gibson et al., 1993 and 2002; Leng and Anderson, 2003; Maric, 2003; Edwards et al., 2004; Yi et al., 2008; Birks and Gibson, 2009; Turner et al., 2010 and 2014; Tondu et al., 2013; Anderson et al., 2013; MacDonald et al., 2017). Multi-year datasets are most informative, as they reflect seaonal and interannual variability in isotope composition and response of lake water balances to climate conditions (Gibson, 2002). In cold-regions, lake isotope compositions are seasonally influenced by surges of inflow during spring snowmelt, followed by relatively short, arid summers with high evaporation rates (Gibson and Reid, 2014). With a sensativity to varying meteorological conditions (temperature and precipitation types), lake isotope compositions (i.e., $\delta^{18}O$ and δ^2H) provide quantitative information about the relative importance of input water contributions (e.g., snowmelt, rain and permafrost thaw) and evaporation. These data can be used to calculate additional useful water balance metrics including evaporation-to-inflow ratio (*E/I*; Turner et al., 2010; MacDonald et al., 2017). Water isotope tracers provide an efficient means of identifying hydrological information, which allows for broad-scale studies of lakes of varying catchment characteristics.

Combining quantitative water isotope analyses with remote sensing catchment modelling has been previously demonstrated to be highly informative for hydrological characterization of northern lakes in North America (Turner et al., 2014). Recent studies in the Western Siberian Lowlands (WSL) have also attempted to use stable water isotopes to improve our understanding of dominant landscape controls on northern hydrological systems (Ala-aho et al., 2018). Studies in high-latitude regions indicate that lakes, bogs and permafrost are important influencers of runoff attenuation or enhancing near-surface flow (Hayashi et al., 2004; Cooper et al., 2008; Yi et al., 2012; Turner et al., 2014; Connon et al., 2015; Streletskiy, et al., 2015; Lachniet et al., 2016). Building on these findings, Ala-aho et al. (2018) sampled rivers along a 1,700 km south-north transect in WSL (i.e., from permafrost-free to continuous permafrost) over three years to establish isotope proxies for catchment hydrological responsiveness and connectivity. Water isotope correlations in WSL suggest that lakes and wetlands are intimately connected to rivers. Further, it was found that catchment responsiveness to rain and snow events increases (i.e., reduced mean transit time) with the presence of permafrost (Ala-aho et al., 2018). This study provides unique evidence through isotope analyses that permafrost and lakes/wetlands influence hydrological pathways across wide spatial distributions (10-10^5 km^2) and permafrost coverage (0-70%; Ala-aho et al., 2018). These studies reinforce our understanding of the complex interactions of northern hydrological systems under warming climate scenarios. Such isotope tracer methods may be further employed across a broad scale in the North Slave Region to evaluate meteorological and catchment-specific drivers of lake hydrology.

2.3.2 Isotope Framework

Analyses of water body hydrological conditions using isotope tracers are completed through comparison of δ^2H and $\delta^{18}O$ isotope values among sites and relative to a regionally-established isotope framework. The framework represents gradients of influence by inflow

(precipitation) and outflow (evaporation) hydrological drivers. The strong linear trends exhibited in hydrogen and oxygen isotope compositions of precipitation and surface waters can be traced to the systematic mass-dependent isotopic partitioning of water molecules in the hydrologic cycle (Edwards et al., 2004). Globally, the isotopic composition of precipitation plots along the *Global Meteoric Water Line (GMWL)*, which is described by $\delta^2H = 8\ \delta^{18}O + 10$ (Craig, 1961; Figure 2.12). Where precipitation plots along the GMWL, or *Local Meteoric Water Line (LMWL)*, for a given region is dependent on the trajectory and distillation history of atmospheric moisture contributing to precipitation (Turner et al., 2010). In a region with a seasonal climate, snow typically plots along an isotopically-depleted section of the GMWL (or LMWL) relative to rain.

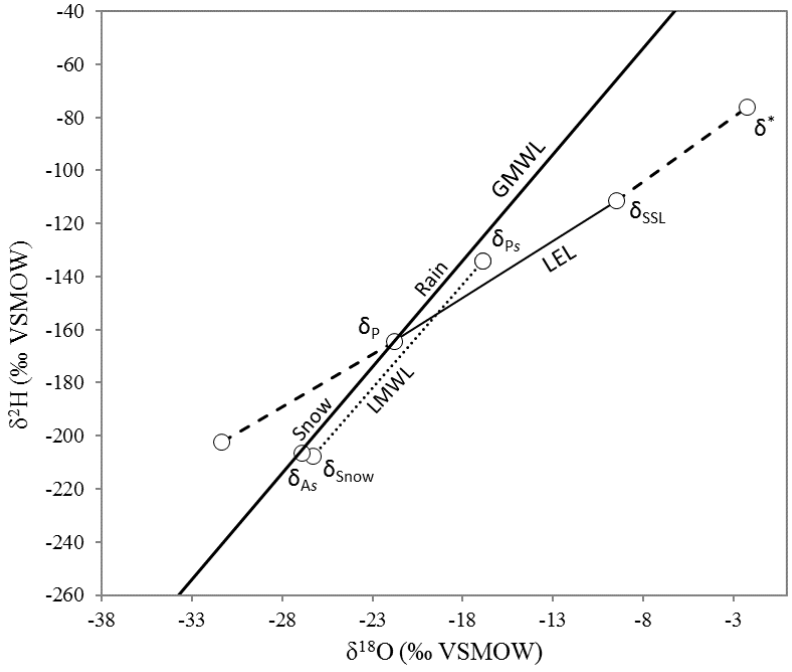

Figure 2.12 – Isotope labelling of water balance components along the GMWL (reproduced from Edwards et al., 2004). Descriptions of the labelled components are provided below and in Table 2.1.

The isotope compositions of water from lakes in the region will typically cluster along another trendline, known as the *Local Evaporation Line (LEL)*. The slope of the LEL is usually 4-6. The point at which the LEL intersects the LMWL is recognized as the average annual

isotopic composition of precipitation (δ_p) for the region. As such, the LEL reflects the isotopic evolution of regional lakes undergoing evaporation while being replenished by waters having the composition of δ_p (Turner et al., 2010). The LEL deviates from the intersection of the GMWL at δ_P. Water from regional lakes will plot along the LEL during the ice-free season. The progression of lake water compositions along the LEL, away from δ_p, is a reflection of evaporative loss. As lakes become isotopically enriched by evaporation through summer (assuming typical rainfall conditions), the lake compositions will generally migrate up the LEL towards the steady-state composition (δ_{SSL}). This point represents the isotopic composition of a terminal lake basin where evaporative loss is equal to inflow. As lake waters become increasingly isotopically enriched through summer, they will migrate further up the LEL towards the δ^* composition, which represents the isotopic composition of a lake nearing complete desiccation. Lake water compositions will laterally deviate from the LEL as source water (rainfall or snowmelt) mixing occurs, as the isotope compositions of these source waters tend to plot on the GMWL or LMWL (Turner et al., 2010). Lake water compositions that plot above the LEL indicate more dominant rainfall input/influence, while those that plot below the LEL suggest more dominant snowfall input/influence. A summary of the main isotope framework components is provided in Table 2.1.

Table 2.1 – Summary of isotope framework components.

Component	Symbol/ Abbreviation	Description
Global Meteoric Water Line	GMWL	Isotopic composition of precipitation globally (trendline), described by $\delta^2H = 8\ \delta^{18}O + 10$.
Local Meteoric Water Line	LMWL	Isotope composition of precipitation regionally (trendline), developed from mean local snow and rain isotopic compositions.
Local Evaporation Line	LEL	Regional evaporation trendline. Isotopic compositions of water from lakes in the region will typically cluster/migrate along the trendline during the ice-free season.

Component	Symbol/ Abbreviation	Description
Evaporating flux isotopic composition	δ_E	Mean isotopic composition of the regional evaporating flux.
Ambient atmospheric moisture isotopic composition	δ_{As}	Isotopic composition of ambient atmospheric moisture in the region.
Precipitation isotopic composition	δ_P	Mean annual isotopic composition of precipitation, estimated from the intersection of the observed LEL and the GMWL.
Summer rain isotopic composition	δ_{Ps}	Summer rain isotopic composition derived from mean regional sampling data.
Snow isotopic composition	δ_{Snow}	Snow isotopic composition derived from mean regional sampling data.
Steady-state isotopic composition	δ_{SSL}	Isotopic composition of a terminal lake basin at steady-state (i.e., evaporation equal to inflow).
Complete desiccation isotopic composition	δ^*	Isotopic composition of lake approaching complete desiccation.

Lake isotope data from the North Slave Region may be collected and used to derive a LEL for regional hydrological analyses. The development of this framework will enhance the evaluation of key drivers of lake hydrology under variable precipitation and catchment conditions.

2.3.3 Evaporation/Inflow Ratio

The relative importance of lake vapour loss relative to input can be determined for individual lakes using water isotope tracers and calculation of additional metrics including the evaporation/inflow (E/I) ratio and the isotopic composition of lake-specific input (δ_I). E/I ratio calculations are based on isotope mass balance calculations described by

$$E/I = (\delta_I - \delta_L) / (\delta_E - \delta_L) \quad (1)$$

where δ_L is the measured isotopic composition of lake water and δ_E is the isotopic composition of the associated evaporating flux, calculated using the Craig and Gordon (1965) model as formulated by Gonfiantini (1986) in decimal notation (refer to Equations and Calculations, Appendix One). These calculations require meteorological parameters (flux-weighted

temperature and relative humidity) for the region of interest, as well as several other modelled isotope parameters calculated using methods developed by Gonfiantini (1986) and Horita and Wesolowski (1994), which are described in Appendix One. The calculations reveal important information about lake water balance conditions, specifically, isotopic deviation from the "steady-state" of lakes as the inflow versus evaporation influences change. Lake steady-state is a useful benchmark of the isotopic composition of lakes when inflow is equal to evaporative loss.

E/I ratios and lake water isotopic distributions in δ^2H–$\delta^{18}O$ space were used here to provide insight of the role of specific hydrological processes influencing study lakes (i.e., temporally and spatially) in the Yellowknife region. Study lake E/I ratios representative of the beginning (May) and end (August) of the 2017 and 2018 ice-free seasons. The δ_I value of each lake, as calculated using input water composition, is assumed to plot at the intersection of the GMWL and lake-specific evaporation line. Overall, the isotope framework, associated components and E/I values are useful for comparing differences among the hydrological conditions of many lakes across the region surrounding Yellowknife. Coupling these water isotope approaches with analysis of catchment properties provides the capacity to elucidate the influence that the surrounding landscape has on mediating individual lake hydrological conditions.

REFERENCES

Ahlenius, H. 2007. Permafrost extent in the northern hemisphere [map]. Global Outlook for Ice and Snow. UNEP/GRID-Arendal. Obtained online from http://www.grida.no/resources/5234 on November 19, 2019.

Ala-aho, P., Soulsby, C., Pokrovsky, O.S., Kirpotin, S.N., Karlsson, J., Serikova, S., Manasypov, R., Lim, A., Krickov, I., Kolesnichenko, L.G., Laudon, H. and Tetzlaff, D. 2018. Permafrost and lakes control river isotope composition across a boreal Arctic transect in the Western Siberian lowlands. *Environ. Res. Lett*. 13, 034028.

Anderson, L., Birks, S.J., Rover, J. and Guldager, N. 2013. Controls on recent Alaskan lake changes identified from water isotopes and remote sensing. *Geophys. Res. Lett.* 40, 1-6.

Araguás-Araguás, L., Froehlich, K. and Rozanski, K. 2000. Deuterium and oxygen-18 isotope composition of precipitation and atmospheric moisture. *Hydrol. Proc.*, 14, 1341-1355.

Birks, S.J. and Gibson, J.J. 2009. Isotope hydrology research in Canada, 2003-2007. *Can. Water Resour. J*. 34 (2), 163-176.

Bouchard, F., Turner, K.W., MacDonald, L.A., Deakin, C., White, H., Farquharson, N., et al. 2013. Vulnerability of shallow subarctic lakes to evaporate and desiccate when snowmelt runoff is low. *Geophys. Res. Lett*. 40(23), 6112-6117. Doi: 10.1002/2013GL058635.

Bracken, L.J. and Croke, J. 2007. The concept of hydrological connectivity and its contribution to understanding runoff-dominated geomorphic systems. *Hydrological Processes*. 21(13), 1749-63.

Brock, B.E., Yi, Y., Clogg-Wright, K.P., Edwards, T.W.D., Wolfe, B.B., 2009. Multi-year landscape-scale assessment of lakewater balances in the Slave River Delta, NWT, using water isotope tracers. *Journal of Hydrology*, 379, 81-91.

Brown, J., Ferrians, O., Heginbottom, J.A. and Melnikov, E.S. 2002. Circum-arctic map of permafrost and ground-ice conditions, version 2. NSIDC: National Snow and Ice Data Center/World Data Center for Glaciology, Boulder, Co. Obtained from http://nsidc.org/data/ggd318 [accessed November 16, 2019].

Bryson, R.A. 1966. Air masses, streamline, and the boreal forest. *Geographical Bulletin*, 8(3), 228-69.

Burgman, J.O., Calles, B. and Westman, F. 1987. Conclusions from a ten year study of oxygen-18 in precipitation and runoff in Swedon. Symposium on Isotope Techniques in Water Resources Development. International Atomic Energy Agency, Vienna, 30 March-3 April 1987, IAEA-SM-299/107.

Burke, J.M., Prepas, E.E. and Pinder, S. 2005. Runoff and phosphorous export patterns in large forested watersheds on the western Canadian Boreal Plain before and for 4 years after wildfire. *J. Environ. Eng. Sci*. 4, 319-325.

Burles, K. and Boon, S. 2011. Snowmelt energy balance in a burned forest plot. Crowsnest Pass, Alberta. Canada. *Hydrol. Process*. 25, 3012-3029.

Burton, P.J., Parisien, M.-A., Hicke, J.A., Hall, R.J. and Freeburn, J.T. 2008. Large fires as agents of ecological diversity in the North American boreal forest. *Int. J. Wildl. Fire*. 17, 754.

Carroll, M.L., Townshend, J.R.G., DiMiceli, C.M., Loboda, T. and Sohlberg, R.A. 2011. Shrinking lakes of the Arctic: spatial relationships and trajectory of change. *Geophysical Research Letters*. 38, L20406, http://dx.doi.org/10.1029/2011GL049427.

Connon, R., Quinton, W., Craig, J., Hanisch, J. and Sonnentag, O. 2015. The hydrology of interconnected bog complexes in discontinuous permafrost terrains. *Hydrol. Process*. 29, 3831-3847.

Cooper, L.W. et al. 2008. Flow-weighted values of runoff tracers ($\delta^{18}O$, DOC, Ba, alkalinity) from the six largest Arctic rivers. *Geophys. Res. Lett*. 35, L18606.

Craig, H. 1961. Isotopic variations in meteoric waters. *Science*, 133, 1702-1703.

Craig, H., Gordon, L.I. 1965. Deuterium and oxygen 18 variations in the ocean and the marine atmosphere. In: Tongiorgi, E. (Ed.), Stable Isotope in Oceanographic Studies and Paleotemperatures. Laboratorio di Geologia Nucleare, Pisa, Italy, pp. 9-130.

Dalton, A.S., Patterson, R.T, Roe, H.M., Macumber, A.L., Swindles, G.T., Galloway, J.M., Vermaire, J.C., Crann, C.A. and Falck, H. 2018. Late Holocene climatic variability in subarctic Canada; insights from a high-resolution lake record from the central Northwest Territories. *PLoS One*. Vol. 2018, 1-21.

Darwent, R., ed. 2016. Fire severest in the 2014 Northwest Territories fires. Nat. Resour. Can., Can. For. Serv., North. For. Cent., Edmonton, AB. *Insights*. No 4b.

deMontigny, P.A. 2014. The climatic implications of lake level expansion in the Mackenzie Bison Sanctuary, Fort Providence, Northwest Territories. MSc Thesis. Carleton University.

Eaton, B.C., Andrews, C.A.E., Giles, T.R. and Phillips, J.C.C. 2010a. Wildfire, morphologic change and bed material transport at Fishtrap Creek, British Columbia. *Geomorphology*. 118, 409-424.

Eaton, B.C., Moore, R.D.D., Giles, T.R. 2010b. Forest fire, bank strength and channel instability: the "unusual" response of Fishtrap Creek, British Columbia. *Earth Surf. Process. Landforms*. 35, 1167-1183.

Ecological Framework of Canada. 2019a. Taiga Plains Ecozone. Retrieved from http://ecozones.ca/english/zone/TaigaPlains/land.html.

Ecological Framework of Canada. 2019b. Taiga Shield Ecozone. Retrieved from http://ecozones.ca/english/zone/TaigaShield/land.html.

Ecosystem Classification Group. 2007 (rev. 2009). Ecological regions of the Northwest Territories–Taiga Plains. Department of Environment and Natural Resources, Government of the Northwest Territories, Yellowknife, NT, Canada. viii + 173 pp. + folded insert map.

Ecosystem Classification Group. 2008. Ecological regions of the Northwest Territories–Taiga Shield. Department of Environment and Natural Resources, Government of the Northwest Territories, Yellowknife, NT, Canada. viii + 146 pp. + insert map.

Edwards, T.W.D., Wolfe, B.B., Gibson, J.J., Hammarlund, D. 2004. Use of water isotope tracers in high latitude hydrology and paleohydrology. In: Pienitz, R., Douglas, M.S.V., Smol, J.P. (Eds.), Long-Term Environmental Change in Arctic and Antarctic Lakes. Springer, Dordrecht, The Netherlands, pp. 187-207.

Environment and Climate Change Canada (ECCC). 2018a. Historical data (hourly, daily, monthly). Yellowknife, Northwest Territories (station: Yellowknife A; climate identifier: 2204101). Retrieved between 2018 and 2019 from http://climate.weather.gc.ca/historical_data/search_historic_data_e.html.

Environment and Climate Change Canada (ECCC). 2018b. Canadian climate normals 1981-2010 station data. Yellowknife, Northwest Territories (station: Yellowknife A; climate identifier: 2204101). Retrieved in 2018 from https://climate.weather.gc.ca/climate_normals/results_1981_2010_e.html?searchType=stnName&txtStationName=yellowknife&searchMethod=contains&txtCentralLatMin=0&txtCentralLatSec=0&txtCentralLongMin=0&txtCentralLongSec=0&stnID=1706&dispBack=1.

Erni, S., Arseneault, D. and Parisien, M.-A. 2018. Stand age influence on potential wildfire ignition and spread in the boreal forest of northeastern Canada. *Ecosystems*. 21(7), 1471-1487.

Essery, R., Pomeroy, J. 2004. Vegetation and topographic control of wind-blown snow distributions in distributed and aggregated simulations for an arctic tundra basin. *Journal of Hydrometeorology*, Special Section 5, 735-744.

Flannigan, M.D. and Wotton, B.M. 2001. Climate, weather and area burned. In Forest fires: behavior and ecological effects. Edited by E.A. Johnson and K. Miyanishi. Academic Press, San Diego, California. pp. 335-357.

Flannigan, M.D., Cantin, A.S., de Groot, W.J., Wotton, M., Newbery, A. and Gowman, L.M. 2013. Global wildland fire season severity in the 21st century. *Forest Ecology and Management*. 294, 54-61.

Frohn, R.C., Hinkel, K.M. and Eisner, W.R. 2005. Satellite remote sensing classification of thaw lakes and drained thaw lake basins on the North Slope of Alaska. *Remote Sensing of Environment*. 97, 116-126.

Gates, C.C. Freese, C.H., Gogan, P.J.P. and Kotzman, M. (eds. and comps). 2010. American Bison: status survey and conversation guidelines 2010. Gland, Switzerland: IUCN.

Gavin, D.G., Hu, F.S., Lertzman, K. and Corbett, P. 2006. Weak climatic control of stand-scale fire history during the late Holocene. *Ecology*. 87(7), 1722-1732.

Gergel, S.E., Turner, M.G. and Kratz, T.K. 1999. Dissolved organic carbon as an indicator of the scale of watershed influence on lakes and rivers. *Ecological Applications*. 9, 1377-90.

Gibson, J.J., Edwards, T.W.D., Bursey, G.G. and Prowse, T.D. 1993. Estimating evaporation using stable isotopes: quantitative results and sensitivity analysis for two catchments in northern Canada. *Nordic Hydrol*. 24, 79-94.

Gibson, J.J. 2001. Forest-tundra water balance signals traced by isotopic enrichment in lakes. *J. Hydrol.* 251, 1-13.

Gibson, J.J. 2002. Short-term evaporation and water budget comparisons in shallow arctic lakes using non-steady isotope mass balance. *J. Hydrol*. 264, 247-266.

Gibson, J.J. and Edwards, T.W.D. 2002. Regional surface water balance and evaporation-transpiration partitioning from a stable isotope survey of lakes in northern Canada. *Glob. Biogeochem. Cyc*. 16, 10.1029/2001GB001839.

Gibson, J.J., Prepas, E.E. and McEachern, P. 2002. Quantitative comparison of lake throughflow, residency, and catchment runoff using stable isotopes: modelling and results from a regional survey of Boreal lakes. *J. Hydrol*. 262, 128-144.

Gibson, J.J. and Reid, R. 2014. Water balance along a chain of tundra lakes: a 20-year isotopic perspective. *J. Hydrol*. 519, 2148-2164.

Gibson, J.J. 2019. Isotope-based evaporation and water balance studies at Pocket Lake and Baker Creek: 2019 update. Submitted to Shawne Kokelj, Government of Northwest Territories. InnoTech Alberta. December 31, 2019.

Gonfiantini, R. 1986. Environmental isotopes in lake studies. In: Fritz, P., Fontes, J.C. (Eds.), Handbook of Environmental Isotope Geochemistry, The Terrestrial Environment, vol. 2. Elsevier, New York, pp. 113-168.

Government of Northwest Territories (GNWT). 2016. North Slave hydro system. Yellowknife, NT. 2 pp.

Grosse, G. and Jones, B.M. 2013. Thermokarst lakes, drainage, and drained basins. Elsevier. Amsterdam, Netherlands. 29p.

Hayashi, M., Quinton, W.L., Pietroniro, A. and Gibson, J.J. 2004. Hydrologic functions of wetlands in a discontinuous permafrost basin indicated by isotopic and chemical signatures. *J. Hydrol*. 296, 81-97.

Heginbottom, J.A., Dubreuil, M.A. and Harker, P.A. 1995. Canada-Permafrost. National Atlas of Canada, Fifth Edition. National Atlas Information Service, Natural Resources Canada: Ottawa, ON, Canada; Plate 2.1. MCR 4177.

Hinkel, K.M., Jones, B.M., Eisner, W.R., Cuomo, C.J., Beck, R.A. and Frohn, R. 2007. Methods to assess natural and anthropogenic thaw lake drainage on the western Arctic coastal plain of northern Alaska. *Journal of Geophysical Research*. 112, F02S16, http://dx.doi.org/10.1029/2006jf000584.

Horita, J., Wesolowski, D. 1994. Liquid-vapour fractionation of oxygen and hydrogen isotopes of water from the freezing to the critical temperature. *Geochimica et Cosmochimica Acta*, 58, 3425-3437.

Jalal, W., Pinel-Alloul, B., Méthot, G. 2005. Suivi à moyen terme des impacts écologiques des feux et des coupes forestières sur la communauté zooplanctonique des lacs de l'écozone boréale. Rev. *des Sci. l'eau*. 18, 221-248.

James, M., Lewkowicz, A.G., Smith, S.L. and Miceli, C.M. 2013. Multi-decadal degradation and persistence of permafrost in the Alaska Highway corridor, northwest Canada. *Environmental Research Letters*. 8, 045013 (10pp.). DOI: 10.1088/1748-9326/8/4/045013.

Jespen, S.M., Voss, C.I., Walvoord, M.A., Rose, J.R., Minsley, B.J. and Smith, B.D. 2012. Sensitivity analysis of lake mass balance in discontinuous permafrost: the example of disappearing Twelvemile Lake, Yukon Flats, Alaska (USA). *J. Hydrol*. 21, 185-200, http://dx.doi.org/10.1007/s10040-012-0896-5.

Jones, B.M., Grosse, G., Arp, C.D., Jones, M.C., Walter Anthony, K.M. and Romanovsky, V.E. 2011. Modern thermokarst lake dynamics in the continuous permafrost zone, northern Seward Peninsula, Alaska. *Journal of Geophysical Research*. 116, G00M03, http://dx.doi.org/10.1029/2011JG001666.

Jorgenson, M.T., Romanovsky, V.E., Harden, J., Shur, Y., O'Donnell, J., Schurr, E.A.G., Kanevskiy, M. and Marchenko, S. 2010. Resilience and vulnerability of permafrost to climate change. *Canadian Journal of Forestry Research*. 40, 1219-1236. doi:10.1139/X10-060.

Jorgenson, M.T. and Shur, Y.L. 2007. Evolution of lakes and basins in northern Alaska and discussion of the thaw lake cycle. *Journal of Geophysical Research*. 112, F02S17, http://dx.doi.org/10.1029/2006JF000531.

Karlsson, J.M., Bring, A., Peterson, G.D., Gordon, L.J. and Destouni, G. 2011. Opportunities and limitations to detect climate-related regime shifts in inland Arctic ecosystems through eco-hydrological monitoring. *Environmental Research Latters*. 6, http://dx.doi.org/10.1088/1748-9326/6/1/0140159.

Karlson, J.M., Lyon, S.W. and Destouni, G. 2012. Thermokarst lake, hydrological flow and water balance indicators of permafrost change in Western Siberia. *Journal of Hydrology*. 464/465, 459-466, http://dx.doi.org/10.1016/j.jhyrol.2012.07.037.

Kochtubajda, B., Flannigan, M.D., Gyakum, J.R., Stewart, R.E., Logan, K.A., Nguyen, T.V. 2006. Lighting and fires in the Northwest Territories and responses to future climate change. *Arctic*. 59(2), 211-221.

Kokelj, S.V., Zajdlik, B. and Thompson, M.S. 2009. The impacts of thawing permafrost on the chemistry of lakes across the subarctic boreal-tundra transition, Mackenzie Delta region, Canada. *Permafrost and Periglacial Processes*. 20(2), 185-199.

Kokelj, S.V. and Jorgenson, M.T. 2013. Advances in thermokarst research. *Permafrost and Periglacial Processes.* 24, 108-119.

Korosi, J.B., Thienpont, J.R., Pisaric, M.F.J., deMontigny, P.A., Perreault, J., McDonald, J., Simpson, M.J., Armstrong, T., Kokelj, S.V., Smol, J.P.. and Blais, J.M. 2017. Broad-scale lake expansion and flooding inundates essential wood bison habitat. *Nature Communications*. 8 10.1038/ncomms14510.

Kreutzweiser, D.P., Sibley, P.K., Richardson, J.S. and Gordon, A.M. 2012. Introduction and a theoretical basis for using disturbance by forest management activities to sustain aquatic ecosystems. *Freshw. Sci*. 31, 224-231.

Labrecque, S., Lacelle, D., Duguay, C.R., Lauriol, B. and Hawkings, J. 2009. Contemporary (1951-2001) evolution of lakes in the Old Crow Basin, northern Yukon, Canada: remote sensing, numerical modeling, and stable isotope analysis. *Arctic*. 62, 225-238.

Lachniet, M.S., Lawson, D.E., Stephen, H., Sloat, A.R. and Patterson, W.P. 2016. Isotopes of $\delta^{18}O$ and $\delta^{2}H$ reveal climatic forcings on Alaska and Yukon precipitation. *Water Resourc. Res.* 52, 6575-6586.

Larsen, J.N., Anisimov, O.A., Constable, A., Hollowed, A.B., Maynard, N., Prestrud, P., et al. Polar Regions. In: Barros, V.R., Field, C.B., Dokken, D.J., Mastrandrea, M.D., Mach, K.J., Bilir, T.E., et al., editors. Climate change 2014: impacts, adaptation, and vulnerability part b: regional aspects contribution of working group II to the fifth assessment report of the Intergovernmental Panel on Climate Change. Cambridge, United Kingdom and New York, NY, USA. Cambridge University Press. 2014, p. 1567-1612.

Larter, N. C., Sinclair, A. R. E., Ellsworth, T., Nishi, J. and Gates, C. C. 2000. Dynamics of reintroduction in an indigenous large ungulate: the wood bison of northern Canada. *Anim. Conserv*. 4, 299-309.

Leng, M.J. and Anderson, N.J. 2003. Isotopic variation in modern lake waters from western Greenland. *The Holocene*. 13, 605-611.

Lewis, T.L., Lindberg, M.S., Schmutz, J.A. and Bertram, M.R. 2014. Multi-trophic resilience of boreal lake ecosystems to forest fires. *Ecology*. 95, 1253-1263.

Liu, Z. and Wimberly, M.C. 2015. Climatic and landscape influences on fire regimes from 1984 to 2010 in the Western United States. *Plos ONE*. 10(10), 1-20.

MacDonald, L.A., Turner, K.W., Balasubramaniam, A.M., Wolfe, B.B., Hall, R.I. and Sweetman, J.N. 2012. Tracking hydrological responses to a thermokarst lake in the Old Crow Flats (Yukon Territory, Canada) to recent climate variability using aerial photographs and paleolimnological methods. *Hydrological Processes*. 26, 117-129.

MacDonald, L.A., Wolfe, B.B., Turner, K.W., Anderson, L., Arp, C.D., Birks, S.J., Bouchard, F., Edwards, T.W.D., Farquharson, N., Hall, R.I., McDonald, I., Narancic, B., Ouimet, C., Pienitz, R., Tondu, J. and White, H. 2017. A synthesis of thermokarst lake water balance in high-latitude regions of North America from isotope tracers. *Arctic Science*. 3, 118-149.

Mahat, V., Anderson, A. and Silins, U. 2015. Modelling of wildfire impacts on catchment hydrology applied to two case studies. *Hydrol. Process*. 29, 3687-3698.

Marsh, P., Russel, M., Pohl, S., Haywood, H. and Onclin, C. 2009. Changes in thaw lake drainage in the Western Canadian Arctic from 1950 to 2000. *Hydrological Processes*. 23(10), 145-158.

Maric, R. 2003. Coupled isotope-mass balance studies in tundra lakes, Lac de Gras area, N.W.T., Canada. M.Sc. Thesis, University of Waterloo, 145 pp.

Morse, P.D., Wolfe, S.A., Kokelj, S.V. and Gaanderse, A.J.R. 2016. The occurrence and thermal disequilibrium state of permafrost in forest ecotopes of the Great Slave Region, Northwest Territories, Canada. *Permafrost and Periglac. Process*. 27, 145-162.

Moser, K.A., Smol, J.P., Lean, D.R.S. and MacDonald, G.M. 1998. Physical and chemical limnology of northern boreal lakes, Wood Buffalo National Park, northern Alberta and the Northwest Territories, Canada. *Hydrobiologia*. 377(1-3), 25-43.

Mustaphi, C.C. and Pisaric, M.F.J. 2013. Varying influence of climate and aspect as controls of montane forest fire regimes during the late Holocene, south-eastern British Columbia, Canada. *Journal of Biogeography*. 40(10), 1983-1996.

Mustaphi, C.C. and Pisaric, M.F.J. 2014. Holocene climate-fire-vegetation-interactions at a subalpine watershed in southeastern British Columbia, Canada. *Quaternary Research*. 228-239.

Natural Resources Canada (NRCAN). 2017. *Forest Classification*. Retrieved from https://www.nrcan.gc.ca/our-natural-resources/forests-and-forestry/sustainable-forest-management/measuring-and-reporting/forest-classification/13179.

Natural Resources Canada (NRCAN). 2019a. 1980-2018 forest fire perimeters [map]. Canadian National Fire Database (CNFDB). Retrieved online from http://cwfis.cfs.nrcan.gc.ca/ha/nfdb on November 19, 2019.

Natural Resources Canada (NRCAN). 2019b. Forest fires. Retrieved from https://www.nrcan.gc.ca/our-natural-resources/forests-forestry/wildland-fires-insects-disturban/forest-fires/13143 on November 19, 2019.

Ombradovic, M.M. and Sklash, M.G. 1986. An isotopic and geochemical study of the snowmelt runoff in a small arctic watershed. *Hydrol. Process*. 1, 15-30.

Owens, P.N., Giles, T.R., Petticrew, E.L., Leggat, M.S., Moore, R.D.D. and Eaton, B.C. 2013. Muted responses of streamflow and suspended sediment flux in a wildfire-affected watershed. *Geomorphology*. 202, 128-139.

Pausas, J.G. 2015. Evolutionary fire ecology: lessons learned from pines. *Trends in Plant Science*. 5, 318-325.

Payette, S. 2004. Accelerated thawing of subarctic peatland permafrost over the last 50 years. *Geophysical Research Letters*. 31, L18208, http://dx.doi.org/10.1029/2004g1020358.

Pelster, D.E., Burke, J.M. and Prepas, E.E. 2008. Runoff and inorganic nitrogen export from Boreal Plain watersheds six years after wildfire and one year after harvest. *J. Environ. Eng. Sci*. 7, 51-61.

Phillips, D. 1990. The climates of Canada. Ottawa: Supply and Services Canada, 176 p.

Pientz, R., Smol, J.P. and Lean, D.R.S. 1997. Physical and chemical limnology of 24 lakes located between Yellowknife and Contwoyto Lake, Northwest Territories (Canada). *Can. J. Fish. Aquat. Sci*. 54, 347-358. doi: 10.1139/f96-275.

Pienitz, R., Douglas, M.S.V. and Smol, J.P. 2004. Long-term environmental change in Arctic and Antarctic lakes. Published by Springer. Dordrecht, The Netherlands. 272-275.

Piper, L. 2018. Great Slave Lake. In The Canadian Encyclopedia. Retrieved from https://www.thecanadianencyclopedia.ca/en/article/great-slave-lake on November 17, 2019.

Pohl, S., Marsh, P., Onclin, C. and Russell, M. 2009. The summer hydrology of a small upland tundra thaw lake: implications to lake drainage. *Hydrological Processes*. 23, 2536-2546.

Pomeroy, J.W., Fang, X. and Ellis, C. 2012. Sensitivity of snowmelt hydrology in Marmot Creek, Alberta, to forest cover disturbance. *Hydrol. Process*. 26, 1891-1904.

Price, C. and Rind, D. 1994. Possible implications of global climate change on global lightning distributions and frequencies. *Journal of Geophysical Research*. 99, 10823-10831.

Prowse, T.D., Furgal, C., Wrona, F.J. and Reist, J.D. 2009. Implications of climate change for northern Canada: freshwater, marine, and terrestrial ecosystems. *Ambrio*. 35, 282-289.

Quinton, W.L., Hayashi, M. and Chasmer, L.E. 2009. Peatland hydrology of discontinuous permafrost in the Northwest territories: overview and synthesis. *Can. Wat. Res. Journ*. 34(4), 311-328.

Riordan, B., Verbyla, D. and McGuire, A.D. 2006. Shrinking ponds in subarctic Alaska based on 1950-2002 remotely sensed images. *J. Geophys. Res*. 111(G4): G04002. Doi: 10.1029/2005JG000150.

Robinne, F.-N., Hallema, D.W., Bladon, K.D. and Buttle, J.M. 2020. Wildfire impacts on hydrologic ecosystem services in North America high-latitude forests: A scoping review. *Journ. of Hydrol.* 581, 124360.

Roach, J., Griffith, B., Verbyla, D. and Jones, J. 2011. Mechanisms influencing changes in lake area in Alaskan boreal forest. *Global Change Biology*. 17(8), 2567-2583.

Rozanski, K., Araguás-Araguás, L. and Gonfiantini, R. 1993. Isotopic patterns in modern global precipitation. In: Swart, P.K., McKenzie, J., Lohmann, K.C. and Savin, S. (eds.), Climate change in continental isotopic records. *Geophysical Monograph,* 78, American Geophysical Union, Washington, 1-36.

Schindler, D.W., Newbury, R.W., Beaty, K.G., Prokopowich, J., Ruszczynski, T. and Dalton, J.A. 1980. Effects of a windstorm and forest fire on chemical losses from forested watersheds and on the quality of receiving streams. *Can. J. Fish. Aquat. Sci*. 37, 328-334.

Schindler, D.W. and Smol, J.P., 2006. Cumulative effects of climate warming and other human activities on freshwaters of Arctic and subarctic North America. *Ambrio*. 35, 160-168.

Shur, Y.L. and Jorgensen, M.T. 2007. Patterns of permafrost formation and degradation in relation to climate and ecosystems. *Permafrost and Periglacial Processes*. 18, 7-19. doi:10.1002/ppp.582.

Smith, L.C., Sheng, Y., MacDonald, G.M. and Hinzman, L.D. 2005. Disappearing arctic lakes. *Science*. 308(5727), 1429. Doi: 10.1126/science.1108142.

Smol, J.P., Wolfe, A.P., Birks, H.J.B., Douglas, M.S.V., Jones, V.J., Korhola, A., Pienitz, R., Ruhland, K., Sorvari, S., Antoniades, D., Brooks, S.J., Fallu, M.A., Hughes, M., Keatley, B.E., Laing, T.E., Michelutti, N., Nazarova, L., Nyman, M., Paterson, A.M., Perren, B., Quinlan, R., Rautio, M., Saulinier-Talbot, E., Siitonen, S., Solovieva, N. and Weckstrom, J. 2005. Climate-driven regime shifts in the biological communities of Arctic lakes. *Proceedings of the National Academy of Sciences of the United States of America*. 102, 4397-4402.

Spence, C. 2000. The effect of storage on runoff from a headwater subarctic shield basin. *Arctic*. 53. 237-47.

Spence, C., Guan, X.J., Phillips, R., Hedstrom, N., Granger, R. and Reid, B. 2010. Storage dynamics and streamflow in a catchment with a variable contributing area. *Hydrol. Process*. 24, 2209-2221.

Spence, C., Kokelj, S.V., Kokelj, S.A., McKluskie, M. and Hedstrum, N. 2015. Evidence of a change in water chemistry in Canada's subarctic associated with enhanced winter streamflow. *Journal of Geophysical Research: Biogeosciences*. 120, 113-27.

Spence, C., Ali, G., Oswald, C.J. and Wellen, C. 2019. An application of the T-TEL assessment method to evaluate connectivity in a lake-dominated watershed after drought. *Journal of the American Water Resources Association*. 55(2), 1-16.

Springer, J., Ludwig, R., Kienzle, S.W. 2015. Impacts of forest fires and climate variability on the hydrology of an alpine medium sized catchment in the Canadian Rocky Mountains. *Hydrology*. 2, 23-47.

Streletskiy, D.A. et al. 2015. Permafrost hydrology in changing climatic conditions: seasonal variability of stable isotope composition in rivers in discontinuous permafrost. *Environ. Res. Lett*. 10, 095003.

Tank, S.E., Mengistu, S.G., Olefeldt, D., Spence, C., Quinton, W.L. and Dion, N. 2017. Evaluating the effects of fire and landscape on stream water concentrations of carbon, nutrients and ions in watersheds of the Taiga Plains and Taiga Shield, NT [Poster]. GNWT Cumulative Impacts Monitoring Program (CIMP) workshop. Yellowknife, NT. January 2017.

Thompson, D.K., Parisien, M.-A., Morin, J., Millard, K., Larsen, C.P.S. and Simpson, B.N. 2017. Fuel accumulation in a high-frequency boreal wildfire regime: from wetland to upland. *Canadian Journal of Forest Research.* 47(7), 957-964.

Tondu, J.M.E., Turner, K.W., Wolfe, B.B., Hall, R.I., Edwards, T.W.D. and McDonald, I. 2013. Using water isotope tracers to develop the hydrological component of a long-term aquatic ecosystem monitoring program for a northern lake-rich landscape. *Arct. Antarct. Alp. Res.* 45, 594-614.

Turner, K.W., Wolfe, B.B., Edwards, T.W.D. 2010. Characterizing the role of hydrological processes on lake water balances in Old Crow Flats, Yukon Territory, Canada, using water isotope tracers. *Journal of Hydrology*. 386 (2010), 103-117.

Turner, K.W., Wolfe, B.W., Edwards, T.W.D., Lantz, T.C., Hall, R.I. and Larocque, G. 2014. Controls on water balance of shallow thermokarst lakes and their relations with catchment characteristics: a multi-year, landscape-scale assessment based on water isotope tracers and remote sensing in Old Crow Flats, Yukon (Canada). *Glob. Change Biol*. 20(5), 1585-1603. Doi: 10.1111/gcb.12465.

Veraverbeke, S., Rogers, B.M., Goulden, M.L. Jandt, R.R., Miller, C.E., Wiggins, E.B. and Randerson, J.T. 2017. Lightning as a major driver of recent large fire years in North American boreal forests. *Nature Climate Change*. 7(7), 529-534.

Ward, P.C. and Mawdsley, W. 2000. Fire management in the boreal forest of Canada. In: Kasischke, E.S., and Stocks, B.J.,eds. Fire, climate change and carbon cycling in the boreal forest. New York: Springer-Verlag, 66-84.

Weber, M.G. and Stocks, B.J. 1998. Forest fires and sustainability in the boreal forests of *Canada. Ambio*, 27(7), 544-550.

Whelan, R.J. 1995. The ecology of fire. Cambridge Studies in Ecology. Cambridge University Press. Cambridge, United Kingdom.

Winkler, R., Spittlehouse, D.L., Boon, S. and Zimonick, B. 2015. Forest disturbance effects on snow and water yield in interior British Columbia. *Hydrol. Res.* 46, 521-532.

Wolfe, B.B., and Edwards, T.W.D. 1997. Hydrologic control on the oxygen-isotope relation between sediment cellulose and lake water, Taimyr Peninsula, Russia: Implications for the use of surface-sediment calibrations in paleolimnology. *J. Paleolim*. 18, 283-291.

Wolfe, B.B., Karst-Riddoch, T.L., Hall, R.I., Edwards, T.W.D., English, M.C., Palmini, R., McGowan, S., Leavitt, P.R. and Vardy, S.R. 2006. Classification of hydrological regimes of northern floodplain basins (Peace–Athabasca Delta, Canada) from analysis of stable isotopes ($\delta^{18}O$, $\delta^{2}H$) and water chemistry. *Hydr. Proc*. 21(2), 151-168.

Wolfe, B.B. and Turner, K.W. 2008. Near record precipitation causes rapid drainage of Zelma Lake, Old Crow Flats, northern Yukon Territory. *Meridian*. Spring, 7-12.

Wolfe, B.B., Light, E.M., Macrae, M.L., Hall, R.I., Eichel, K., Jasechko, S., White, J., Fishback, L. and Edwards, T.D.W. 2011. Divergent hydrological responses to 20th century climate change in shallow tundra ponds, western Hudson Bay Lowlands. *Geophysical Research Letters*. 38, L23402, http://dx.doi.org/10.1029/2011g1049766.

Wrona, F.J., Prowse, T.D., Reist, J.D., Hobbie, J.E., Levesque, L.M.J. and Vincent, W.F. 2006. Climate change effects on aquatic biota, ecosystem structure and function. *Ambio*. 35, 359-369.

Yi, Y., Brock, B.E., Falcone, M.D., Wolfe, B.B., Edwards, T.W.D. 2008. A coupled isotope tracer method to characterize input water to lakes. *Journal of Hydrology*, 350, 1-13.

Yi, Y. et al. 2012. Isotopic signals (^{18}O, ^{2}H, ^{3}H) of six major rivers draining the pan-Arctic watershed. *Glob. Biogeochem. Cycles*. 26, GB1027.

Yoshikawa, K.S. and Hinzman, L.D. 2003. Shrinking thermokarst ponds and groundwater dynamics in discontinuous permafrost near Council, Alaska. *Permafrost Periglacial Process*. 14(2), 151-160. Doi:10.1002/ppp.451.

Zhang, Y., Olthof, I., Fraser, R. and Wolfe, S.A. 2014. A new approach to mapping permafrost and change incorporating uncertainties in ground conditions and climate projections. *The Cryosphere Discussions*. 8, 1895-1935. DOI:10.5194/tcd-8-1895-2014.

CHAPTER THREE

THE HYDROLOGY OF NORTHERN BOREAL LAKES IN THE TAIGA SHIELD AND PLAINS, NORTHWEST TERRITORIES AND THE IMPORTANCE OF CATCHMENT CHARACTERISTICS IN MEDIATING RESPONSES TO CLIMATE

Abstract

Freshwater lakes are prominent features across northern boreal regions and are sensitive to changing climate conditions. This study aims to broaden our understanding of how variable climate and landscape conditions (including wildfire) influence subarctic lake hydrology in the North Slave Region near Yellowknife, Northwest Territories (NT), Canada. To accomplish this, we integrated analyses of water isotope tracers, lake level changes, local meteorological conditions and remotely sensed catchment data for 20 study lakes located within the Taiga Shield and Taiga Plains ecozones. Lake water isotope data (δ^2H and $\delta^{18}O$) were obtained twice during the ice-free season (May and August) during 2017 and 2018 to identify the relative importance of hydrological controls. Water level was also measured to provide additional insight of lake hydrological conditions. Hydrological data were compared to measured and modelled catchment characteristics, including relative lake/catchment size, slope, land cover and recent wildfire burn area. Overall, precipitation was a major driver of seasonal and interannual lake hydrological change, while evaporation was a major driver of summer water loss. During spring 2017, lake levels increased following typical snowmelt conditions (isotopic dilution) and then progressively decreased by late summer under normal rainfall conditions and a stronger influence from evaporation (isotopic enrichment). During spring 2018, following a drier fall 2017 and below-average winter snowfall, lake levels were relatively low due to less input, before increasing by late summer following heavy summer rainfall, which offset evaporative water loss. Relative catchment size (lake area to catchment area (LA/CA)) was found to be an important driver of

lake hydrology, however, this relationship is complicated by storage deficits associated with variable meteorological conditions. During wet conditions (e.g., freshet and periods of high rainfall), lakes with larger catchments (low LA/CA) had more positive water balances than lakes with high LA/CA. Under drier conditions, lake catchment size and associated fill-and-spill hydrological connectivity was reduced. Lake basins with high LA/CA (particularly those with shallower depth and greater surface area) were more prone to evaporative water loss. Lake hydrological conditions were less influenced by catchment land cover compositions, including burn area. Findings presented here highlight important drivers of lake water balances in subarctic boreal regions, which are sensitive to variable climate conditions.

3.1 Introduction

In subarctic boreal (Taiga) regions of North America, freshwater lakes provide important habitat for abundant plant and wildlife species, and are integral to the culture and lifestyle of local communities. These northern lakes and interconnected streams, rivers and wetlands serve as significant stores of water on the landscape and represent an important component of regional hydrological cycles (Spence et al., 2019). It has been well documented that Arctic and subarctic landscapes are sensitive to accelerating climate warming, and are undergoing increasing ecosystem change (Pientz et al., 2004; Smol et al., 2005; Schindler and Smol, 2006; Prowse et al., 2009; MacDonald et al., 2012; Kokelj and Jorgenson, 2013; Larsen et al., 2014). However, more research is needed to evaluate how variable climate conditions may influence northern boreal lake hydrological processes across regional scales.

Due to access and the wealth of lake systems, the northern Great Slave Lake region (North Slave Region) near Yellowknife, Northwest Territories (NT), Canada represents a prime region for studying climate-driven hydrological change. For example, drought-like conditions during 2013-15 led to an intense wildfire year during 2014 (Darwent, 2016; GNWT, 2016), with potential hydrological implications not yet fully understood. It is important to continue to develop monitoring approaches that can be used to investigate the complex relations among climate, catchment characteristics and lake hydrological conditions over long-term durations.

The response of lakes to variable climate scenarios are highly complex and can depend on the direct impacts of meteorological conditions and the catchment characteristics that are influenced by changing climate and disturbance (Turner et al., 2014). These landscape changes include shrub proliferation, which has been widespread across northern regions (Elmendorf et al., 2012; Myers-Smith et al., 2011; Tape et al., 2016; IPCC, 2014; Wang et al., 2018). For

example, an increasing presence of vegetation (e.g., larger trees and shrubs) within a catchment likely provides a windbreak for deposited snow and promotes snowpack development during the winter months (Essery and Pomeroy, 2004; Brock et al., 2009; Turner et al., 2010 and 2014). Wildfire may also influence the hydrological conditions of boreal lakes, however, a recent screening of relevant studies conducted by Robinne et al. (2020) determined that responses of northern aquatic ecosystems to fire may be highly variable. There still exists substantial gaps in the understanding of freshwater cycling processes, which limits predictive forecasting of flows and storage following climate and burn disturbances (Quinton et al., 2009).

Previous hydrological studies of the Pocket Lake and Baker Creek (Taiga Shield basins) near Yellowknife have provided key insights about northern hydrological processes since 1991 (Gibson, 2019). These studies indicate that hydrological connectivity is a complex driver that plays a crucial role in the watershed dynamics of northern systems, especially for Canadian Shield lakes (Spence and Phillips, 2015; Spence et al. 2019). Hydrological connectivity will vary depending on the seasonal timing of precipitation, lake storage deficits and the intensity of rainfall events (Spence, 2000; Bracken and Croke, 2007; Spence et al., 2019). Recent studies also confirm that seasonal and interannual hydrological variation are common in these northern boreal regions (Gibson, 2019). Increasingly, these studies have emphasized the importance of integrating data about basin heterogeneity, geometry, topology and connectivity (Western et al., 2001; Sidle et al., 2000; Beven and Freer, 2001; Spence, 2001; Wolfe et al., 2014). For example, differences in physiography will result in variable storage capacity within a given basin, with hydrological connectivity among basin elements being a critical factor in determining water storage and downstream flow (Spence and Woo, 2006). These cascading systems increasingly pass runoff downstream as the landscape becomes saturated and storage capacities are exceeded

(Spence and Woo, 2006). This heterogeneous downslope flow through intermitent channels results in the "fill-and-spill" flow mechanism that is charactersitic of Taiga Shield basins where overland flow is dominant (Spence and Woo, 2003). Lake connectivity downstream is likely to increase or decrease depending on whether conditions are wet (e.g., during freshet or greater rainfall) or dry (Gibson and Reid, 2014; Spence et a., 2019). Lakes near the lower end of a basin have been found to be particularly prone to evaporative water loss under drier conditions (Spence et al., 2019). Identifying multi-year periods of drier and low flow conditions is very important for interpreting the hydrological conditions of regional watersheds (Gibson, 2019).

An effective approach used to evaluate water balance interactions across vast hydrological systems includes the monitoring of water isotope tracers (Burgman et al., 1987; Rozanski et al., 1993; Wolfe and Edwards, 1997; Wolfe et al., 2002, 2005 and 2011; Maric, 2003, Gibson 2001 and 2002; Gibson and Edwards, 2002; Gibson et al., 1993 and 2002; Leng and Anderson, 2003; Edwards et al., 2004; Wolfe and Turner, 2008; Yi et al., 2008 and 2012; Birks and Gibson, 2009; Labrecque et al., 2009; Turner et al., 2010 and 2014; Tondu et al., 2013; Anderson et al., 2013; MacDonald et al., 2017). Water isotope studies typically utilize comparison of hydrogen (δ^2H; deuterium) and oxygen ($\delta^{18}O$) isotope compositions to characterize lake and river hydrological conditions. In cold-regions, lake isotope compositions are seasonally influenced by surges of inflow during spring snowmelt, followed by relatively short and drier summers with high evaporation rates (Gibson and Reid, 2014). Long-term isotope records provide valuable information about vapour loss mechanisms (evaporation versus transpiration), effective drainage areas of basins and relative connectivity (Gibson, 2002 and 2019). Further, lake isotope compositions provide quantitative information about relative input of various water contributions (e.g., snowmelt, rain and permafrost thaw) in relation to the

relative influence of evaporation, which is often expressed as evaporation-to-inflow ratio (*E/I*; MacDonald et al., 2017).

In this study, we aim to apply and evaluate similar isotope approaches to assess hydrological conditions across a broader scale in the North Slave Region. Water isotope data are integrated with in-situ lake level monitoring to evaluate the hydrology of 20 lake basins of variable physiographic settings in the Taiga Shield and Plains. Here, we present a two-year lake water isotope dataset from 2017-18, obtained from bi-annual (May and August) sampling during the ice-free season, to capture seasonal and interannual lake water balance responses under variable meteorological conditions. The timing of the study allows for assessment of hydrological changes under relatively average (2017) versus above-average (2018) summer rainfall conditions. The study years reflect a period of general hydrological recovery in the region following an extended dry period from 2013-2016. The study also provides an opportunity to evaluate the utility of using water isotope tracers to capture the hydrological conditions of lakes spanning different catchment characteristics.

We present an inventory of lake catchment characteristics derived from remotely-sensed (Landsat) datasets, and an evaluation of how landscape properties influence lake responses to meteorological conditions. Primary catchment conditions of interest for this study include lake area to catchment area ratio (LA/CA), physiography and land cover characteristics (including recent catchment burn area from 2012-16). The specific objectives of this study include 1) identifying the seasonal and interannual lake hydrological conditions of 20 study lakes across the Taiga Shield and Plains ecozones of the North Slave Region, 2) identifying the relative importance of catchment characteristics (e.g., physiography, land cover and burn area) in determining lake hydrological responses, and 3) determining the effectiveness of our integrated

approach for elucidating the complex relations among climate, catchment and lakes. We hypothesize that lake hydrology will be variable among sites and depend strongly on precipitation, catchment connectivity and land cover properties.

3.2 Study Site

3.2.1 Sampling Locations

The study examined 20 lakes located along the northern extent of Great Slave Lake (North Slave Region), within 300-kilometres (km) of Yellowknife, NT (Figure 3.1). Lakes were categorized based on three main study regions including: 1) Ingraham Trail, 2) Mackenzie Bison Sanctuary and 3) Snare River Basin. Study lakes ranged in size and form, from relatively small upland and lowland lakes (minimum surface area of 1.8 ha) to relatively large, deep lakes (maximum surface area of 3,284 ha). The overall median lake size was 10.9 ha. The lakes were selected to reflect a range of catchment characteristics, including regional location, size, land cover and recent wildfire activity. In total, nine study lakes are situated within catchments having experienced full or partial burn in the recent five-year period prior to study (2012-16).

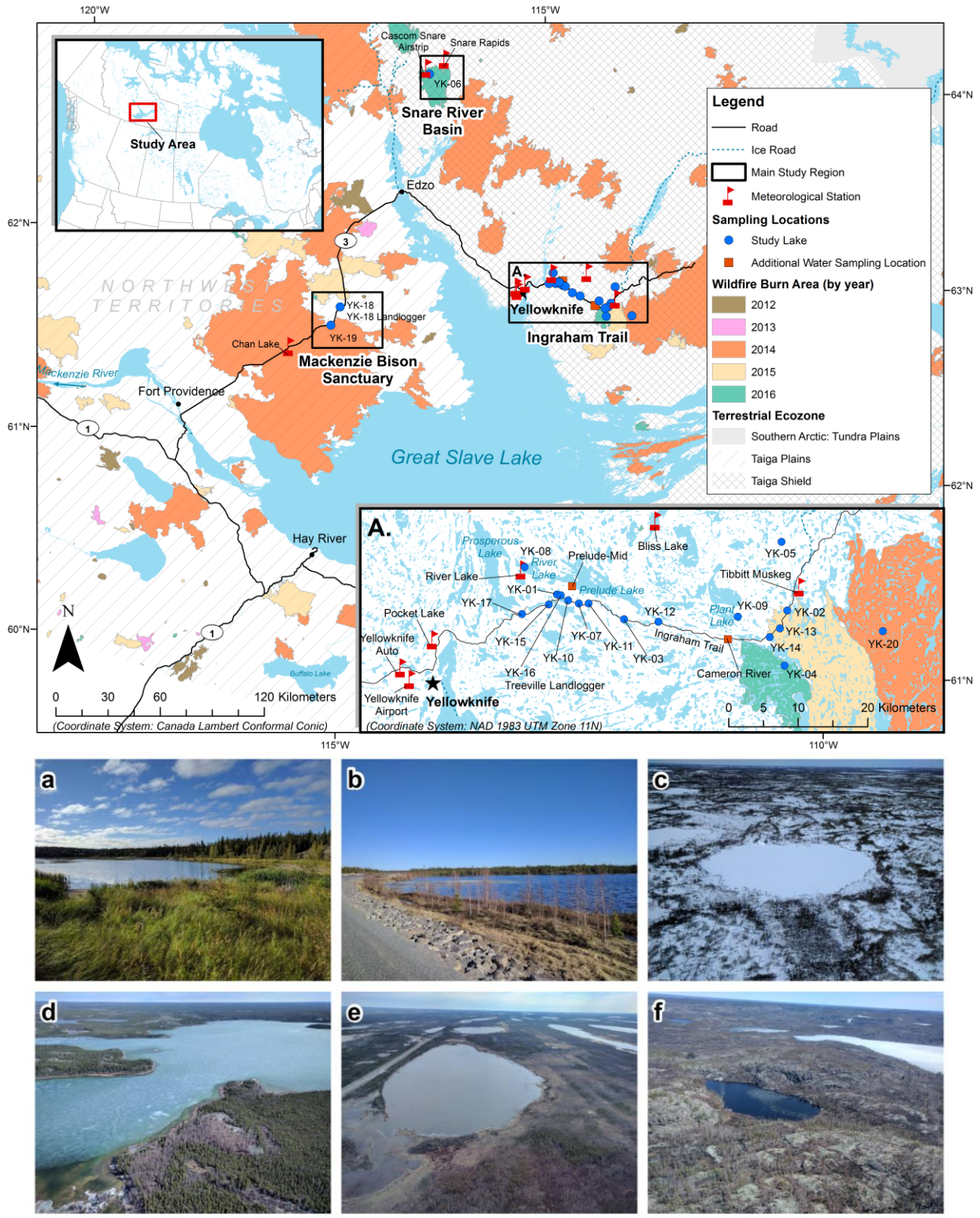

Figure 3.1 – Map of Yellowknife, NT region illustrating main study regions, terrestrial ecozone boundaries, lake sampling locations, meteorological stations and recent wildfire burn areas by year (2012-16; GNWT, 2017). The 2014 year, in particular, represented an extensive and severe wildfire season within the region. Beneath, photographs of select study lakes highlight various physiographic settings and hydrological conditions: (a) small, shallow lake (YK-15) situated along the Ingraham Trail, as photographed during August 2017; (b) small, shallow lake (YK-07)

situated along the Ingraham Trail, as photographed during May 2017; (c) small lake (YK-05) situated in the Ingraham Trail region under frozen conditions, as photographed during April 2018; (d) relatively large/deep lake (River Lake (YK-08)) situated in the Ingraham Trail region, as photographed during May 2018; (e) shallow lake (YK-19) situated in the relatively flat Mackenzie Bison Sanctuary plains region, as photographed during May 2018; and (f) small, relatively deep lake (YK-06) perched within rugged Snare River basin, as photographed during May 2018.

Seventeen study lakes are situated along or near the Ingraham Trail, within a 65-km extent east of Yellowknife in the Taiga Shield ecozone, which is comprised of mixed forests with wetlands, bogs and bare outcrops dominated by lichens and shrubs (Figures 3.1a-d, Ecosystem Classification Group, 2008; Ecological Framework of Canada, 2019b). This includes several larger lake systems such as Prelude Lake (fed by the Cameron River to the east; mean depth = 18 m and maximum depth = 53.3 m; Roberge et al., 1990), River Lake (fed from Prelude Lake to the east; measured centre depth = 23.6 m) and Plant Lake (measured centre depth = 10.2 m). Two study lakes are located along Highway 3 within the Mackenzie Bison Sanctuary of the Taiga Plains ecozone, approximately 110 km west of Yellowknife on the western side of the north arm of Great Slave Lake (Figure 3.1e). This region is comprised of broad extents of nearly level to gently rolling plains with large wetlands, muskeg, small lakes and stream channels (Ecosystem Classification Group, 2007; Ecological Framework of Canada, 2019a). One study lake is situated within the more rugged Snare River basin of the Taiga Shield ecozone, approximately 140 km north of Yellowknife (Figure 3.1f). Important study lake and catchment information are provided in Table 3.1, including key metrics such as median catchment slope, maximum *lake surface area to catchment area (LA/CA)*, *lake surface area to lake centre depth (LA/LD)* and proportion of recent catchment burn (2012-16).

Table 3.1 – Study lake general information.

Study Lake ID	Common Name	Study Region	Coordinates (Decimal Degrees)		Elevation (masl)	Surface Area (ha)	Centre Depth (m)	Catchment Area (ha)	Median Catchment Slope (°)	LA/CA (%)	LA/LD (%)	Catchment Burn 2012-16 (%)
			Northing	Easting								
YK-01	N/A	Ingraham Trail	62.56144	-114.01993	233.2	1.9	N/A	37.3	4.9	5.2	N/A	0
YK-02	N/A	Ingraham Trail	62.52552	-113.37851	268.8	7.7	N/A	701.6	3	1.1	N/A	67.7 (2015)
YK-03	N/A	Ingraham Trail	62.52545	-113.83582	199.6	3	N/A	90.7	4.6	3.3	N/A	0
YK-04	N/A	Ingraham Trail	62.45475	-113.39454	222.5	1.6	1.4 (1)	13.7	7	11.9	1.2	100 (2016)
YK-05	N/A	Ingraham Trail	62.61439	-113.38393	260.2	2.3	1.8 (1)	163.5	2.6	1.4	1.3	0
YK-06	N/A	Snare River Basin	63.40971	-116.12493	295.2	2.1	8.3 (1)	21.4	10.3	9.6	0.3	100 (2016)
YK-07	N/A	Ingraham Trail	62.54850	-113.95967	205.6	14.1	2 (1)	77.3	2.4	18.2	7 .1	0
YK-08	River Lake	Ingraham Trail	62.59863	-114.10643	154.6	497	23.6 (1)	774,527	3.1	0.06	21.0	0.5 (2016) 1.9 (2015) 19.6 (2014) 0.2 (2012)
YK-09	Plant Lake	Ingraham Trail	62.52106	-113.51747	204.3	541	10.2 (1)	2,399	3.1	22.6	53.0	0
YK-10	N/A	Ingraham Trail	62.55314	-113.98939	208.9	81.2	N/A	420.7	2.6	19.3	N/A	0
YK-11	N/A	Ingraham Trail	62.54795	-113.93246	203.6	7.4	N/A	87.5	3.7	8.5	N/A	0
YK-12	Prelude Lake	Ingraham Trail	62.51999	-113.73997	169.6	3,284	53.3 (2)	762,313	3.1	0.4	61.6	0.5 (2016) 1.9 (2015) 19.9 (2014) 0.2 (2012)
YK-13	N/A	Ingraham Trail	62.50314	-113.40197	243.7	1.8	N/A	26.7	3.3	6.6	N/A	100 (2015)
YK-14	N/A	Ingraham Trail	62.49262	-113.43156	215.4	48.6	N/A	173.1	3.5	28.1	N/A	54 (2015)
YK-15	N/A	Ingraham Trail	62.54903	-114.04402	197.9	9.3	N/A	2,730	2.6	0.3	N/A	0
YK-16	Rainbow Lake	Ingraham Trail	62.56008	-114.00924	227.7	17.3	7 (1)	57.9	3.2	29.8	2.5	0
YK-17	N/A	Ingraham Trail	62.53825	-114.11970	186.0	6.4	N/A	31	3.5	20.6	N/A	0
YK-18	N/A	Mackenzie Bison Sanctuary	62.10711	-116.29725	212.0	45.8	1.1 (1)	148.8	2	30.8	42.4	0
YK-19	N/A	Mackenzie Bison Sanctuary	62.00099	-116.33416	202.8	67.4	1.2 (1)	5,711	1.8	1.9	55.7	100 (2014)
YK-20	N/A	Ingraham Trail	62.49185	-113.11520	192.1	12.5	5.4 (1)	74.7	3.2	16.7	2.3	100 (2014)

Note:

"N/A" – Not Available.

Study lake coordinates correlate to water level logger locations, where installed.

Catchment slope determined from median elevation change of 5-m/10-m DEM raster data (ArcticDEM, 2017; GNWT Centre for Geomatics, 2018).

Fire history data obtained from GNWT Centre for Geomatics (2018).

(1) Lake centre depth measured during present study; (2) Prelude Lake centre depth measured during previous study (Roberge et al., 1990).

LA/CA = lake surface area (ha) / lake catchment area (ha); LA/LD = lake surface area (ha) / lake depth (m).

3.2.2 Climate

Regional climate data were obtained from the Yellowknife Airport meteorological station maintained by Environment and Climate Change Canada (ECCC), which represents the most complete and reliable climate information available for the region. The historical (1943-2018) mean annual temperature in Yellowknife is -4.7 degrees Celsius (°C), with a notable warming trend of $R^2 = 0.30$ (with $p = 0.11$; Figure 3.2a; ECCC, 2018a). The mean ice-free season (May-September) temperature during this time period is 11.2 °C. Yellowknife Airport climate normal data (1981-2010) indicate a mean peak summer (July) temperature of 17 °C and a mean winter (October-April) temperature of -15.4 °C (ECCC, 2018b). The average date of last spring frost is May 25, while the average date of first autumn frost is September 18 (ECCC, 2018b). During the years of study, mean annual temperatures were similar, including -3.2 °C during 2017 and -3.1 °C during 2018. Mean ice-free season (May-September) temperatures were 13.3 °C during 2017 (slightly warmer than the long-term mean) and 10.4 °C during 2018 (slightly cooler than the long-term mean).

Mean annual precipitation in Yellowknife (1943-2018) is 270.8 mm ($R^2 = 0.07$ with $p < 0.05$ over this duration; Figure 3.2b). This includes approximately 142.4 mm of rainfall (May-September), as well as 140.1 cm of total annual snowfall (October-April), comprised of 121.7 mm of snow water equivalent (ECCC, 2018a)). Since 1980, mean annual rainfall has been higher (162.6 mm), while mean total annual snowfall accumulation (153.4 cm) and snow water equivalent (123.3 mm) have been generally similar to the longer-term values (ECCC, 2018a). During 2013-2016 leading up to the study, relatively lower precipitation levels occurred in Yellowknife.

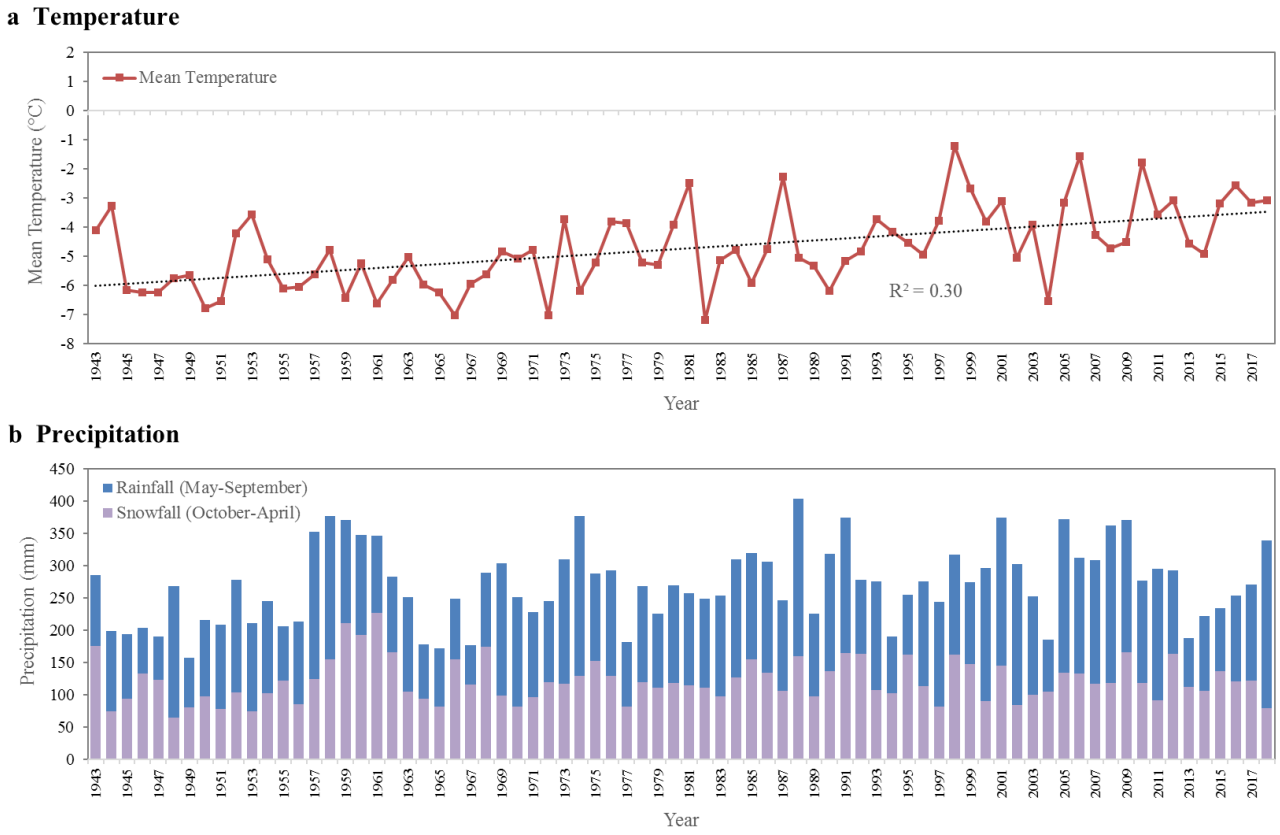

Figure 3.2 – Historical (1943-2018) climate data for Yellowknife as recorded at the Yellowknife Airport met station (ECCC, 2018a), including (a) mean annual temperature, with warming trend ($R^2 = 0.30$) identified, and (b) precipitation ($R^2 = 0.07$), presented as proportion of inferred snowfall (snow water equivalent from previous October-April) and rainfall (May-September). Relatively lower precipitation was experienced leading up to the study during 2013-2016. 2017 saw average snowmelt and summer rainfall; while 2018 saw lower than average snowmelt and heavy summer rainfall.

During the period of study, precipitation was highly variable. Average May-September rainfall (147.1 mm) was recorded during 2017, while more pronounced rainfall (256.4 mm) was recorded during 2018 (Figure 3.2b; ECCC, 2018a). Notably, 2018 saw the most ice-free season rainfall recorded at the Yellowknife Airport since data collection commenced in 1942-43. During winter 2016-17 (October-April) snowfall accumulation was similar to the longer-term averages (162.2 cm, with 122.4 mm of snow water equivalent). In contrast, during winter 2017-18, snowfall accumulation was lower than average (139.2 cm; with 80.1 mm snow water equivalent; ECCC, 2018a). Available regional snow survey data suggest reasonably similar snowfall accumulation patterns within the major study areas during 2016-18 (GNWT, 2019).

3.3 Methodology

3.3.1 Regional Rainfall Analysis

May-September rainfall data from a total of nine meteorological stations located throughout the greater study region (Figure 3.1; Table A3.1, Appendix Three) were obtained and investigated to evaluate the spatial variability of precipitation during the 2017 and 2018 study years.

3.3.2 Lake Water Isotope Sampling and Analyses

To evaluate varying seasonal and interannual hydrological conditions, water samples for isotope analyses were collected, wherever possible, from the 20 study lakes twice during the 2017 and 2018 ice-free seasons (late May and August). Study lakes were primarily accessed by truck and on foot, as well as by helicopter and watercraft for remote lakes. Samples were analysed to determine the composition of water isotopes $\delta^{2}H$ and $\delta^{18}O$. During 2017, lake water samples were collected between 16-18 May and 28-29 August. Additional water sampling of several remote lakes was completed under frozen lake conditions during 23-28 April 2018, with conditions deemed representative of the late-summer 2017 isotopic state. Lake water sampling during 2018 was completed between 20-21 May and 13-17 August.

Lake water samples were typically collected near shore. Samples were also collected near the centre of several remote lakes (accessed by helicopter with floats). It was assumed that lakes were relatively well-mixed (with the potential exception of larger study lakes, including Prelude Lake, River Lake and Plant Lake) with similar isotopic conditions near shore and in the centre. During April 2018, several remote lakes had water samples collected through augured holes in the lake ice. Water samples were collected in 30-ml high-density polyethylene bottles from at least 15 cm below the water surface. Additional precipitation (snowpack) samples for isotope analyses were collected in April 2018. These samples were collected and sealed in plastic bags

and allowed to melt with limited headspace prior to being transferred to 30 ml bottles. Water was prepared for analysis of water isotope values ($\delta^{18}O$ and $\delta^{2}H$) by filtering samples through 0.45 µm cellulose acetate filters into 2-ml glass vials.

Isotope analysis was carried out at the University of Alberta Biological Analytical Service Laboratory (BASL). The laboratory method consisted of laser spectroscopic analysis of liquid water samples for stable hydrogen and oxygen isotopes using a *Picarro Water (H_20) Isotopes Analyzer L2130-I* with a liquid sample precision of 0.025/0.1‰ for $\delta^{18}O/\delta^{2}H$ and drift over 24 hours of 0.2/0.8‰ for $\delta^{18}O/\delta^{2}H$. Using conventional approaches, water isotopic compositions were expressed as δ-values, representing deviations in per mil (‰) from *Vienna Standard Mean Ocean Water (VSMOW)* such that

$$\delta_{sample} = [(R_{sample}/R_{VSMOW}) - 1] \times 10^{3} \quad (1)$$

where R is the $^{18}O/^{16}O$ or $^{2}H/^{1}H$ ratio in sample, and VSMOW (Epstein and Mayeda, 1953; Morrison et al., 2001; refer to Isotope Data, Appendix Two).

Isotope Framework Development

Lake hydrological conditions were evaluated by comparison of $\delta^{2}H$ and $\delta^{18}O$ isotope values and relative to an isotope hydrology framework developed for the North Slave Region near Yellowknife. The framework represents gradients of influence by inflow (snowmelt and rainfall runoff) and outflow (evaporation) hydrological drivers. The strong linear trends exhibited in hydrogen and oxygen isotope compositions of precipitation and surface waters can be traced to the systematic mass-dependent isotopic partitioning of water molecules in the hydrologic cycle (Edwards et al., 2004). Globally, the isotopic composition of precipitation plots along the *Global Meteoric Water Line (GMWL)*, which is described by $\delta^{2}H = 8\ \delta^{18}O + 10$ (Craig, 1961). Where precipitation plots along the GMWL, or *Local Meteoric Water Line (LMWL)*, for a given region is dependent on the trajectory and distillation history of atmospheric moisture contributing

to precipitation. In a region with a seasonal climate, snow typically plots along a more isotopically-depleted section of the GMWL (or LMWL) relative to rain.

The isotope compositions of water from lakes (δ_L) in the region will typically cluster along another trendline known as the *Local Evaporation Line (LEL)*. The slope of the LEL is usually 4-6. The point at which the LEL intersects the LMWL is recognized as the average annual isotopic composition of precipitation (δ_P) for the region. The LEL reflects the isotopic evolution of regional lakes undergoing evaporation (Turner et al., 2010). The LEL deviates from the intersection of the GMWL at δ_P. Water from lakes will plot along and around the LEL during the ice-free season according to lake-specific hydrological conditions. As lakes become isotopically enriched by evaporation through summer, isotope values plot further away from the summer precipitation (rainfall) composition (δ_{Ps}) and up the LEL towards the steady-state composition (δ_{SSL}). Rain isotope composition data were obtained during a previous 2016 study at Pocket Lake near Yellowknife (Gibson, 2017). The derived δ_{SSL} point represents the isotopic composition of a terminal lake basin where evaporative loss is equal to inflow. Lakes experiencing higher proportions of evaporative water loss may plot beyond δ_{SSL}, towards the isotopic composition of a lake nearing complete desiccation (δ^*). Rainfall and snowmelt isotopic compositions typically plot along the GMWL (or LMWL). Inflow of these source waters can offset the relative influence of evaporation, which is represented by lower δ_L values that will typically deviate from the LEL depending on the amount of mixing. Lake water compositions that plot above the LEL indicate more dominant rainfall input/influence, while those that plot below the LEL indicate more dominant snowfall input/influence. The isotope framework is an invaluable tool which provides the basis for calculating additional metrics used to characterize lake hydrological conditions.

Evaporation/Inflow (E/I) Ratios

Lake-specific *evaporation/inflow (E/I)* ratios were calculated to estimate the relative importance of vapour loss relative to input for the 2017-18 sampling periods. Together, E/I ratios and lake water isotopic distributions in δ^2H–$\delta^{18}O$ space provide useful water balance metrics to evaluate the role of specific hydrological processes influencing study lakes (temporally and spatially) in the Yellowknife region. Study lake E/I ratios were calculated for all lake samples using the coupled-isotope tracer approach developed by Yi et al. (2008) and utilized by Turner et al. (2010 and 2014), which is based on the linear resistance model of Craig and Gordon (1965). Lake E/I calculations are based on isotope mass balance calculations described by the equation

$$E/I = (\delta_I - \delta_L) / (\delta_E - \delta_L) \quad (2)$$

where δ_L is the measured isotopic composition of lake water. δ_I is the calculated input water composition to the lake, assumed to plot at the intersection of the GMWL and lake-specific evaporation line (Yi et al., 2008). δ_E is the isotopic composition of the associated evaporating flux, calculated using the Craig and Gordon (1965) model as formulated by Gonfiantini (1986) and Horita and Wesolowski (1994) in decimal notation (refer to Equations and Calculations, Appendix One; and Isotope Data, Appendix Two).

3.3.3 Lake Water Level Monitoring

Lake water levels were monitored for the duration of the study to obtain complementary information about lake hydrological change. *Onset* HOBO U20 series water level loggers (model numbers: U20-001-04 and/or U20L-04 for up to 4 m depth and 0.21 cm accuracy) were installed in 19 of the 20 study lakes (YK-01 through YK-19) between September 2016 and May 2017 (Table A3.2 and Figure A3.1, Appendix Three). HOBO loggers record temperature and pressure data, which are used to calculate water level using a reference logger outside of the lake. The loggers were programmed to collect hourly readings. Water level loggers were initially deployed

among six study lakes (YK-01, YK-02, YK-03, YK-07, River Lake (YK-08), Plant Lake (YK-09)), with data collection commencing on 29 September 2016. An additional 13 lakes (YK-04, YK-05, YK-06, YK-10, YK-11, Prelude Lake (YK-12), YK-13, YK-14, YK-15, YK-16, YK-17, YK-18, YK-19) had water level loggers installed and commenced recording on 19 May 2017. Changes in water level were compared to isotope data to evaluate the relative importance of climate and catchment controls on lake hydrological conditions.

3.3.4 Catchment Delineation

Catchment characteristics were identified using remote sensing approaches to evaluate linkages with lake hydrological conditions. Study lake surface area boundaries were manually traced and delineated at fine resolution (up to 1:1,000) using *Esri ArcMap* software (version 10.5) and the World Imagery basemap layer (DigitalGlobe, 2017; GeoEye, 2017). Study lake delineations were supplemented by field observations and ground/air photographs to improve accuracy. Study lake catchment area boundaries were delineated using available digital elevation model (DEM) data in ArcMap 10.5 software, utilizing the Spatial Analyst extension and *Arc Hydro* plugin (version 10.2). The primary data used for the catchment area modelling were 5-m ArcticDEM raster tiles (ArcticDEM, 2017). Minor coverage gaps of these data in several areas were accounted for using secondary 10-m resolution DEM layers obtained from the GNWT Centre for Geomatics (GNWT Centre for Geomatics, 2018; Table A3.3, Appendix Three).

3.3.5 Catchment Land Cover Classification

Lake catchment land cover classifications were derived using Landsat 8 Operational Land Imager (OLI) satellite images obtained online from the United States Geological Survey (USGS) *EarthExplorer* interface (USGS, 2018; Table A3.4, Appendix Three). The Level 1 Landsat 8 OLI scenes provide 11 bands between 15 to 30-m resolution. Tier 1 (T1) Landsat scenes include Level-1 Precision and Terrain (L1TP) geometrically and radiometrically corrected

data that are inter-calibrated across the different Landsat instruments (USGS, 2018). Low (<10%) to cloud-free Landsat scenes were obtained across the entire lake catchments within the three main study regions. Scenes acquired during July to August were used to capture high plant phenology within the region when vegetation foliage is clearly identifiable for differentiating broad land cover types. Landsat scenes from the 2017 summer season were primarily utilized. Due to excessive cloudiness during 2017 covering the western plains region (containing the YK-18 and YK-19 study lake catchments), a 2018 summer scene was utilized for this region.

Study lake catchment land cover was modelled for the Landsat scenes using the maximum likelihood classification tool (supervised classification) in ArcGIS 10.5 software. The maximum likelihood classification method is a widely accepted approach (Osunmadewa et al., 2018; Pal and Mather, 2003; Sun et al., 2009) that provides useful results when ground-truth data are limited, as was the case in this study. The maximum likelihood classifier evaluates the probability of a given pixel belonging to a particular class (ERDAS, 1999; Benediktsson et al., 1990; Foody, 2002; Otukei et al., 2010; Paola and Schowengerdt, 1995; Richards and Xiuping, 2006). Land cover classification was completed for each of the three main study regions: (1) Ingraham Trail (23,336 square kilometres (km^2)); (2) Mackenzie Bison Sanctuary (368 km^2); and (3) Snare River Basin (112 km^2). The modelling of the Ingraham Trail study region included 17 study lake catchments, including the relatively larger Prelude Lake (YK-12; 7,623 km^2) and River Lake (YK-08; 7,745 km^2) catchments. The Mackenzie Bison Sanctuary study region modelling included the catchments of study lakes YK-18 and YK-19, located west of the north arm of Great Slave Lake. The Snare River basin study region modelling included the catchment of study lake YK-06; the lone lake located in the region northwest of the north arm of Great Slave Lake.

Three broad land cover classes were defined using the Landsat data including *open water*, *mixed vegetation* and *open terrestrial*. This classification scheme was selected since the scope of this study requires a general comparison of land cover type and potential for snowpack retention. For example, it is expected that tall vegetation will have greater snowpack, producing greater meltwater input during spring than open terrestrial surface areas. The open terrestrial land cover class included open bedrock, exposed soil, sand and rock, roads and recently burned land with relatively sparse foliage or scorched/dead vegetation. Classification training data polygons, referred to as regions of interest (ROI), were developed for the Landsat raster datasets using oblique aerial and in-situ photographs of the study sites (Table A3.5, Appendix Three). Approximately 100 ROI (covering 60.3 km^2) were delineated for the Ingraham Trail region, while approximately 50 ROI were delineated for each the Mackenzie Bison Sanctuary (18.9 km^2) and Snare regions (8.7 km^2). Training pixels were evenly distributed across each study region and land cover class. Maximum likelihood classification was run (using 11 bands) to output 30-m resolution land cover classification results for each of the three, respective study regions. An accuracy assessment of the land cover classification modelling was derived using a confusion matrix (or error matrix) and several associated metrics including overall accuracy, user's and producer's accuracy, and kappa statistic (Table A3.6, Appendix Three).

Wildfire Burn Area

The extent of recent wildfire burn areas within study lake catchments (where applicable) were identified to evaluate the potential influence of fire disturbance on lake hydrology. Recent burn history in this study was defined as the five-year period prior to study commencement (2012 to 2016). The areal coverage of wildfire burns during 2012-16 within each study lake catchment were identified using the fire history spatial (polygon) data available from the GNWT

Centre for Geomatics (GNWT Centre for Geomatics, 2017). The intersection of the fire history polygon data and study lake catchment areas were determined in ArcGIS 10.5.

3.4 Results and Interpretation

3.4.1 Regional Rainfall Patterns

Rainfall recorded at nine met stations located throughout the greater study region highlights spatial variability in precipitation conditions during the 2017 and 2018 study years (Cascom, 2018; ECCC, 2018a; GNWT 2018a-e). During the 2017 ice-free season (May-September), rainfall ranged from 107 mm (Bliss Lake met station) to a maximum of 230 mm (Cascom Snare Airstrip met station; Figure 3.3a). The 2017 ice-free season included a notable dry period during 5-26 July, when very little rainfall fell across the Yellowknife region. The Cascom Snare Airstrip met station recorded several heavy rainfall events leading to greater seasonal rainfall compared to the other sites during 2017. The met stations of similar latitude situated east of the north arm of Great Slave Lake and along the Ingraham Trail (including Yellowknife Airport, River Lake, Tibbitt Muskeg, Yellowknife Auto and Bliss Lake) recorded similar rainfall during 2017 (Figure 3.3a). Mean total monthly rainfall data indicate that August (56.8 mm) was the wettest month during 2017, while September (9.2 mm) was the driest (Figure 3.3c).

The 2018 ice-free season experienced greater rainfall. Total May-September rainfall ranged from 135.6 mm (Chan Lake met station) to a maximum of 271.3 mm (River Lake met station; Figure 3.3b). Mean total monthly rainfall data were similar among met stations and indicated that June (101.8 mm) was the wettest month during 2018 while September (7.1 mm) was the driest (Figure 3.3d).

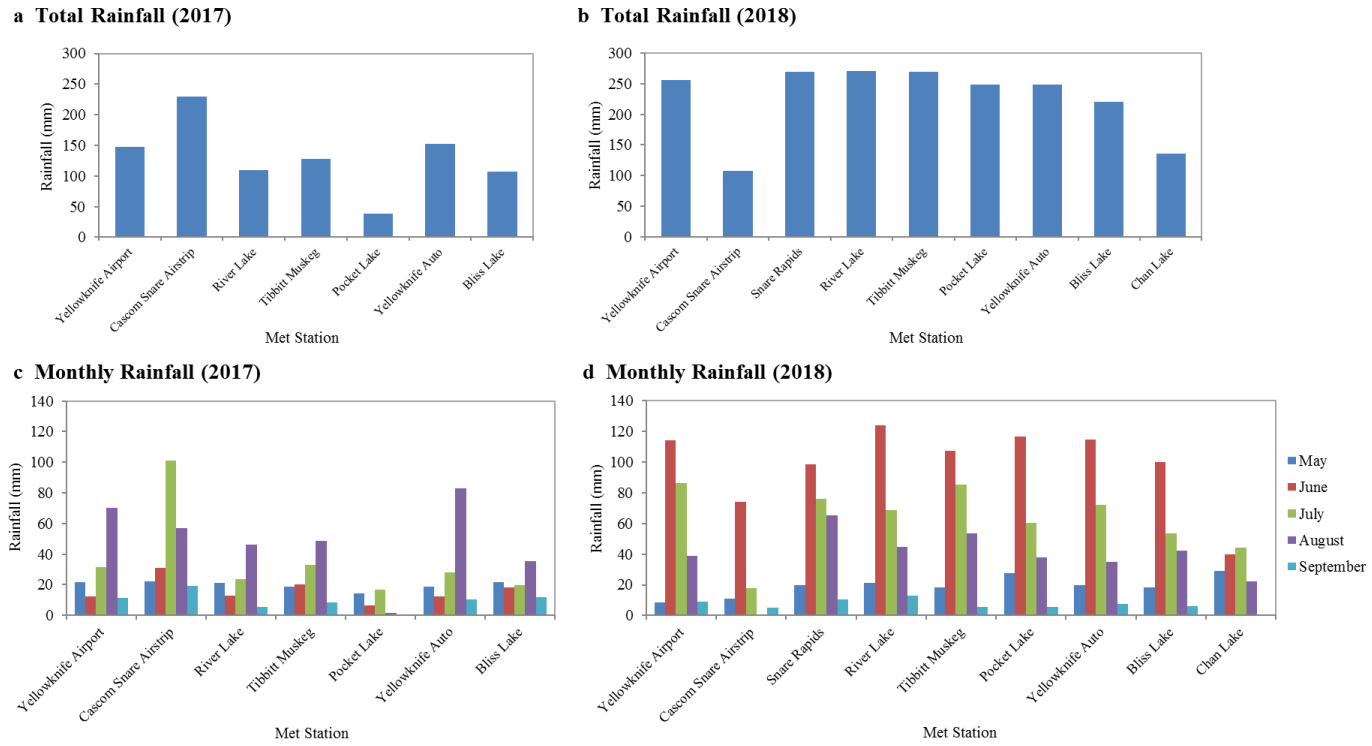

Note:
Pocket Lake met station rain gauge suspected to have malfunctioned during 2017 and, as such, 2017 data were not used in analyses.
No data available for Chan Lake or Snare Rapids met stations during the 2017 ice-free season.
Cascom Snare Airstrip met station experienced several prolonged shutdown periods during 2018 and, as such, 2018 data from this station were not used in analyses.

Figure 3.3 – Graphs illustrating rainfall in the Yellowknife region during the ice-free season as recorded by regional met stations (Cascom, 2018; ECCC, 2018a; GNWT, 2018a-e), including (a) 2017 total rainfall (1 May – 30 September), (b) 2018 total rainfall (1 May – 30 September), (c) 2017 monthly rainfall, and (d) 2018 monthly rainfall. Overall, the 2017 ice-free season saw relatively normal rainfall (147.1 mm) as recorded at the Yellowknife Airport met station; while the 2018 ice-free season saw pronounced rainfall (256.4 mm; ECCC, 2018a).

3.4.2 Lake and Catchment Physical Properties

Study lake surface areas ranged from 1.8 ha (YK-13) to 3,284 ha (Prelude Lake (YK-12)), with a median size of 10.9 ha (Table 3.1). Catchment areas ranged from 13.7 ha (YK-04) to 774,527 ha (River Lake (YK-08)), with a median size of 120 ha. Study lake centre depths (where measured) were found to range from approximately 1 m (YK-04, YK-18 and YK-19) to 53 m (Prelude Lake (YK-12)), with a median of approximately 5.4 m. LA/CA values ranged from approximately 0.06% (River Lake (YK-08)) to 30.8% (YK-18), with a median of 9.1%. LA/LD values ranged from approximately 0.3% (YK-06) to 61.6% (Prelude Lake (YK-12)), with a median of 5%. The median slope of each catchment in degrees (°) was determined using the

slope terrain analysis tool in *QGIS* software (version 2.18.16), through identifying the median elevation change value from the available 5-m/10-m resolution DEM raster data (ArcticDEM, 2017; GNWT Centre for Geomatics, 2018). The median catchment slope for all sites ranged from 1.8 ° (YK-19, located in the relatively flat Mackenzie Bison Sanctuary region of the Taiga Plains) to 10.3 ° (YK-06, located in the hilly Snare River basin of the Taiga Shield), with a median value of 3.1 °.

3.4.3 Isotope Hydrology

Precipitation Isotope Composition

An estimate of the average isotopic composition of precipitation (δ_P) used in the development of the isotope framework were obtained from the *Canadian Network for Isotopes in Precipitation* (CNIP, 2017). The $\delta_{P\ CNIP}$ precipitation compositions for Yellowknife between 1961-1990 were -21.2 for $\delta^{18}O$ and -161.8 for $\delta^{2}H$. These precipitation isotopic composition values, in conjunction with the derived, ice-free season flux-weighted temperature and relative humidity values (2014-18 mean), were used to calculate key parameters across the isotope hydrology framework. Notably, $\delta_{P\ CNIP}$ provides an estimated intersection between the LEL with the LMWL.

The isotopic composition of snow and rainfall samples collected during this study were used to establish the LMWL (refer to Isotope Data, Appendix Two). The isotopic composition of snow samples ranged from -27.4 to -25.1 for $\delta^{18}O$ (-212.3 to -202.5 for $\delta^{2}H$), whereas rain samples ranged from -20.4 to -15.11 for $\delta^{18}O$ (-159.3 to -118.1 for $\delta^{2}H$; Gibson, 2017). Snow and rain isotope compositions show distinct clustering, with snow being isotopically-depleted compared to rain (Figure 3.4a). The snow and rain isotope values deviate slightly from the GMWL. The LMWL was identified as the line extending through the average isotopic compositions of snow (δ_{Snow} = -26.3 for $\delta^{18}O$ and -207.6 for $\delta^{2}H$) and rainfall (δ_{Ps} = -16.9 for

$\delta^{18}O$ and -134 for $\delta^{2}H$). The mean isotopic composition of these precipitation values (weighted by volume as 47% rain and 53% snow, as recorded in Yellowknife during 2014-18; ECCC, 2018a) was -21.9 for $\delta^{18}O$ and -173.1 for $\delta^{2}H$. As such, these values were reasonably similar to the 1961-1990 $\delta_{P\ CNIP}$ values (-21.2 for $\delta^{18}O$ and -161.8 for $\delta^{2}H$), which were used in framework development. The final isotope framework is presented in Figure 3.4b.

Lake Water Isotope Composition

Ice-free season (May and August) isotope compositions of the study lakes during 2017 and 2018 were superimposed on the isotopic framework, illustrating a range of evolution patterns (Figures 3.4c-f; Figures A3.2 and A3.3, Appendix Three). Considering the 2017-18 isotope data from all study lakes, the mean lake LEL slope was found to be 4.12.

During May 2017 following spring freshet, the influence of snowmelt dilution is evident in the lake water compositions (Figure 3.4c). The lakes largely plot low along, and below the LEL towards the mean isotopic composition of snow (δ_{Snow}). By August 2017 (Figure 3.4d), under average seasonal rainfall conditions, the lake compositions move up along the LEL towards the steady-state composition (δ_{SSL}). This highlights the influence of summer evaporation, as the lake waters become increasingly isotopically enriched. Study lake YK-06, the lone lake in the northern Snare River basin, stands out as the lowest value along the LEL during all 2017-18 sampling seasons, suggestive of greater inflow influence during spring and summer as verified by regional precipitation data.

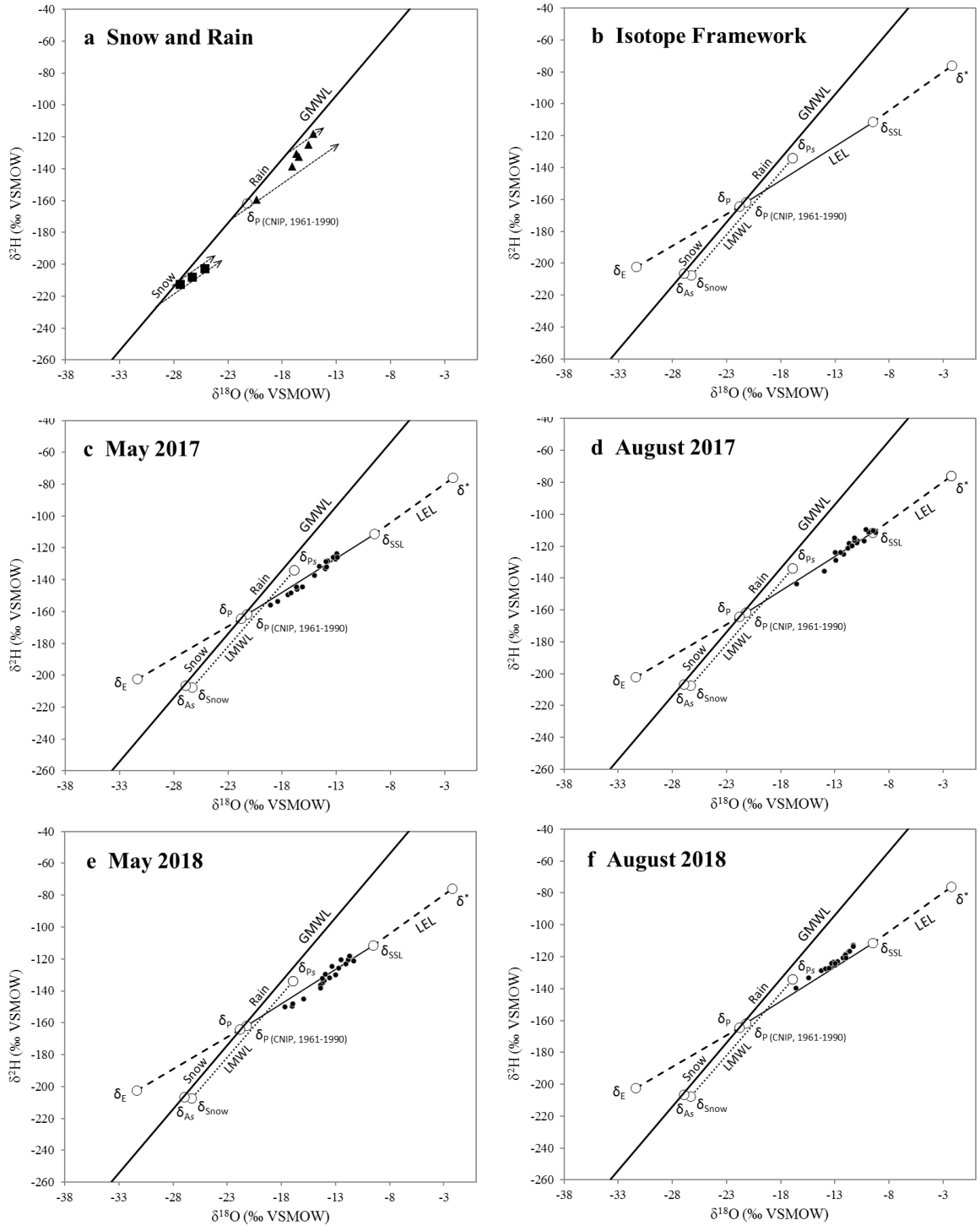

Figure 3.4 – (a) Isotope compositions of snow and rain samples in relation to the Global Meteoric Water Line (GMWL: $\delta^2H = 8\ \delta^{18}O + 10$; Craig, 1961). Dashed arrows identify the general isotopic alteration of rainfall and snowmelt due to evaporation. The "Rain" and "Snow" labels are positioned to identify their approximate ranges along the GMWL. (b) Isotope framework for the Yellowknife region for 2017-18, highlighting the GMWL, Local Meteoric Water Line (LMWL) and Local Evaporation Line (LEL). The LEL extends from the intersection of the GMWL (i.e., the precipitation isotopic composition, δ_{Ps}) to the calculated steady-state composition (δ_{SSL}) and the limiting isotope composition of a lake approaching desiccation (δ^*). The mean isotope composition of the calculated

evaporating flux is also displayed (δ_E). Further figures illustrate isotopic composition of study lakes sampled during 16-18 May 2017 (a), 28-29 August 2017 (b), 20-21 May 2018 (c), and 13-17 August 2018 (d), superimposed on the isotopic framework.

During May 2018 following spring freshet, the influence of snowmelt dilution is again evident in the lake water compositions. The lakes generally plot low along, and below the LEL towards δ_{Snow}; however, not to the extent seen during May 2017 (Figure 3.4e). This is likely the result of less spring snowmelt dilution during 2018 (approximately 139 cm or 80 mm snow water equivalent) compared to 2017 (approximately 162 cm or 122 mm snow water equivalent), in conjunction with the isotopic enrichment established at the end of the 2017 ice-free season. Following wet June and July summer conditions during 2018, August lake isotope values plot above and along the LEL, in contrast to the strong isotopic enrichment experienced during the 2017 ice-free season (Figure 3.4f). The stronger rainfall influence results in lake isotope values clustering above the LEL during August 2018, as the lake water compositions migrate towards the summer precipitation composition (δ_{Ps}). These findings demonstrate the influence of persistent summer rainfall on lake water isotope compositions, with inflow generally offsetting evaporative water loss.

Lake E/I Ratios

Study lake E/I ratios calculated for the 2017-18 ice-free seasons provide a relative measure of lake evaporation relative to inflow. For a terminal lake, E/I values can range from near 0 to >1, with 1 representing steady-state conditions where evaporation equals inflow. Lakes across our study sites are not typically terminal and maintain connectivity with adjacent water bodies and streams when levels are sufficient. Hence, E/I values presented here reflect differences in the relative importance of hydrological controls among lakes.

During 2017 following freshet, May E/I ratios for the study lakes ranged from 0.13 (YK-06) to 0.50 (YK-17), with a median value of 0.35 (Figure 3.5b). By August, E/I ratios increased

for all study lakes, ranging from 0.25 (YK-06) to 1.20 (YK-15), with a median value of 0.66. YK-06 in the Snare River basin received greater rainfall during the 2017 ice-free season, resulting in a stronger inflow influence during August (lower E/I) compared to the other lakes. Overall E/I ratio change from May-August 2017 ranged from 0.08 (Prelude Lake (YK-12)) to 0.84 (YK-15), with a median value of 0.31 and a statistical range of 0.77. The comparatively large Prelude Lake system was shown to change relatively little in E/I from spring to summer 2017 under average seasonal rainfall conditions.

During May 2018 following freshet, study lake E/I ratios were generally higher than during May 2017 as a result of less snowmelt dilution, ranging from 0.20 (YK-06) to 0.78 (YK-17), with a median value of 0.46 (Figure 3.5b). During August 2018, E/I ratios were lower than August 2017 as a result of the increased summer rainfall influence which offset the influence of evaporation. August 2018 E/I ratios ranged from 0.19 (YK-06) to 0.58 (YK-20), with a median value of 0.46 (similar to May 2018). Overall E/I ratio change from May-August 2018 ranged from -0.27 (YK-17) to 0.14 (YK-19), with a median value of -0.02 and a range of 0.41.

In summary, the E/I data indicate that from May-August 2017 under normal rainfall conditions the study lakes largely experienced greater evaporative water loss (increasing summer E/I) compared to May-August 2018, which experienced greater rainfall and inflow. Seasonal E/I change provides a valuable metric for comparison to other hydrological indicators (e.g., water level) and catchment details when identifying controls on lake conditions.

3.4.4 Lake Water Level and E/I Change

Water level loggers installed in 19 of the 20 study lakes provided relative water level change data for a time period spanning the 2016-2018. Measured lake water level closely tracked lake water isotope results (Figure 3.5; Figure A3.4, Appendix Three). Seasonal water level change data from the early to late ice-free season for each study lake are presented in Table 3.2.

Values were standardized to zero at the beginning of the data recording so that comparison of level change could be made among sites. Positive values indicate water level increase, while negative values indicate water level decrease.

Table 3.2 – Summary of study lake water level change (2016-18).

Study Lake/ Logger ID	HOBO Water Level Logger ID	Relative Water Level Change by Date (m)					Date of Final Data Download
		30 September, 2016	19 May, 2017	30 September, 2017	19 May, 2018	August/ September 2018 (Final Download)	
YK-01	10860580	0	0.346	-0.507	0.378	-0.184	14 August, 2018
YK-02	10860574	0	0.271	-0.293	0.421	0.089	13 August, 2018
YK-03	10766050	0	0.254	-0.214	0.295	-0.044	13 August, 2018
YK-04	20081847	N/A	0	-0.079	0.199	0.078	16 August, 2018
YK-05	20081850	N/A	0	-0.367	0.209	0.144	16 August, 2018
YK-06	20075768	N/A	0	0.021	-0.023	0.058	15 August, 2018
YK-07	10766329	0	0.359	-0.247	0.147	0.220	14 August, 2018
River Lake (YK-08)	10860583	0	0.131	-0.082	0.079	0.122	1 September, 2018
Plant Lake (YK-09)	10860576	0	0.161	-0.191	0.061	0.035	15 September, 2018
YK-10	20081846	N/A	0	-0.278	0.142	0.242	14 August, 2018
YK-11	20081852	N/A	0	-0.239	0.274	0.243	13 August, 2018
Prelude Lake (YK-12)	20081857	N/A	0	-0.137	0.074	0.249	13 August, 2018
YK-13	20081848	N/A	0	-0.291	0.262	0.227	13 August, 2018
YK-14	20081853	N/A	0	-0.228	0.172	0.279	13 August, 2018
YK-15	20081851	N/A	0	-0.252	0.196	0.196	14 August, 2018
YK-16	20081858	N/A	0	-0.253	0.204	0.219	14 August, 2018
YK-17	20081941	N/A	0	-0.138	-0.038	0.415	14 August, 2018
YK-18	20081855	N/A	0	-0.127	0.139	-0.100	17 August, 2018
YK-19	20081845	N/A	0	-0.270	0.356	-0.050	17 August, 2018

Note:
"N/A" – Not Available.

With near-average snowmelt dilution during 2017, lake water levels of the initial six study lakes generally increased following the May freshet (Table 3.2). Water level increase ranged from 0.13 m (River Lake (YK-08) to 0.36 m (YK-07) from October 2016-May 2017. During May-September 2017 under relatively normal ice-free season rainfall conditions, all study lakes (with the exception of YK-06 in the Snare River basin) experienced water level drawdown. Seasonal water level change ranged from a decrease of -0.51 m (YK-01) to an

increase of 0.02 m (YK-06). Lake YK-01 exhibits limited inflow retention and appears to pass accumulated flow downstream more actively. The slight water level increase seen in YK-06 (0.02 m) during 2017 was likely the result of relatively greater rainfall in the Snare River basin.

With below-average snowmelt dilution during 2018, lake water levels experienced less of an increase during spring compared to spring 2017 (Table 3.2). Water level change from October 2017-May 2018 ranged from a decrease of -0.04 m (YK-17) to an increase of 0.4 m (YK-02). During the 2018 ice-free season under pronounced rainfall conditions, most study lakes experienced water level increase from May-August/September. The Mackenzie Bison Sanctuary lakes (YK-18 and YK-19) experienced more notable drawdown, however, likely due to less summer rainfall in this region. Water level change from May-August/September 2018 ranged from a decrease of -0.18 m (YK-01) to an increase of 0.42 m (YK-17). Once again, the notable drawdown exhibited by lake YK-01 compared to other study lakes in the region (under heavy rainfall conditions during 2018) provides an indication that it has a low residence time and high lateral outflow. In contrast, the notable increase exhibited by lake YK-17 under heavy rainfall conditions during 2018 suggests that the lake experiences low lateral outflow and has greater storage capacity.

Overall, lake water level and E/I ratio change during the ice-free season are intrinsically linked through an inversely proportional relationship (Figures 3.5a and b). Lake levels generally decrease as E/I increases, and vice versa. However, fill-and-spill mechanisms related to lake storage capacity thresholds and hydrological connectivity along a chain-of-lakes system under variable precipitation conditions add complexity to this relationship and increase variability. In summary, median lake level change showed a decrease of -0.24 m during May-September 2017, increase of 0.20 m during October-May 2018, and an increase of 0.18 m during May-August

2018 (Figure 3.5a). The greatest variability (inter-quartile range; IQR) among lakes was observed from May-September 2017 (0.14 m) under normal rainfall conditions, while the lowest occurred from May-August 2018 (0.20 m) under heavy rainfall conditions. Median lake E/I ratios were found to be 0.35 during May 2017, 0.66 during August 2017, 0.46 during May 2018 and 0.46 during August 2018 (Figure 3.5b). Seasonal variability of lake E/I ratios was the greatest during August 2017 (IQR = 0.19) under normal summer rainfall conditions, and the lowest during August 2018 (IQR = 0.12) under heavy summer rainfall conditions.

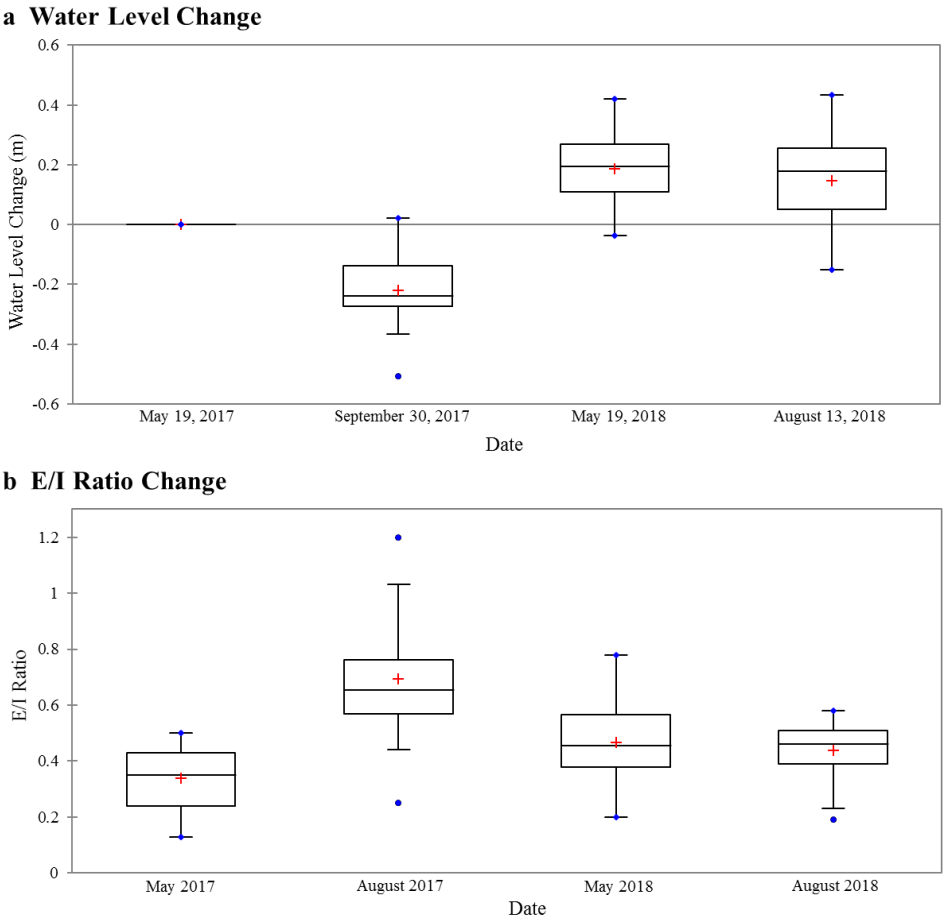

Figure 3.5 – Boxplots illustrating (a) relative study lake water level change and (b) E/I ratio change during the 2017-18 ice-free seasons. As the graphs indicate, E/I ratio change is generally inversely proportional to water level change (broadly linked with high variability). E/I was relatively lower during spring (May 2017) following freshet and snowmelt dilution. By August 2017, E/I ratios of the lakes generally increased under normal/drier conditions, and lake levels decreased from the stronger summer evaporation influence. Following the May 2018 freshet, snowmelt dilution caused lake E/I to fall once again, with lake levels increasing from the greater inflow influence. By August 2018, following an early summer season of relatively heavy rainfall, E/I levels remained fairly steady among the lakes (similar to spring) and were more tightly grouped, as the relatively strong influence of inflow

largely offset the summer evaporation influence. Lake levels, in turn, mostly increased from May-August 2018 under these wetter conditions.

Spring-summer seasonal change in E/I was plotted against water level change in Figure 3.6. This comparison indicated a weak, negative correlation following normal snowmelt dilution and rainfall conditions during 2017 ($R^2 = 0.15$ with $p < 0.05$). On the other hand, the negative relationship was stronger under lighter snowmelt dilution and heavy rainfall conditions during 2018 ($R^2 = 0.38$ with $p < 0.05$). Hence, overall ice-free season E/I ratio change and water level change of the lakes were more strongly linked during the high-rainfall conditions experienced during summer 2018. Hence, precipitation is identified here as a primary driver of lake hydrology.

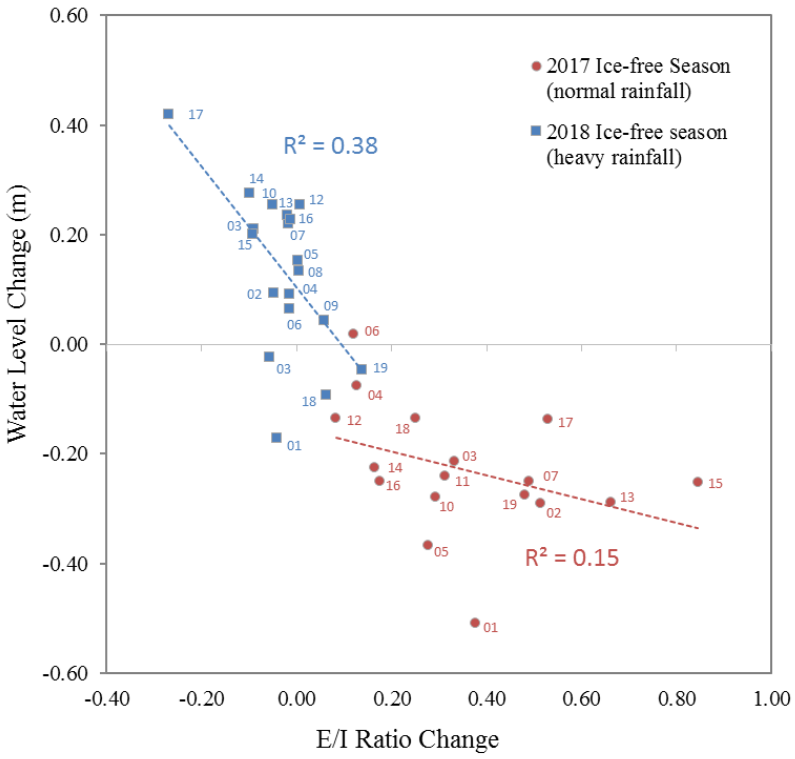

Note:
Water level data ranged from 19 May-30 September for the 2017 ice-free season; and 19 May-13 August /15 September for the 2018 ice-free season (refer to Table 3.2 for further details).
Study lake names abbreviated.

Figure 3.6 – Scatterplot illustrating study lake ice-free season (May-September) overall water level change versus overall EI ratio change for 2017 and 2018. Overall ice-free season E/I ratio and water level change of lakes were found to be more strongly linked under greater rainfall-induced inflow conditions during 2018, when catchment hydrological connections were increasingly active and passing along flow, replenishing the lakes.

Influence of LA/CA on Lake Hydrology

The influence of catchment characteristics on lake hydrological responses were explored by evaluating the relationship between maximum LA/CA and ice-free season lake E/I change. During May 2017 following freshet, lake E/I ratios showed weak, positive correlation to LA/CA ($R^2 = 0.28$ with $p < 0.05$); however, no relationship was detected during August 2017 under normal/drier conditions (Figure 3.7a).

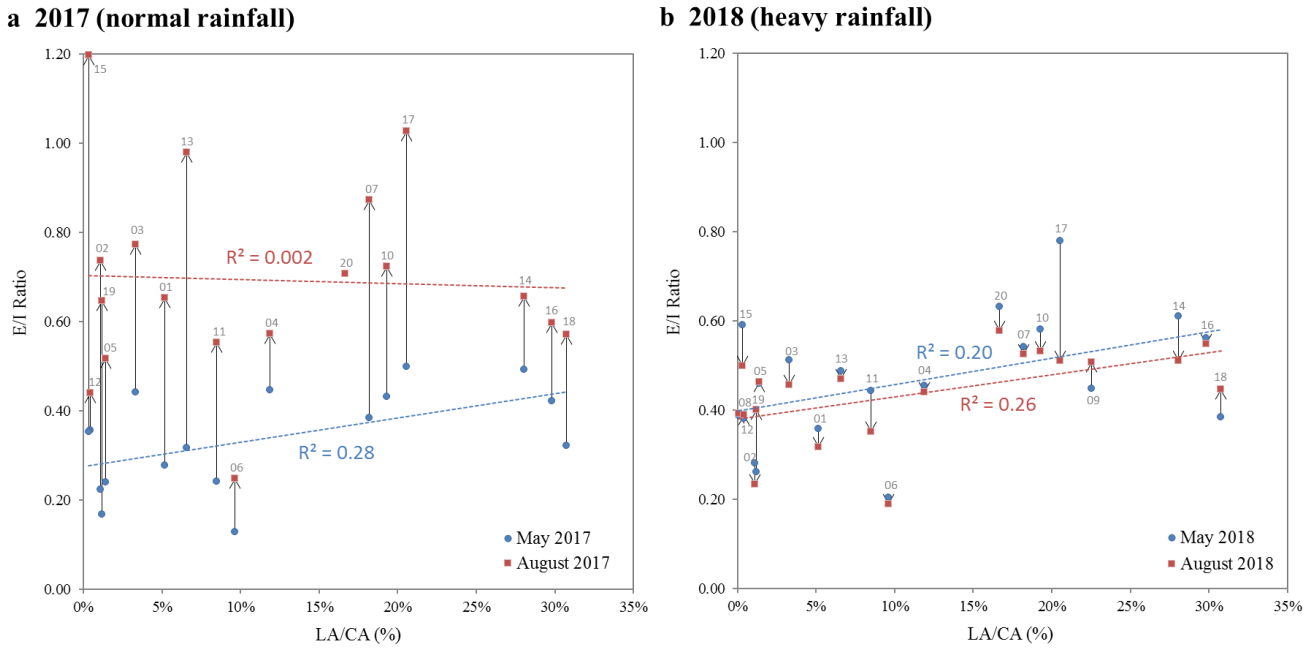

Note:
Study lake names abbreviated.

Figure 3.7 – Scatterplots illustrating study lake ice-free season (May-August) EI ratios versus maximum LA/CA during (a) 2017 and (b) 2018. The comparison yielded a weak, positive correlation during times of increased catchment inflow, including May 2017 ($R^2 = 0.28$ with $p < 0.05$), May 2018 ($R^2 = 0.20$ with $p < 0.05$) and August 2018 ($R^2 = 0.26$ with $p < 0.05$). No correlation was observed under normal/drier summer conditions during August 2017, when catchment hydrological connectivity was diminished.

During May 2018 following freshet, as well as during August 2018 under wet summer conditions, lake E/I ratios showed weak, positive correlations with LA/CA ($R^2 = 0.20$ and 0.26, respectively, with $p < 0.05$; Figure 3.7b). Lakes exhibiting E/I increases during the 2018 ice-free season included YK-17 as well as YK-18 and YK-19 (located in the Mackenzie Bison Sanctuary region), which likely experienced less rainfall during 2018 compared to the other study lakes.

Overall, maximum LA/CA had a notable influence on gauging the response of lake hydrological conditions when conditions were relatively wet during spring (2017 and 2018), and late summer 2018. For instance, lakes with lower LA/CA are likely to be more influenced by inflow through catchment hydrological connections during periods of higher flow (e.g., freshet and periods of heavy rainfall), while lakes with higher LA/CA are likely to be more influenced by evaporation during these time periods. Under drier, low-flow conditions (e.g., summer 2017), the influence of catchment connectivity diminished, and no trend was observed between E/I and maximum LA/CA as catchment water bodies increasingly function as more isolated systems.

Lake Depth and E/I

The relationships between lake depth and E/I were explored for the study lakes of similar size category (surface area < 70 ha) which had approximate centre depth measurements collected in the field, including YK-04, YK-05, YK-06, YK-07, YK-16, YK-18, YK-19 and YK-20. Centre depths among these lakes ranged from approximately 1 m (YK-04, YK-18 and YK-19) to 8 m (YK-06), with a median of 1.9 m. While depths are only point measurements, they provide an indication of the relationship between LA/LD and hydrology.

During the early season (May 2017 and 2018), no relationships were identified when comparing lake E/I to centre depth. During August 2017 (drier), study lake E/I showed weak, negative correlation to approximate centre depth ($R^2 = 0.26$ with $p < 0.05$), while no meaningful correlation ($R^2 = 0.08$) was found during August 2018 (wetter). A comparison of overall ice-free season lake E/I change to centre depth showed weak, negative correlation during both 2017 ($R^2 = 0.31$ with $p < 0.05$) and 2018 ($R^2 = 0.24$ with $p < 0.05$). These findings suggest that the ice-free season evaporation influence is likely to be greater under shallower lake conditions.

Comparison of lake E/I to LA/LD yielded additional insights. During the early season (May), study lake E/I showed weak, negative correlation to LA/LD ($R^2 = 0.10$ with $p < 0.05$

during 2017; and $R^2 = 0.21$ with $p < 0.05$ during 2018). During the late season (August 2017 and 2018), no relationships were found to exist between lake E/I and LA/LD. A comparison of overall ice-free season lake E/I change to LA/LD showed weak, positive correlation during 2017 ($R^2 = 0.31$ with $p = 0.09$) and strong, positive correlation during 2018 ($R^2 = 0.90$ with $p = 0.17$). These findings suggest that spring-summer E/I variability may be greater for lakes with higher LA/LD (larger lake surface area compared to depth), especially under wetter conditions. Shallower lakes with increasing surface area (greater solar heating) can be expected to experience the greatest spring-summer change in hydrological conditions as a result of the stronger influence from evaporation. Subsequent research should include more robust measurements of lake morphology to confirm these observations.

Catchment Slope and E/I

The relationship between median catchment slope (as determined using available 5-m/10-m DEM data) and study lake E/I was evaluated. During summer (August), in particular, study lake E/I ratios showed weak, negative correlation to median catchment slope, with $R^2 = 0.23$ (with $p < 0.05$) during 2017 under normal rainfall conditions and $R^2 = 0.28$ (with $p < 0.05$) during 2018 under heavy rainfall conditions. No correlation was identified during spring ($R^2 = 0.03$ during May 2017 and 0.06 during May 2018). Lakes with catchments having relatively greater median slope included YK-06 (10.3°), followed by YK-04 (4.6°), YK-01 (4.9°) and YK-03 (4.6°). These lakes are more likely to be influenced by hydrological connectivity and associated lateral inflow (landscape runoff of rainfall) during the ice-free season as indicated by relatively lower E/I values. The slope-E/I relationship likely does not exist following the spring freshet since snowmelt inflow is high enough to mask the importance of lateral flow direction and slope. During subsequent months, however, lakes with greater catchment slope are likely to experience increased drainage efficiency into the lake basin following rainfall events.

3.4.5 Catchment Land Cover Classification

Maximum likelihood classification was performed for each lake catchment to identify the spatial distribution of three broad land cover types within the study regions, including open water, mixed vegetation and open terrestrial (e.g., open bedrock, roads and rock face, as well as recently burned land; Figure 3.8). Accuracy of the final land cover classification layer was evaluated using a confusion matrix and associated metrics. Previous studies have noted that acceptable overall accuracy is ≥85% (Anderson, 1976; Thomlinson et al., 1999; Foody, 2002;). The Kappa coefficient, ranging from -1 to 1, with a value closer to 1 indicating strong data agreement and acceptability was also calculated to verify land cover classification accuracy (Cohen, 1960; McHugh, 2012). Overall accuracy scores for the three main study areas were high, including 94.5% for the Ingraham Trail area, 94.7% for the Snare River basin and 100% for the Mackenzie Bison Sanctuary area. Kappa coefficient scores were similarly high at 91.8% for the Ingraham Trail area, 92% for the Snare River basin and 100% for the Mackenzie Bison Sanctuary area. The relatively high accuracy is likely due to the inclusion of only three generalized land cover types.

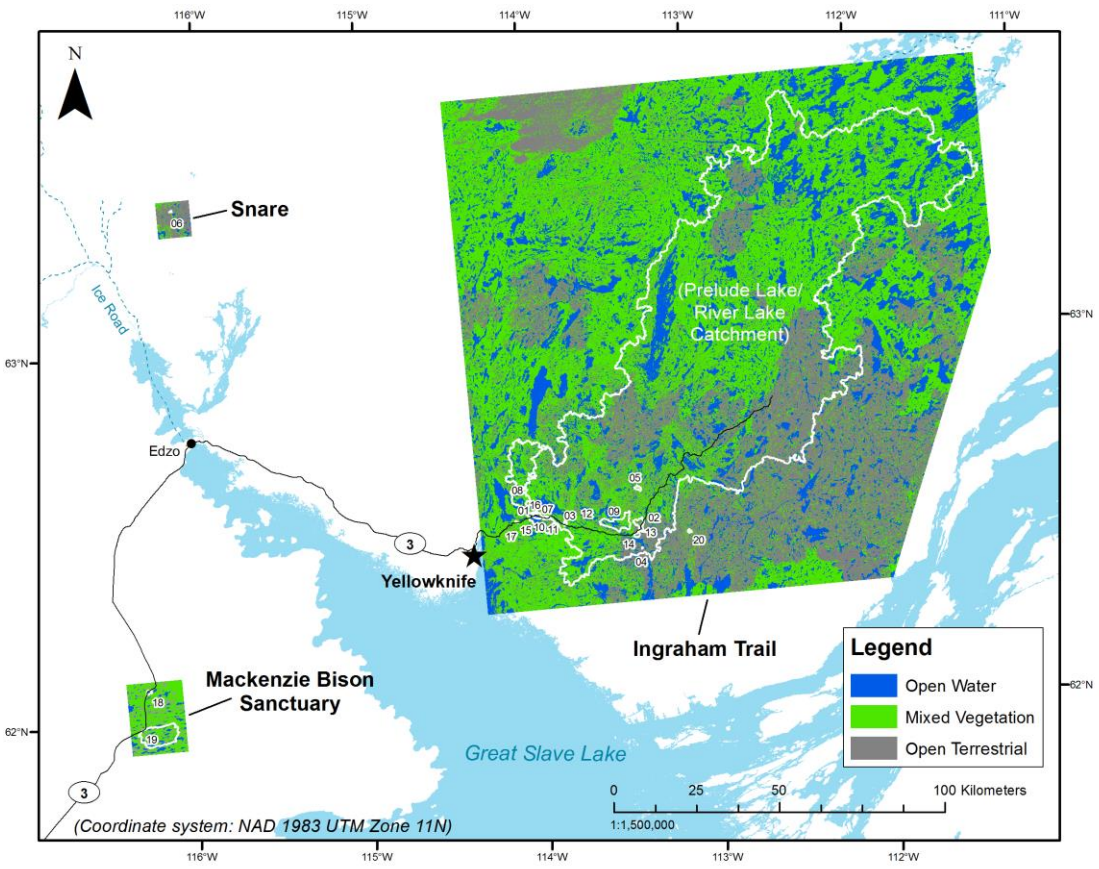

Figure 3.8 – Map illustrating land cover classification modelling for the three main study regions, including (1) Ingraham Trail (23,336 km^2); (2) Mackenzie Bison Sanctuary (368 km^2); and (3) Snare River Basin (112 km^2). Study lake catchments are outlined in white, superimposed over the modelled land cover rasters. Land cover classes include open water, mixed vegetation and open terrestrial.

Land cover classification results for all study lake catchments show median land cover proportions of 16% for open water, 39% for vegetation and 46% for open terrestrial. The study lake catchment with the greatest proportion of open water land cover was YK-18 (29%), while YK-05 had the least (1%; Figure 3.9a). The proportion of vegetation land cover was greatest for the YK-17 catchment (75%), while YK-04 and YK-14 each had the least (5%). Catchments having experienced recent burn (as detailed below) had a relatively higher proportion of open terrestrial land cover. Overall, the proportion of open terrestrial land cover was greatest for the YK-04 catchment (90%) and the least for the YK-17 catchment (5%; Figure 3.9a). An example

of catchment land cover modelling results compared alongside associated satellite imagery and aerial photography is provided in Figure 3.9b.

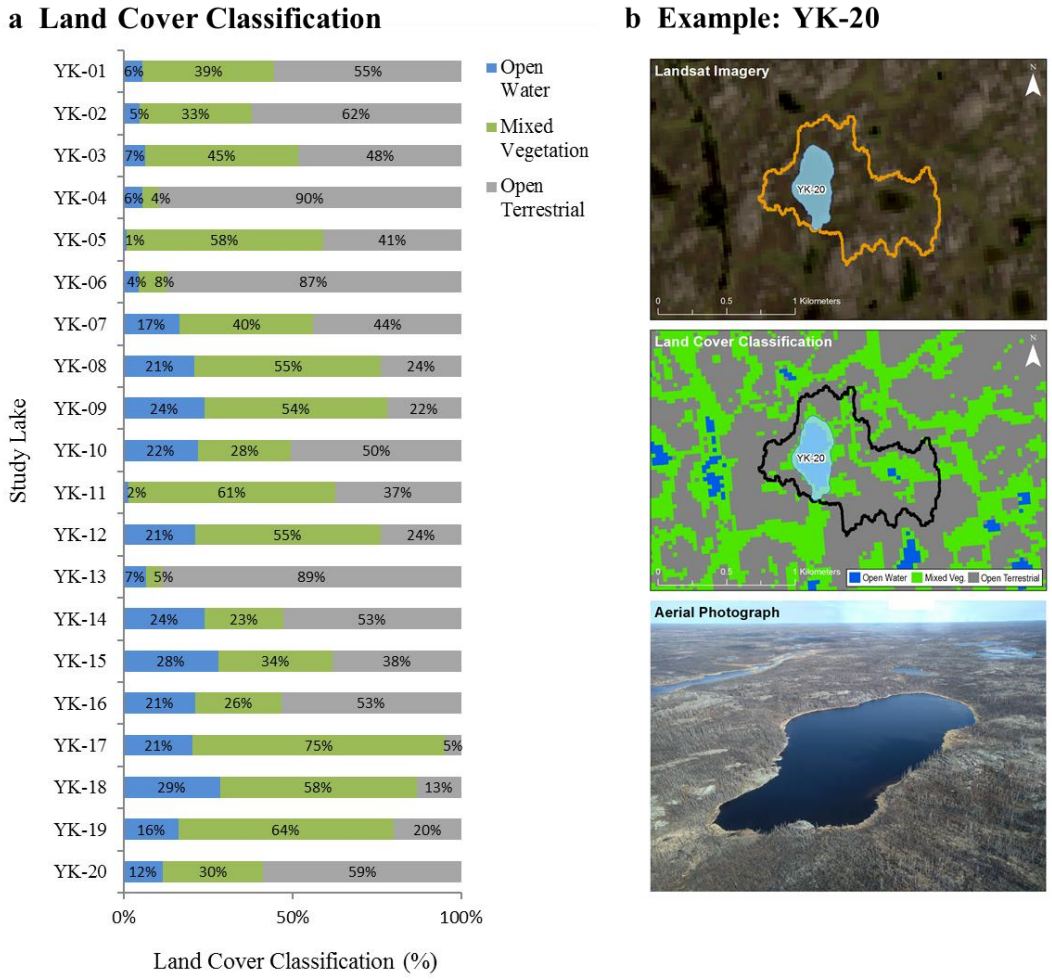

Figure 3.9 – (a) Stacked-column graph illustrating study lake catchment land cover classification results. (b) Study lake YK-20 example, illustrating several catchment views, including Landsat imagery (30-m resolution), land cover classification results and aerial reference photograph (May 2018). YK-20's catchment experienced 100% burn from wildfire during 2014, as is visible in the aerial photograph.

Recent Burn Area

Nine study lake catchments experienced either full or partial burn within the five-year period prior to study (2012-16; Figure 3.1 and Table 3.1). Lake catchments experiencing 100% burn between 2012-16 included: YK-04 (2016), YK-06 (2016), YK-13 (2015), YK-19 (2014) and YK-20 (2014). The catchments of the comparatively large lake systems, including River Lake (YK-08) and Prelude Lake (YK-12), experienced partial burn during multiple years

between 2012-16, but most notably in 2014 when approximately 20% of each of their catchment areas burned. No data related to fire severity was available for these burn records and, as such, this parameter was not assessed.

3.4.6 Influence of Catchment Land Cover on Lake Hydrology

Both qualitative and quantitative analyses were used to evaluate catchment drivers of lake hydrological conditions. Quantitatively, study lake land cover classification proportions were compared to E/I ratio data from 2017-18. A summary of the R^2 value correlations generated from these scatterplot comparisons is provided in Table 3.3.

Table 3.3 – Summary of scatterplot R^2 correlations of E/I ratio versus land cover proportion (2017-18).

Land Cover Class	R^2 Correlation E/I Ratio versus Land Cover Proportion			
	May 2017	**August 2017**	**May 2018**	**August 2018**
Open Water	**0.23**	**0.17**	**0.18**	**0.33**
Mixed Vegetation	-0.01	**0.02**	0.01	0.01
Open Terrestrial	**-0.01**	**-0.07**	-0.10	-0.10

Note:
Bold values indicate statistical significance ($p < 0.05$).
Plant Lake (YK-09) not included in May and August 2017 analyses due to unavailable data.
Study lake YK-20 not included in May 2017 analysis due to unavailable data.
River Lake (YK-08) and Prelude Lake (YK-12) omitted from these analyses to minimize bias, as the seasonal E/I ratios of these comparatively large catchments were found to show little variance.

Among the three main land cover classes assessed, study lake E/I ratios were found to be most correlated with the open water class. E/I ratios showed weak, positive correlation with open water composition during all sampling intervals, including May 2017 ($R^2 = 0.23$), August 2017 ($R^2 = 0.17$), May 2018 ($R^2 = 0.18$) and August 2018 ($R^2 = 0.33$). This correlation was found to strengthen with increasing inflow conditions. The relationship between study lake E/I ratios and open terrestrial land cover composition showed no relationship during most sampling intervals, including August 2017 ($R^2 = 0.07$) as well as May and August 2018 ($R^2 = 0.10$). No correlations were identified when comparing the mixed vegetation composition to E/I ratios (Table 3.3).

3.4.7 Summary of Relations among Lake Hydrology and Catchment Conditions

The influence of catchment physical characteristics on study lake hydrology was further evaluated using a multivariate principal component analysis (PCA) approach, completed in Microsoft XLSTAT using the correlation matrix setting (Pearson correlation coefficient). The PCA utilized five, key catchment variables for eigenvalues, including LA/CA, median slope, open water land cover proportion, mixed vegetation land cover proportion, and open terrestrial land cover proportion (Figure A3.5, Appendix Three). PCA ordination plots showcasing early season and later season hydrological responses during 2017 and 2018 were generated (Figures 3.10a-d). Catchment characteristics spanning Axis 1 (55.16%) and Axis 2 (26.50%) of the PCA explained 81.66% of the variability in the data. Axis 1 separated catchments mainly based on proportion (%) open terrestrial, slope, % open water and % vegetation. For instance, catchments with higher % of open terrestrial surface and greater slope (and lower % open water and vegetation) plotted to the right along Axis 1; while catchments with lower % open terrestrial surface and lower slope (and higher % open water and vegetation) plotted to the left along Axis 1. Axis 2 separated catchments mainly based on proportion (%) open water, % vegetation and LA/CA. Specifically, catchments with higher % of open water and LA/CA (and lower % vegetation) positioned to the top along Axis 2; while catchments with lower % of open water and LA/CA (and higher % vegetation) positioned to the bottom along Axis 2. Key study lake hydrological data incorporated into the plots include E/I in Figures 3.10a-d (relative point colour, with darker shading indicative of increasing magnitude), May-August/September water level change in Figures 3.10c and d (relative point type, with a circle representative of water level increase and a square of water level decrease; as well as relative point size indicative of increasing magnitude). Relative catchment burn area (2012-16) is also indicated in Figures 3.10a-d (thicker point border, with low catchment burn (22%) indicated by light grey, moderate

catchment burn (55-68%) indicated by dark grey, and complete catchment burn (100%) indicated by black).

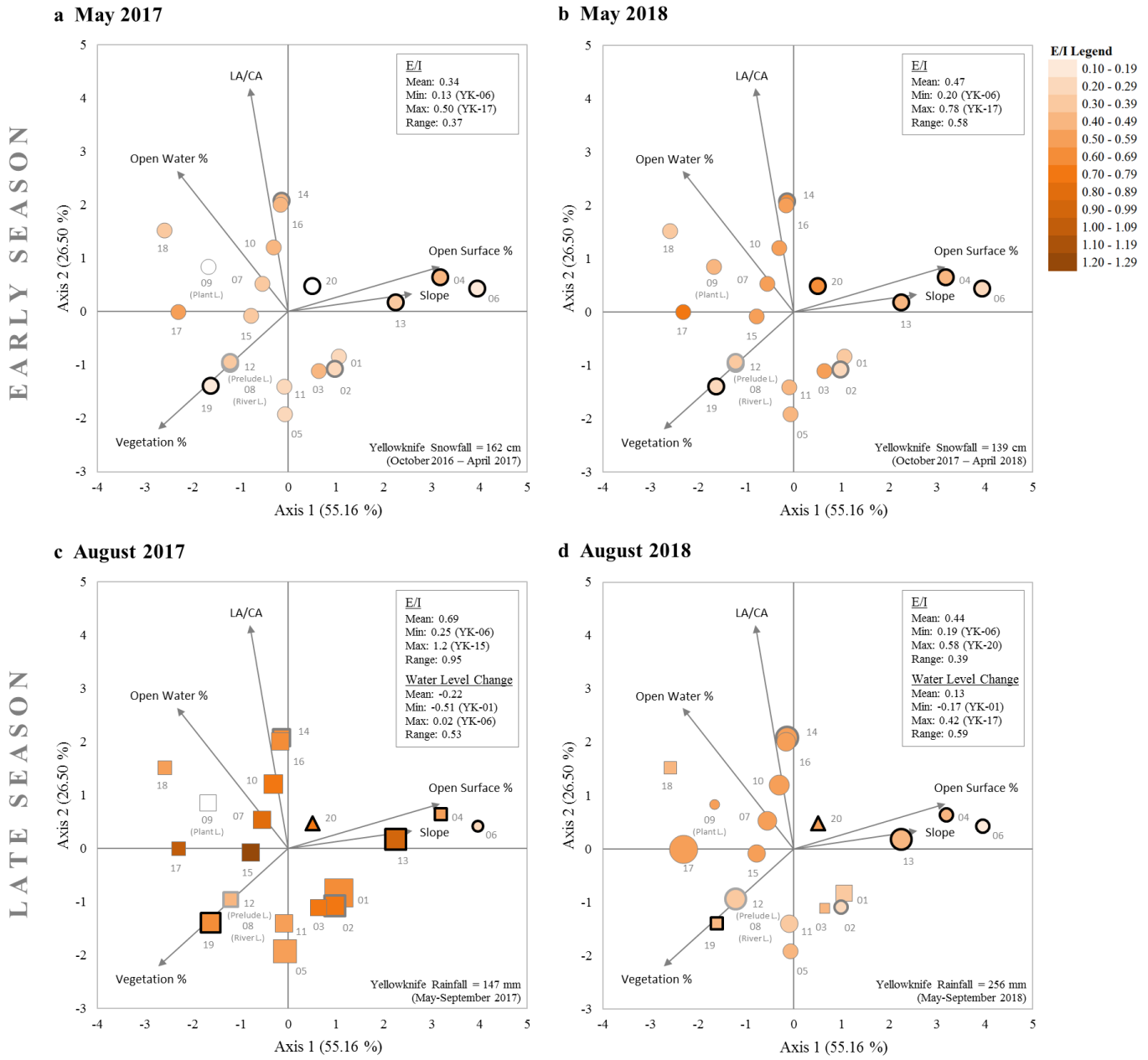

Note:
Study lake names abbreviated.
Water level data presented here covers 19 May – 30 September for the 2017 ice-free season; and 19 May – 13 August/15 September for the 2018 ice-free season (refer to Table 3.2 for further details).

Figure 3.10 – PCA plots illustrating relative distribution of study lakes and hydrological influence from catchment characteristics during the ice-free season, including (a) May 2017 and (b) May 2018 during the early season; and (c) August 2017 and (d) August 2018 during the late season. Lake E/I ratios are indicated by orange/red point colour shading of increasing darkness/magnitude (with hollow points inserted where no E/I data was available). In the late season plots ((c) 2017 under drier conditions and (d) 2018 under wetter conditions), relative May-August/September water level change is indicated by point shape/size. In these plots, circle points indicate water level increase, square

points indicate water level decrease and triangle points (YK-20) indicate no available water level data. Also, point size in these plots (c and d) corresponds to the relative magnitude of ice-free season (spring-summer) water level change, with larger points indicating greater water level increase/decrease and smaller points less increase/decrease. Relative catchment burn area (2012-16) is indicated by a thick point outline, with light grey colouring equal to approximately 22% catchment burn (River Lake (YK-08) and Prelude Lake (YK-12)), dark grey colouring equal to 54-68% burn (YK-02 and YK-14), and black colouring equal to 100% burn (YK-04, YK-06, YK-13, YK-19 and YK-20).

The ordination plots illustrate the hydrological complexity of lakes associated with varying catchment characteristics and precipitation conditions. The early ice-free season (May) data reflect lake hydrological conditions post-freshet when the inflow influence is relatively strong (lower E/I; Figures 3.10a and b). The lakes generally have higher E/I and E/I variability during May 2018 (below-average snowmelt dilution) compared to May 2017 (near-average snowmelt dilution). The hydrology of lakes with relatively larger LA/CA were expected to have lower E/I values during the early season, however, PCA results do not clearly represent this during spring, especially during 2017 (Figures 3.10a and b).

The late ice-free season (August) PCA plots illustrate lake hydrological responses under normal (2017) and heavy (2018) rainfall conditions (Figures 3.10c and d). During the drier 2017 ice-free season, all study lakes (with the exception of YK-06 in the Snare River basin, where heavier rainfall persisted), experienced water level drawdown and increasing E/I. As noted earlier and in the PCA, there was no relationship between LA/CA and E/I during August 2017, which may be explained by reduced hydrological connectivity within increasingly dry and fragmented catchments. The relative importance of evaporation also tends to be stronger for shallower lakes (e.g., YK-07, YK-013, YK-15 and YK – 17). Lakes having catchments with relatively greater proportions of open terrestrial surface (bedrock) and catchment slope (e.g., YK-04, YK-06) experienced less drawdown during 2017 (Figure 3.10c) and may be more influenced by summer rainfall inflow as a result of greater drainage efficiency to the basin (i.e., less groundwater infiltration and catchment storage). Overall, the range of lake E/I values is

higher during the drier 2017 ice-free season compared to the wetter 2018 ice-free season. The predictability of E/I based on catchment characteristics, notably LA/CA, diminishes when dry conditions reduce hydrological connectivity. This suggests that LA/CA values used in this analysis are representative of maximum catchment size when conditions are wet.

During the 2018 ice-free season under wetter conditions, most study lakes experienced water level increases and lower E/I. This was especially true for lakes with higher LA/CA (Figure 3.10d). Study lakes experiencing water level decrease during 2018 included YK-18 and YK-19 owing to less rainfall in the Mackenzie Bison Sanctuary region. Lakes with higher LA/CA generally exhibited higher E/I during 2018 compared to lakes more influenced by hydrological connectivity and inflow from relatively larger catchments. However, lakes with higher LA/CA experienced greater increases in water level as it got wetter through late-summer 2018 (Figure 3.10d; Figure A3.5, Appendix Three). The results also highlight how deeper, stratified lakes with comparatively large catchments (e.g., River Lake (YK-08) and Prelude Lake (YK-12)) exhibit relatively little variation in E/I from spring-summer, and under variable precipitation conditions.

Influence of Catchment Burn on Lake Hydrology

The influence of recent catchment burn area (2012-16) and lake hydrology was variable. Catchments experiencing burn generally have less proportions of vegetation and greater proportions of open terrestrial surface. Some of these lake catchments also exhibit relatively greater catchment slope in Shield environments (e.g., YK-06, YK-04). Study lakes YK-01, YK-11 and YK-13 presented an opportunity to compare lake hydrological conditions of recently burned (2012-16) and unburned catchments. These lakes are located in close proximity to one another (within a 16 km radius) along the Ingraham Trail. YK-13's catchment experienced 100% burn (by area) from wildfires in 2015; while the catchments of YK-01 and YK-11 did not

experience burn between 2012-16. Lakes YK-13, YK-01 and YK-11 have similar physical catchment characteristics, including relatively small lake area (1.8, 1.9 and 7.4 ha, respectively), low LA/CA (6.6, 5.2 and 8.5%, respectively), shallow centre depth (1.5, 2.5 and 1.5 m, respectively), low LA/LD (1.2, 0.8 and 4.9%, respectively), moderate median slope (3.3, 4.9 and 3.7 °, respectively) and relatively low open water composition (7, 6 and 2%, respectively). The burned catchment of YK-13 had relatively low (5%) vegetation land cover compared to (89%) open terrestrial surface. Conversely, the unburned catchments of YK-01 and YK-11 had relatively greater proportions of vegetation land cover (39% and 61%, respectively) and lower proportions of open terrestrial land cover (55% and 37%, respectively).

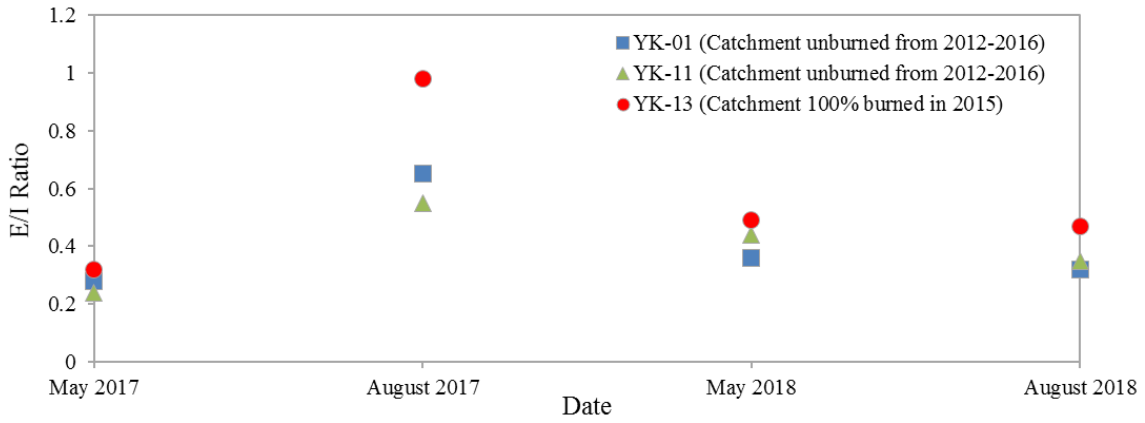

Figure 3.11 – Comparison of 2017-18 E/I ratio change for study lakes within recently (2012-16) burned versus unburned catchments. YK-13's catchment experienced 100% burn (by area) from wildfire during 2015; while the reasonably similar catchments of YK-01 and YK-11 did not experience burn during 2012-16. Slightly higher E/I values were exhibited by YK-13 (burned catchment) potentially due to diminished vegetation from fire and, subsequently, less winter snowpack accumulation and dilution during spring freshet.

With a fully burned catchment (burned during 2015), YK-13 was more influenced by evaporation during all sampling periods, reaching a peak of 0.98 during August 2017 (Figure 3.11). While other catchment factors may help drive higher E/I, the effect may be exacerbated by diminished vegetation from fire and, potentially, less winter snowpack accumulation and dilution during spring freshet.

The influence of catchment physiography and burn proportion on lake hydrology was also demonstrated by YK-04 (Ingraham Trail region), which experienced 100% catchment burn during 2016. The lake has relatively high median catchment slope (7°), high open terrestrial surface catchment composition (90%), shallow depth (1.4 m), moderate LA/CA (11.9%), and is the only water body within its catchment. With a relatively small and open catchment, YK-04 receives less spring snowmelt input, allowing E/I to be greater (i.e., 0.45) during May. Furthermore, the seasonal hydrological variability of YK-04 was relatively low (i.e., May-August E/I change = 0.12, and lake level drawdown = -0.12 m). This indicates that the catchment exhibits greater runoff efficiency, which is facilitated by open terrestrial surface and high catchment slope.

3.5 Discussion

Previous studies have indicated that lakes across northern regions are highly sensitive to ongoing changes in climate (Pientz et al., 2004; Smol et al., 2005; Schindler and Smol, 2006; Prowse et al., 2009; MacDonald et al., 2012; Kokelj and Jorgenson, 2013; Larsen et al., 2014). However, the hydrological responses of lakes to meteorological conditions can be highly individual depending on catchment characteristics (Turner et al., 2014). Studies at Pocket Lake and Baker Creek, NT since 1991 showed that lake hydrological conditions can vary seasonally and interannually (Gibson, 2019). Gibson (2019) demonstrated the importance of using multi-year water isotope records to evaluate hydrological processes. Here, we build on the regional lake water isotope and level records for 2017-19 and provide insight into the complexities of lake hydrological responses to meteorological conditions that are associated with catchment characteristics including catchment size relative to lake area, physiography, and land cover. This study was conducted during a period of general hydrological recovery following a series of

particularly dry years, from approximately 2013-16. The North Slave Region experienced average ice-free season rainfall during 2017 and more pronounced rainfall during 2018 (especially during June-July).

We detected a complex interplay of catchment characteristics that mediate the influence of meteorological conditions on lakes across the Taiga Shield and plains. Overall, precipitation is the main driver of lake water balances in this region (Gibson, 2019). The influence of precipitation on the hydrology of our study lakes was associated with hydrological connectivity, which is consistent with findings from other studies conducted within Shield environments (Spence and Phillips, 2015; Spence et al. 2019). We found that when connectivity among basins was high (i.e., following spring snowmelt or during heavy rainfall in August 2018), the hydrological conditions of individual basins were associated with maximum catchement extent. For instance, lakes with lower LA/CA received greater inflow during wet conditions. As many hydrological systems are connected through a chain-of-lakes, water balances respond according to connectivity among water bodies (Gibson and Reid, 2014; Spence et al., 2010 and 2019). However, during drier or even typical summer conditions (e.g., August 2017), LA/CA (utilizing maxium catchment size) was not a useful predictor of lake hydrological conditions since less hydrological connectivity existed across the catchments. During periods of low rainfall, lake inflow is likely to decrease as hydrological connectivity from the upper catchment is reduced, with greater influence from evaporation (Gibson and Reid, 2014). This occurs when upstream water body levels do not rise above outlet elevation thresholds (Spence et al., 2019). Lakes further down a chain-of-lakes system, near the terminal end, are likely to be most influenced by evaporation and drawdown during drier conditions when hydrological connectivity diminishes (Spence et al., 2019).

Catchment physiography also influences water body storage capacity and downstream flow dynamics within these cascading shield systems (Spence and Woo, 2003 and 2006). As shown here, steeper overall catchment slope may result in greater drainage efficiency and inflow to lake basins during the ice-free season. Findings presented here also suggest that lake surface area relative to centre depth (LA/LD) influences lake hydrology. Shallower lakes with increasing surface area (high LA/LD) are likely to experience the greatest spring-summer change in hydrological conditions due to the stronger evaporative influence. This supports previous research findings of past studies (e.g., Bouchard et al., 2013), where shallow subarctic lakes were found to be more susceptible to evaporative drawdown and desiccation when snowmelt runoff was low.

Previous research of multi-year lake hydrology using isotope tracers has also been conducted in the Slave River Delta (Brock et al., 2009), located south of the present study area. While the lakes in this environment are largely deltaic in form as opposed to Shield lakes, a number of common parallels to the current study can be drawn. Results from Slave River Delta suggest that annual flooding of lakes is not required to maintain positive water balances ($E/I < 1$). However, multiple years without spring flooding will clearly lead to greater cumulative evaporation in deltaic lakes (Brock et al., 2009). Where lake water balances are largely influenced by connectivity with the Slave River or Great Slave Lake, late season E/I ratios were found to be relatively low, with little variation during the three-year monitoring period from 2003-2006 (Brock et al., 2009). This highlights the important role precipitation-driven catchment hydrological connectivity plays in regulating lake water balances across the greater landscape.

In addition to catchment extent, lake size and morphometry were highly variable among study sites, which also influenced hydrological conditions. The two, comparably large study

lakes, Prelude Lake (YK-12) and River Lake (YK-08) have more prominent hydrological drainage inlets/outlets. Most notably, the Cameron River system drains west into Prelude Lake and River Lake. Overall, the presence of hydrologically active drainage outlets from lakes can limit lake level increase during the ice-free season and result in water level drawdown as input decreases (e.g., YK-01; Figure A3.6, Appendix Three). It is important to couple water level measurements with water isotope tracers to capture hydrological drivers within these relatively open-flow systems where residence time is low. For example, E/I is relatively low during periods of high inflow, however, it may remain consistent following a substantial water level decrease. In these lakes, water isotope tracers will only provide an indication of water loss when evaporative water loss outweighs lateral inflow.

Catchment land cover has been found to have a strong control on lake hydrological responses to meteorological conditions in studies in northwestern Canada (e.g., Turner et al., 2014; Balasubramaniam et al., 2015). For example, larger catchments with high proportions of shrub vegetation accumulate greater snowpack, which enhances spring input to lakes, compared to lakes with catchments having high proportions of surface water and smaller vegetation. We found here that the influence of catchment land cover on lake hydrology was less important compared to the spatial extent of catchments and lateral connectivity. However, comparison of a subset of burned and non-burned lake catchments (with similar catchment characteristics) showcased how lakes without vegetation were indeed more susceptible to water level drawdown, especially during August 2017 under average rainfall conditions.

3.6 Conclusions and Recommendations

Subarctic boreal lakes are prominent features across northern regions, with hydrological conditions that will continue to evolve under variable climate scenarios. Here, we build on

previous research in the North Slave Region to broaden our understanding of how variable climate and landscape conditions (including wildfire burn) influence lake hydrology. The study integrated analyses of water isotope tracers, lake level changes, local meteorological conditions and remotely sensed catchment data for 20 study lakes located within the Taiga Shield and Plains regions. The study lakes represented a range of sizes, catchment conditions and geographical locations. The timing of the study presented an opportunity to assess hydrological changes under relatively normal (2017) and more pronounced (2018) summer rainfall conditions. These years reflected a time of general hydrological recovery following an extended dry period during 2013-16. These cycles (spanning several years) of drier conditions followed by hydrological recovery are evident in the longer-term climate record in Yellowknife since 1943.

The study lakes were found to exhibit a strong degree of hydrological variability (i.e., isotope and water level), with conditions dependent on catchment characteristics and seasonal meteorological conditions. Isotope tracers and derived E/I values provided effective indicators of hydrological conditions. However, additional investigation of catchment properties was required to effectively interpret insight of the hydrological drivers.

Overall, precipitation was a major driver of seasonal and interannual lake hydrological change; while evaporation was a major driver of summer water loss. During spring 2017, lake levels increased following typical snowmelt conditions (isotopic dilution) and then progressively decreased by late summer under normal rainfall conditions and a stronger influence from evaporation (isotopic enrichment). During spring 2018, following a drier fall 2017 and below-average winter snowfall, lake levels were relatively lower with greater influence from evaporation, before increasing by late summer following heavy summer rainfall which offset evaporative water loss. LA/CA was found to be an important driver of lake hydrology, especially

when hydrological connectivity was maintained during wetter conditions. Lakes with lower LA/CA were more likely to be influenced by inflow during freshet and periods of high rainfall, when catchment hydrological connections increasingly passed along accumulated flow. Under low-flow conditions, isolated lake basins and those with high LA/CA (particularly with shallower depth and high LA/LD) underwent greater evaporative drawdown. Future analyses will likely capture this relationship more effectively if employing a more dynamic assessment of catchment extents, considering variable catchment extents based on preceding meteorological conditions.

We found that recent catchment burn (within five-years prior to study) may diminish vegetation communities and reduce snowfall accumulation and subsequent snowmelt to lakes. However, the overall influence of catchment burn on lake hydrology was less influential than other important catchment properties including hydrological connectivity and LA/CA.

The findings presented here highlight important relationships among climate, catchment characteristics and lake water balances within subarctic boreal regions. These relations provide an important reference when interpreting drivers of lake hydrology under variable meteorological conditions and must be considered when anticipating future hydrological responses. The integration of hydrological and remote sensing analyses presented here demonstrates an effective and sustainable approach for long-term monitoring of these complex relations across vast northern landscapes. Future studies should expand on the work presented here and include additional lakes to enhance our knowledge of how variable climate conditions and landscapes may impact lake environments on the Taiga Shield and Plains.

REFERENCES

Anderson, J.R. 1976. *A Land Use and Land Cover Classification System for Use with Remote Sensor Data*. US Government Printing Office. Washington, DC, USA. Volume 964.

Anderson, L., Birks, S.J., Rover, J. and Guldager, N. 2013. Controls on recent Alaskan lake changes identified from water isotopes and remote sensing. *Geophys. Res. Lett.* 40, 1-6.

ArcticDEM. 2017. 5-m digital elevation model raster tiles (digital shapefiles), Yellowknife region. Obtained from https://www.pgc.umn.edu/data/arcticdem/ on November 24, 2017.

Balasubramaniam, A.M., Hall, R.I., Wolfe, B.B., Sweetman, J.N. and Wang, X. 2015. Source water inputs and catchment characteristics regulate limnological conditions of shallow subarctic lakes (Old Crow Flats, Yukon, Canada). *Canadian Journal of Fisheries and Aquatic Sciences*. 72 (7), 1058 (15p).

Benediktsson, J.A., Swain, P.H., Ersoy, O.K. 1990. Neural network approaches versus statistical methods in classification of multisource remote sensing data. NASA, United States. 13 p. Available online: https://ntrs.nasa.gov/search.jsp?R=19900062611 (accessed September 10, 2019).

Beven, K. and Freer, J. 2001. A dynamic TOPMODEL. *Hydrol. Proc.* 15, 1993-2011.

Birks, S.J. and Gibson, J.J. 2009. Isotope hydrology research in Canada, 2003-2007. *Can. Water Resour. J*. 34 (2), 163-176.

Bouchard, F., Turner, K.W., MacDonald, L.A., Deakin, C., White, H., Farquharson, N., et al. 2013. Vulnerability of shallow subarctic lakes to evaporate and desiccate when snowmelt runoff is low. *Geophys. Res. Lett*. 40(23), 6112-6117. Doi: 10.1002/2013GL058635.

Bracken, L.J. and Croke, J. 2007. The concept of hydrological connectivity and its contribution to understanding runoff-dominated geomorphic systems. *Hydrological Processes*. 21(13), 1749-63.

Brock, B.E., Yi, Y., Clogg-Wright, K.P., Edwards, T.W.D., Wolfe, B.B., 2009. Multi-year landscape-scale assessment of lakewater balances in the Slave River Delta, NWT, using water isotope tracers. *Journal of Hydrology*, 379, 81-91.

Burgman, J.O., Calles, B. and Westman, F. 1987. Conclusions from a ten year study of oxygen-18 in precipitation and runoff in Swedon. Symposium on Isotope Techniques in Water Resources Development. International Atomic Energy Agency, Vienna, 30 March-3 April 1987, IAEA-SM-299/107.

Canadian Network for Isotopes in Precipitation (CNIP). 2017. Isotopic composition of precipitation in Yellowknife (1961-1990).

Cascom. 2018. Cascom Snare Airstrip met station (63.43, -116.18) rain gauge data (2017-2018). Obtained from Shawne Kokelj, Government of Northwest Territories.

Cohen, J. 1960. A coefficient of agreement for nominal scales. *Educational and Psychological Measurement*. 20, 37-46.

Craig, H. 1961. Isotopic variations in meteoric waters. *Science*, 133, 1702-1703.

Craig, H., Gordon, L.I. 1965. Deuterium and oxygen 18 variations in the ocean and the marine atmosphere. In: Tongiorgi, E. (Ed.), Stable Isotope in Oceanographic Studies and Paleotemperatures. Laboratorio di Geologia Nucleare, Pisa, Italy, pp. 9-130.

Darwent, R., ed. 2016. Fire severest in the 2014 Northwest Territories fires. Nat. Resour. Can., Can. For. Serv., North. For. Cent., Edmonton, AB. *Insights*. No 4b.

DigitalGlobe. 2017. "Imagery" basemap. ESRI ArcMap 10.5 software. May 2017.

Eaton, B.C., Moore, R.D.D., Giles, T.R. 2010b. Forest fire, bank strength and channel instability: the "unusual" response of Fishtrap Creek, British Columbia. *Earth Surf. Process. Landforms*. 35, 1167-1183.

Ecological Framework of Canada. 2019a. Taiga Plains Ecozone. Retrieved from http://ecozones.ca/english/zone/TaigaPlains/land.html.

Ecological Framework of Canada. 2019b. Taiga Shield Ecozone. Retrieved from http://ecozones.ca/english/zone/TaigaShield/land.html.

Ecosystem Classification Group. 2007 (rev. 2009). Ecological regions of the Northwest Territories–Taiga Plains. Department of Environment and Natural Resources, Government of the Northwest Territories, Yellowknife, NT, Canada. viii + 173 pp. + folded insert map.

Ecosystem Classification Group. 2008. Ecological regions of the Northwest Territories–Taiga Shield. Department of Environment and Natural Resources, Government of the Northwest Territories, Yellowknife, NT, Canada. viii + 146 pp. + insert map.

Edwards, T.W.D., Wolfe, B.B., Gibson, J.J., Hammarlund, D. 2004. Use of water isotope tracers in high latitude hydrology and paleohydrology. In: Pienitz, R., Douglas, M.S.V., Smol, J.P. (Eds.), Long-Term Environmental Change in Arctic and Antarctic Lakes. Springer, Dordrecht, The Netherlands, pp. 187-207.

Elmendorf, S.C., Henry, G.H.R., Hollister, R.D., Björk, R.G., Bjorkman, A.D. and Callaghan, T.V. et al. 2012. Global assessment of experimental climate warming on tundra vegetation: heterogeneity over space and time. *Ecol. Lett.*, 15, 164-175.

ERDAS. 1999. ERDAS field guide, revised and expanded, 15th ed. ERDAS, Inc. Atlanta, GA, USA.

Environment and Climate Change Canada (ECCC). 2018a. Historical data (hourly, daily, monthly). Yellowknife, Northwest Territories (station: Yellowknife A; climate identifier: 2204101). Retrieved between 2018 and 2019 from http://climate.weather.gc.ca/historical_data/search_historic_data_e.html.

Environment and Climate Change Canada (ECCC). 2018b. Canadian climate normals 1981-2010 station data. Yellowknife, Northwest Territories (station: Yellowknife A; climate identifier: 2204101). Retrieved in 2018 from https://climate.weather.gc.ca/climate_normals/results_1981_2010_e.html?searchType=stnName&txtStationName=yellowknife&searchMethod=contains&txtCentralLatMin=0&txtCentralLatSec=0&txtCentralLongMin=0&txtCentralLongSec=0&stnID=1706&dispBack=1.

Epstein, S. and Mayeda, T.K. 1953. Variation of O^{18} content of waters from natural sources. *Geochimica et Cosmochimica*. Acta 4, 213-224.

Essery, R., Pomeroy, J. 2004. Vegetation and topographic control of wind-blown snow distributions in distributed and aggregated simulations for an arctic tundra basin. *Journal of Hydrometeorology*, Special Section 5, 735-744.

Foody, G.M. 2002. Status of land cover classification accuracy assessment. *Remote Sens. Environ*. 80, 185-201.

GeoEye. 2017. "Imagery" basemap. ESRI ArcMap 10.5 software. May 2017.

Gibson, J.J., Edwards, T.W.D., Bursey, G.G. and Prowse, T.D. 1993. Estimating evaporation using stable isotopes: quantitative results and sensitivity analysis for two catchments in northern Canada. *Nordic Hydrol*. 24, 79-94.

Gibson, J.J. 2001. Forest-tundra water balance signals traced by isotopic enrichment in lakes. *J. Hydrol.* 251, 1-13.

Gibson, J.J. 2002. Short-term evaporation and water budget comparisons in shallow arctic lakes using non-steady isotope mass balance. *J. Hydrol*. 264, 247-266.

Gibson, J.J. and Edwards, T.W.D. 2002. Regional surface water balance and evaporation-transpiration partitioning from a stable isotope survey of lakes in northern Canada. *Glob. Biogeochem. Cyc*. 16, 10.1029/2001GB001839.

Gibson, J.J., Prepas, E.E. and McEachern, P. 2002. Quantitative comparison of lake throughflow, residency, and catchment runoff using stable isotopes: modelling and results from a regional survey of Boreal lakes. *J. Hydrol*. 262, 128-144.

Gibson, J.J. and Reid, R. 2014. Water balance along a chain of tundra lakes: a 20-year isotopic perspective. *J. Hydrol*. 519, 2148-2164.

Gibson, J.J. 2017. Isotope-based evaporation and water balance studies at Pocket Lake and Baker Creek, 2016: an update on a 26-year assessment. Submitted to Shawne Kokelj, Government of Northwest Territories. InnoTech Alberta. January 23, 2017.

Gibson, J.J. 2019. Isotope-based evaporation and water balance studies at Pocket Lake and Baker Creek: 2019 update. Submitted to Shawne Kokelj, Government of Northwest Territories. InnoTech Alberta. December 31, 2019.

Gonfiantini, R. 1986. Environmental isotopes in lake studies. In: Fritz, P., Fontes, J.C. (Eds.), Handbook of Environmental Isotope Geochemistry, The Terrestrial Environment, vol. 2. Elsevier, New York, pp. 113-168.

Government of Northwest Territories (GNWT). 2016. North Slave hydro system. Yellowknife, NT. 2 pp.

Government of Northwest Territories (GNWT) Centre for Geomatics. 2017. NWT Fire History (digital shapefile), 1965-2016. Obtained from http://www.geomatics.gov.nt.ca/ dldsoptions.aspx on February 24, 2017.

Government of Northwest Territories (GNWT) Centre for Geomatics. 2018. 10-m digital elevation model raster tiles (digital shapefiles), Yellowknife region. Obtained from Colin Avey, GNWT Centre for Geomatics.

Government of Northwest Territories (GNWT), Department of Environment and Natural Resources (ENR), Forest Management Division. 2018a. Yellowknife Auto met station (62.48, -114.46) rain gauge data (2017-2018). Obtained from Shawne Kokelj, Government of Northwest Territories.

Government of Northwest Territories (GNWT), Department of Environment and Natural Resources (ENR), Forest Management Division. 2018b. Bliss Lake met station (62.65, -113.73) rain gauge data (2017-2018). Obtained from Shawne Kokelj, Government of Northwest Territories.

Government of Northwest Territories (GNWT), Department of Environment and Natural Resources (ENR), Water Resources Division. 2018a. Snare rapids met station (63.51, -116.01) rain gauge data (2018). Obtained from Shawne Kokelj, Government of Northwest Territories.

Government of Northwest Territories (GNWT), Department of Environment and Natural Resources (ENR), Water Resources Division. 2018b. River Lake met station (62.60, -114.12) rain gauge data (2017-2018). Obtained from Shawne Kokelj, Government of Northwest Territories.

Government of Northwest Territories (GNWT), Department of Environment and Natural Resources (ENR), Water Resources Division. 2018c. Tibbitt Muskeg met station (62.56, -113.34) rain gauge data (2017-2018). Obtained from Shawne Kokelj, Government of Northwest Territories.

Government of Northwest Territories (GNWT), Department of Environment and Natural Resources (ENR), Water Resources Division. 2018d. Pocket Lake met station (62.51, -114.37) rain gauge data (2017-2018). Obtained from Shawne Kokelj, Government of Northwest Territories.

Government of Northwest Territories (GNWT), Department of Infrastructure. 2018e. Chan Lake met station (61.50, -116.42) rain gauge data (2018). Obtained from Shawne Kokelj, Government of Northwest Territories.

Government of Northwest Territories (GNWT), Department of Environment and Natural Resources (ENR). 2019. Snow surveys. Retrieved in March 2019 from https://www.enr.gov.nt.ca/en/services/snow-surveys/summary/231/2019.

Horita, J., Wesolowski, D. 1994. Liquid-vapour fractionation of oxygen and hydrogen isotopes of water from the freezing to the critical temperature. *Geochimica et Cosmochimica Acta*, 58, 3425-3437.

Intergovernmental Panel on Climate Change (IPCC). 2014. Climate policy. IPCC lessons from Berlin. *Science* (New York, N.Y.), 345, 34 pp.

Kokelj, S.V. and Jorgenson, M.T. 2013. Advances in thermokarst research. *Permafrost and Periglacial Processes*. 24, 108-119.

Labrecque, S., Lacelle, D., Duguay, C.R., Lauriol, B. and Hawkings, J. 2009. Contemporary (1951-2001) evolution of lakes in the Old Crow Basin, northern Yukon, Canada: remote sensing, numerical modeling, and stable isotope analysis. *Arctic*. 62, 225-238.

Larsen, J.N., Anisimov, O.A., Constable, A., Hollowed, A.B., Maynard, N., Prestrud, P., et al. Polar Regions. In: Barros, V.R., Field, C.B., Dokken, D.J., Mastrandrea, M.D., Mach, K.J., Bilir, T.E., et al., editors. Climate change 2014: impacts, adaptation, and vulnerability part b: regional aspects contribution of working group II to the fifth assessment report of the Intergovernmental Panel on Climate Change. Cambridge, United Kingdom and New York, NY, USA. Cambridge University Press. 2014, p. 1567-1612.

Leng, M.J. and Anderson, N.J. 2003. Isotopic variation in modern lake waters from western Greenland. *The Holocene*. 13, 605-611.

MacDonald, L.A., Turner, K.W., Balasubramaniam, A.M., Wolfe, B.B., Hall, R.I. and Sweetman, J.N. 2012. Tracking hydrological responses to a thermokarst lake in the Old Crow Flats (Yukon Territory, Canada) to recent climate variability using aerial photographs and paleolimnological methods. *Hydrological Processes*. 26, 117-129.

MacDonald, L.A., Wolfe, B.B., Turner, K.W., Anderson, L., Arp, C.D., Birks, S.J., Bouchard, F., Edwards, T.W.D., Farquharson, N., Hall, R.I., McDonald, I., Narancic, B., Ouimet, C., Pienitz, R., Tondu, J. and White, H. 2017. A synthesis of thermokarst lake water balance in high-latitude regions of North America from isotope tracers. *Arctic Science*. 3, 118-149.

Maric, R. 2003. Coupled isotope-mass balance studies in tundra lakes, Lac de Gras area, N.W.T., Canada. M.Sc. Thesis, University of Waterloo, 145 pp.

McHugh M. L. 2012. Interrater reliability: the kappa statistic. *Biochemia medica.* 22(3), 276-282.

Morrison, J., Brockwell, T., Merren, T., Fourel, F. and Phillips, A.M. 2001. A new on-line method for high precision stable-hydrogen isotopic analyses on nanolitre water samples. *Analytical Chemistry*. 73, 3570-3575.

Myers-Smith, I.H., Forbes, B.C., Wilmking, M., Hallinger, M., Lantz, T., Blok, D. and Sass, U.G.W. 2011. Shrub expansion in tundra ecosystems: dynamics, impacts and research priorities. *Env. Res. Let.*, 6, 15 pp.

Onset Computer Corporation. 2008. Barometric compensation assistant. White paper series. http://www.onsetcomp.com.

Osunmadewa, B.A., Gebrehiwot, W.Z., Csaplovics, E., Adeofun, O.C. 2018. Spatio-temporal monitoring of vegetation phenology in the dry sub-humid region of Nigeria using time series of AVHRR NDVI and TAMSAT datasets. *Open Geosci*., 10, 1-11.

Otukei, J.R., Blaschke, T. 2010. Land cover change assessment using decision trees, support vector machines and maximum likelihood classification algorithms. *Int. J. Appl. Earth Obs. Geoinf.* 12, S27-S31.

Pal, M., Mather, P.M. 2003. An assessment of the effectiveness of decision tree methods for land cover classification. *Remote Sens. Environ*. 86, 554-565.

Paola, J.D. and Schowengerdt, R.A. 1995. A detailed comparison of back propagation neural network and maximum-likelihood classifiers for urban land use classification. *IEEE Trans. Geosci. Remote Sens.* 33, 981-996.

Pienitz, R., Douglas, M.S.V. and Smol, J.P. 2004. Long-term environmental change in Arctic and Antarctic lakes. Published by Springer. Dordrecht, The Netherlands. 272-275.

Prowse, T.D., Furgal, C., Wrona, F.J. and Reist, J.D. 2009. Implications of climate change for northern Canada: freshwater, marine, and terrestrial ecosystems. *Ambrio*. 35, 282-289.

Quinton, W.L., Hayashi, M. and Chasmer, L.E. 2009. Peatland hydrology of discontinuous permafrost in the Northwest territories: overview and synthesis. *Can. Wat. Res. Journ*. 34(4), 311-328.

Richards, J.A.. Xiuping, J. 2006. Remote sensing digital image analysis. Springer, Berlin, Heidelberg. 1-439 p. Available online: https://link.springer.com/book/10.1007/3-540-29711-1#toc (accessed September 10, 2019).

Roberge, M.M., J.B. Dunn, M.R. Falk. 1990. Catch, effort and biological data of fish, in particular lake trout (*Salvelinus namaycush*), from Prelude and Prosperous lakes, Northwest Territories, 1973 and 1979. Can. Dat. Rep. Fish. *Aquat. Sci*. 817: v + 52 p.

Robinne, F.-N., Hallema, D.W., Bladon, K.D. and Buttle, J.M. 2020. Wildfire impacts on hydrologic ecosystem services in North America high-latitude forests: A scoping review. *Journ. of Hydrol.* 581, 124360.

Rozanski, K., Araguás-Araguás, L. and Gonfiantini, R. 1993. Isotopic patterns in modern global precipitation. In: Swart, P.K., McKenzie, J., Lohmann, K.C. and Savin, S. (eds.), Climate change in continental isotopic records. *Geophysical Monograph,* 78, American Geophysical Union, Washington, 1-36.

Schindler, D.W. and Smol, J.P., 2006. Cumulative effects of climate warming and other human activities on freshwaters of Arctic and subarctic North America. *Ambrio*. 35, 160-168.

Sidle, R.C., Tsuboyama, Y., Noguchi, S., Hosoda, I., Fukieda, M. and Shimizu, T. 2000. Stormflow generation in steep forested headwaters: a linked hydrogeomorphic paradigm. *Hydrol. Proc.* 14, 369-385.

Smol, J.P., Wolfe, A.P., Birks, H.J.B., Douglas, M.S.V., Jones, V.J., Korhola, A., Pienitz, R., Ruhland, K., Sorvari, S., Antoniades, D., Brooks, S.J., Fallu, M.A., Hughes, M., Keatley, B.E., Laing, T.E., Michelutti, N., Nazarova, L., Nyman, M., Paterson, A.M., Perren, B., Quinlan, R., Rautio, M., Saulinier-Talbot, E., Siitonen, S., Solovieva, N. and Weckstrom, J. 2005. Climate-driven regime shifts in the biological communities of Arctic lakes. *Proceedings of the National Academy of Sciences of the United States of America*. 102, 4397-4402.

Spence, C. 2000. The effect of storage on runoff from a headwater subarctic shield basin. *Arctic*. 53. 237-47.

Spence. 2001. Sub grid runoff processes and hydrological modeling in the subarctic Canadian Shield. In: Soil-vegetation-atmosphere transfer schemes and large scale hydrological models. Proceedings of a symposium held during the Sixth IAHS Scientific Assembly at Maastricht, The Netherlands, July 2001, IAHS Publication #270, pp. 113-116.

Spence, C. and Woo, M-k. 2003. Hydrology of subarctic Canadian Shield: soil-filled valleys. *Journ. of Hydrol*. 279, 151-166.

Spence, C. and Woo, M-k. 2006. Hydrology of subarctic Canadian Shield: heterogeneous headwater basins. *Journ. of Hydrol.* 317, 138-154.

Spence, C., Guan, X.J., Phillips, R.W, Hedstrom, N., Granger, R. and Reid, B. 2010. Storage dynamics and streamflow in a catchment with a variable contributing area. *Hydrol. Process.* 24, 2209-2221.

Spence, C. and Phillips, R.W. 2015. Refining understanding of hydrological connectivity in a boreal catchment. *Hydrol. Processes.* 29, 3491-503.

Spence, C., Ali, G., Oswald, C.J. and Wellen, C. 2019. An application of the T-TEL assessment method to evaluate connectivity in a lake-dominated watershed after drought. *Journal of the American Water Resources Association*. 55(2), 1-16.

Sun, Z., Ma, R., Wang, Y. 2009. Using landsat data to determine land use changes in Datong basin, China. *Environ. Geol.*, 57, 1825-1837.

Tape, K.D., Gustine, D.D., Ruess, R.W., Adams, L.G. and Clark, J.A. 2016 Range expansion of moose in Arctic Alaska linked to warming and increased shrub habitat. *PLoS ONE*, 11(4): e0152636 doi:10.1371/journal.pone.0152636.

Thomlinson, J.R., Bolstad, P.V., Cohen, W.B. 1999. Coordinating methodologies for scaling land cover classifications from site-specific to global: Steps toward validating global map products. *Remote Sens. Environ.* 70, 16-28.

Thornthwaite, C. 1948. An approach toward a rational classification of climate. *The Geographical Review*. 38, 1-94.

Tondu, J.M.E., Turner, K.W., Wolfe, B.B., Hall, R.I., Edwards, T.W.D. and McDonald, I. 2013. Using water isotope tracers to develop the hydrological component of a long-term aquatic ecosystem monitoring program for a northern lake-rich landscape. *Arct. Antarct. Alp. Res.* 45, 594-614.

Turner, K.W., Wolfe, B.B., Edwards, T.W.D. 2010. Characterizing the role of hydrological processes on lake water balances in Old Crow Flats, Yukon Territory, Canada, using water isotope tracers. *Journal of Hydrology*. 386 (2010), 103-117.

Turner, K.W., Wolfe, B.W., Edwards, T.W.D., Lantz, T.C., Hall, R.I. and Larocque, G. 2014. Controls on water balance of shallow thermokarst lakes and their relations with catchment characteristics: a multi-year, landscape-scale assessment based on water isotope tracers and remote sensing in Old Crow Flats, Yukon (Canada). *Glob. Change Biol*. 20(5), 1585-1603. Doi: 10.1111/gcb.12465.

United States Geological Service (USGS). 2018. Landsat 8 OLI data were "Level 1", 30-m resolution raster images. Product identifier: LC08_L1TP_046015_20170815_20170825_01_T1; LC08_L1TP_046016_20170831_20170915_01_T1; LC08_L1TP_048016_20170829_20170914_01_T1;

LC08_L1TP_047017_20180708_20180717_01_T1. Obtained from https://earthexplorer.usgs.gov/.

Wang, P., Limpens, J., Nauta, A., van Huissteden, C, van Rijssel, Q., Mommer, L., de Kroon, H., Maximov, T.C., Heijmans, M.M.P.D. 2018. Depth-based differentiation in nitrogen uptake between graminoids and shrubs in an Arctic tundra plant community. *Journal of Vegetation Science,* 29.1 (2018), 34-41.

Western, A.W., Bloschl, G. and Grayson, R.B. 2001. Toward capturing hydrologically significant connectivity in spatial patterns. *Water Resources Research*. 37, 83-97.

Wolfe, B.B., and Edwards, T.W.D. 1997. Hydrologic control on the oxygen-isotope relation between sediment cellulose and lake water, Taimyr Peninsula, Russia: Implications for the use of surface-sediment calibrations in paleolimnology. *J. Paleolim*. 18, 283-291.

Wolfe, B.B., Edwards, T.D.W. and Hall, R.I. 2002. Past and present ecohydrology of the Peace-Athabasca Delta, northern Alberta, Canada: water isotope tracers lead the way. *PAGES News*. 10, 16-17.

Wolfe, B.B., Karst-Riddoch, T.L., Vardy, S.R., Falcone, M.D., Hall, R.I. and Edwards, T.D.W. 2005. Impacts of climate and river flooding on the hydro-ecology of a floodplain basin, Peace-Athabasca Delta, Canada: A.D. 1700-present. *Quat. Res.* 64, 147-162.

Wolfe, B.B. and Turner, K.W. 2008. Near record precipitation causes rapid drainage of Zelma Lake, Old Crow Flats, northern Yukon Territory. *Meridian*. Spring, 7-12.

Wolfe, B.B., Light, E.M., Macrae, M.L., Hall, R.I., Eichel, K., Jasechko, S., White, J., Fishback, L. and Edwards, T.D.W. 2011. Divergent hydrological responses to 20th century climate change in shallow tundra ponds, western Hudson Bay Lowlands. *Geophysical Research Letters*. 38, L23402, http://dx.doi.org/10.1029/2011g1049766.

Wolfe, S.A., Stevens, C.W., Gaanderse, A.J., Oldenborger, G. 2014. Lithalsa distribution, morphology and landscape associations in the Great Slave Lowland, Northwest Territories, Canada. Geomorphology 204: 302–313. DOI:10.1016/j.geomorph.2013.08.014.

Yi, Y., Brock, B.E., Falcone, M.D., Wolfe, B.B., Edwards, T.W.D. 2008. A coupled isotope tracer method to characterize input water to lakes. *Journal of Hydrology*, 350, 1-13.

Yi, Y. et al. 2012. Isotopic signals (^{18}O, ^{2}H, ^{3}H) of six major rivers draining the pan-Arctic watershed. *Glob. Biogeochem. Cycles*. 26, GB1027.

CHAPTER FOUR

HYDROLOGICAL RESPONSES OF REPRESENTATIVE CASE STUDY LAKES

A number of study lakes provided additional opportunities for evaluation due to their unique catchment characteristics and hydrological responses. These case studies build on the data presented in Chapter Three, providing additional detailed reference of key sites.

4.1 Large Lake with High LA/CA (Plant Lake)

Plant Lake (study lake YK-09) represents a unique case in that the lake is relatively large (surface area = 541 ha; catchment area = 24 km^2; approximate centre depth = 10.2 m with stratification possible), with high LA/CA (22.6%) and proportion of catchment open water coverage (24%; Figure 4.1). Plant Lake had the longest record of water level data available extending to 15 September 2018, which was approximately one month longer than the other study lakes. With its comparably high LA/CA compared to the other large study lakes such as River Lake (YK-08) and Prelude Lake (YK-12), Plant Lake receives less relative inflow from its catchment. Coupled with a relatively large lake surface area, Plant Lake experienced relatively greater water level drawdown from evaporation during the drier 2017 ice-free season and less water level increase during the wet 2018 ice-free season. During an extended period of lower rainfall near the end of the wet 2018 ice-free season (13 August – 15 September), Plant Lake's water level decreased approximately 0.1 m. This highlights the influence evaporation had on lake levels near the end of the 2018 ice-free season, when the heavy rainfall subsided.

Figure 4.1 – Satellite imagery highlighting Plant Lake (study lake YK-09), which is likely to experience relatively greater influence from ice-free season evaporation (high E/I) as a result of its small catchment relative to lake area (high LA/CA) and high proportion of open water land cover (DigitalGlobe, 2017; GeoEye, 2017).

4.2 Lakes with Variable LA/CA in Taiga Plains Region

Study lakes YK-18 and YK-19 represent unique cases for evaluation, as these lakes are located in close proximity to one another (within 11.5 km) in the relatively flat Mackenzie Bison Sanctuary (Taiga Plains) region (Figure 4.2). Highway 3 is situated immediately west of the lakes, running in a general north-south direction. The lakes are of similar size (46 and 67 ha, respectively) and shallow depth (approximate centre depth = 1-1.5 m). However, the lakes differ considerably in their relative catchment size, with YK-18 having a relatively high LA/CA (31%) and YK-19 a low LA/CA (1%). The relatively large catchment of YK-19 includes numerous shallow lakes.

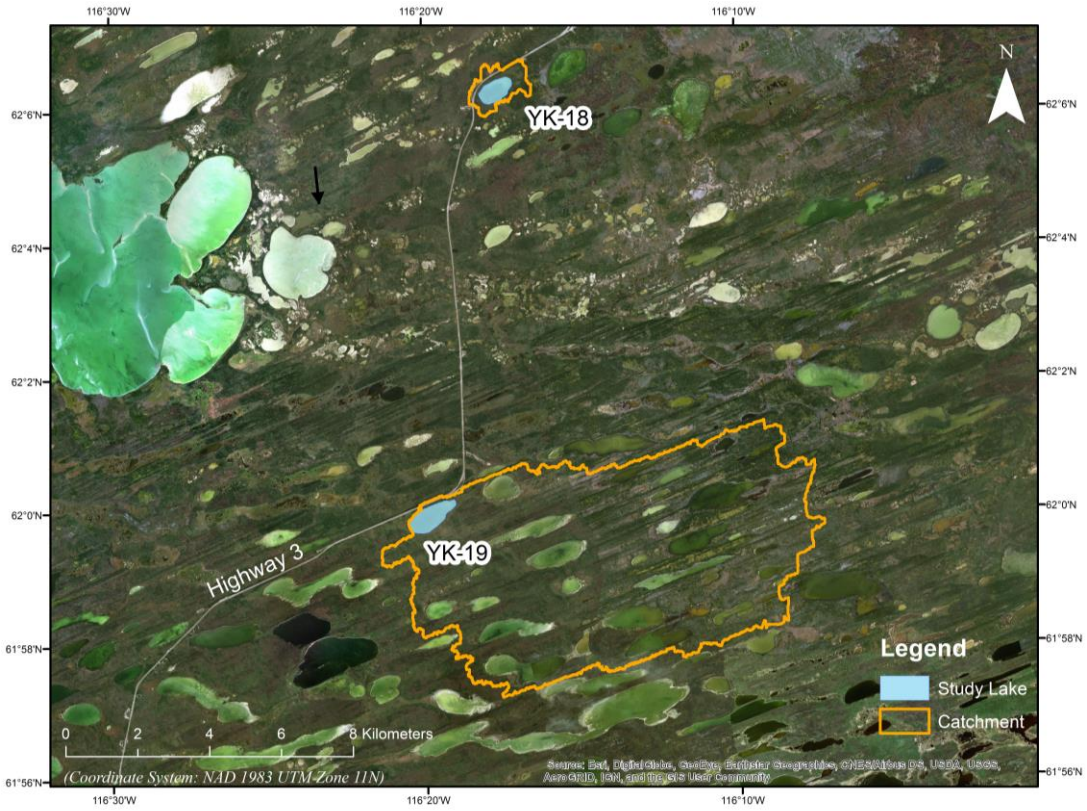

Figure 4.2 – Satellite imagery highlighting study lakes YK-18 and YK-19 within the relatively flat Taiga Plains region. While the lakes have similar surface areas and depth, they differ considerably in relative catchment size. YK-18 has a LA/CA of 31% while YK-19 has a LA/CA of 1%. As such, YK-19 will be more influenced by inflow (lower E/I) during spring snowmelt and following heavy rainfall when catchment hydrological connectivity is maintained (DigitalGlobe, 2017; GeoEye, 2017).

As a result of its larger relative catchment size, the hydrology of YK-19 is more influenced by spring snowmelt than YK-18. During May 2017 following freshet, YK-19 (low LA/CA) had an E/I ratio of 0.17, compared to YK-18 (high LA/CA) with an E/I ratio of 0.32 (Figure 4.3). During August 2017 under drier conditions, hydrologic connectivity within the YK-19 catchment diminished, and the lake was slightly more influenced by evaporation (E/I = 0.65) compared to YK-18 (E/I = 0.57). This influence was also observed in the corresponding water level change data from May-September 2017, with YK-19 drawing down -0.27 m compared to -0.13 m for YK-18. The markedly larger water level decrease observed in YK-19 during summer 2017 is likely related to the drying of catchment hydrological connections and storage capacity limits.

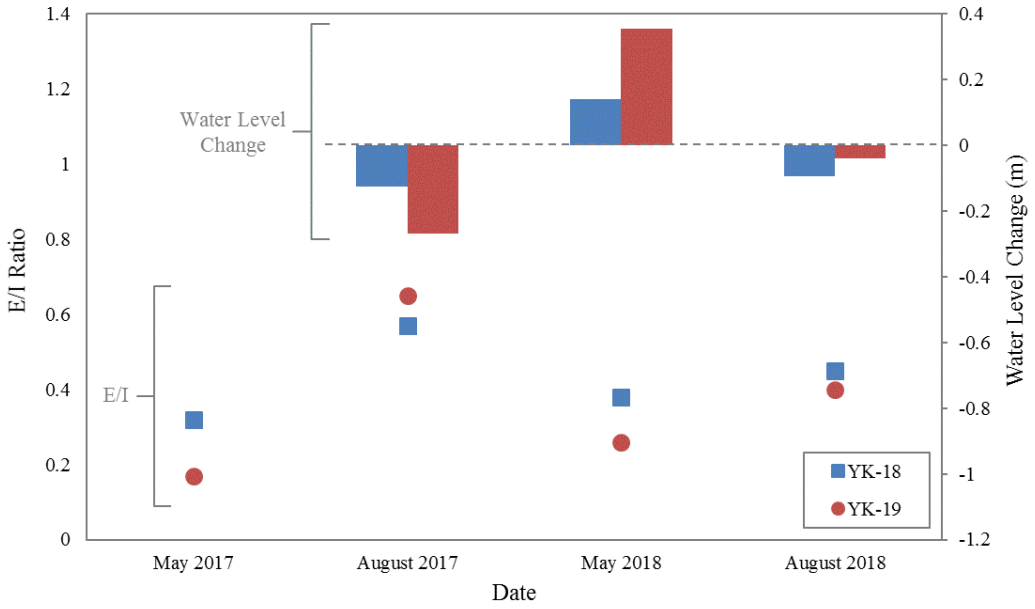

Note:
Summer or "August 2017" water level change presented here refers to 19 May – 30 September 2017 change (to accurately illustrate the full seasonal change).

Figure 4.3 – Comparison of E/I ratio and water level change for study lakes YK-18 (LA/CA = 31%) and YK-19 (LA/CA = 1%), respectively. YK-19 (low LA/CA) is more influenced by inflow (low E/I) via catchment hydrological connections, including during spring snowmelt and during the 2018 ice-free season with heavy rainfall. During August 2017, under low flow conditions when catchment hydrological connectivity is diminished, YK-19 shows slightly higher influence from evaporation than YK-18. YK-19 is also observed to markedly drawdown compared to YK-18 during 2017, and this is likely related to the drying of catchment hydrological connections and storage capacity limits.

During May 2018 following freshet, YK-19 was once again increasingly replenished by snowmelt dilution (E/I = 0.26) from its larger relative catchment compared to YK-18 (E/I = 0.38), with corresponding water level increase reflected in the data (YK-19 = 0.36 m and YK-18 = 0.14 m; Figure 4.3). During August 2018, under relatively heavier summer rainfall conditions, the lakes were more influenced by inflow compared to 2017 (similarly low E/I; YK-19 = 0.4 and YK-18 = 0.45). As such, seasonal lake level drawdown was relatively minor in both lakes during 2018 (YK-19 = -0.04 m and YK-18 = -0.09 m). Together, YK-18 and YK-19 serve as strong examples which demonstrate the complex-nature of relative catchment size (LA/CA) and hydrological connectivity in driving lake hydrology under variable meteorological conditions within the Taiga Plains region.

4.3 Network of Interconnected Study Lake Catchments

The catchment of study lake YK-15 (along the Ingraham Trail) encompasses the full catchments of study lakes YK-01, YK-16, YK-10 and YK-07 (Figure 4.4). This permitted the investigation of seasonal isotopic change for a chain-of-lakes with adjoining and interconnected catchments. YK-15 is a relatively small lake at 9.3 ha, with a catchment of approximately 2,730 ha. As such, the lake has a very low LA/CA (0.34%). The catchment is also made up of a relatively high proportion of open water (28%). The Ingraham Trail bisects the landscape, however, hydrological connectivity among lakes is maintained through ditches and culverts.

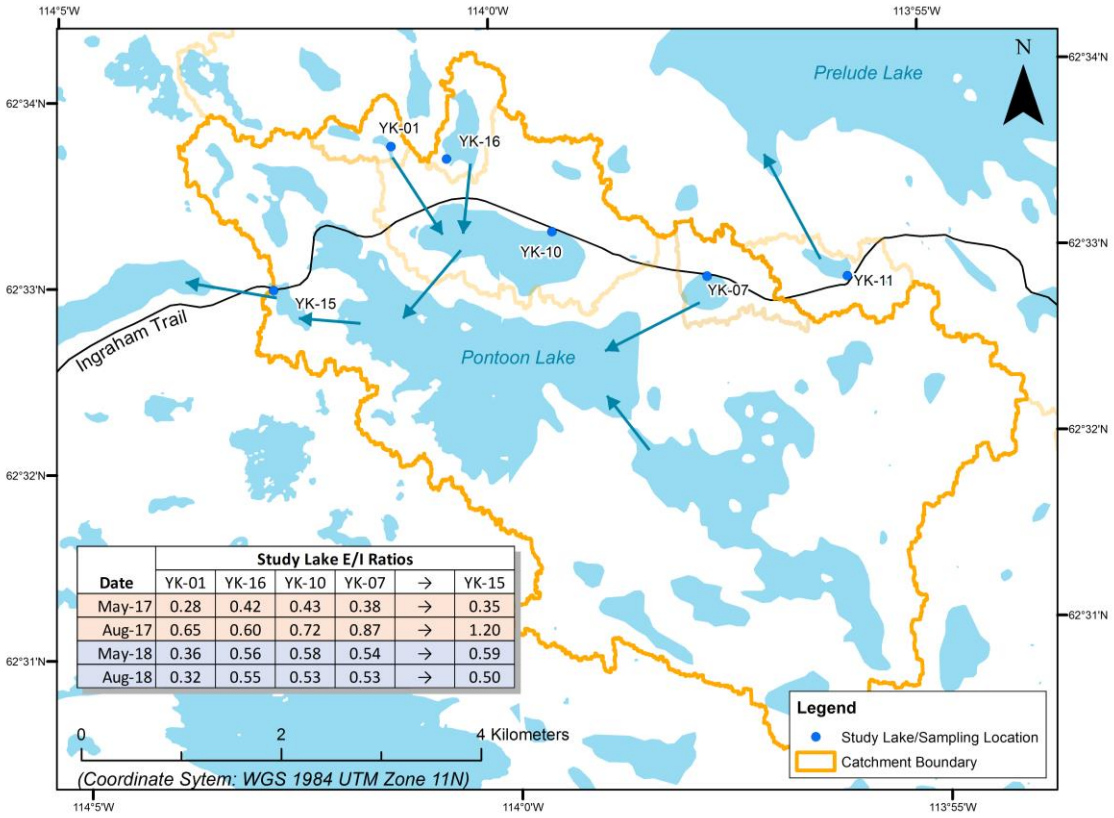

Figure 4.4 – Map illustrating study lakes with adjoining/interconnected catchments as part of the greater YK-15 catchment. Arrows indicate the general drainage direction of the respective catchments. Ice-free season (May and August) lake E/I ratios during 2017 and 2018 are presented in table format for the catchment network. The lakes exhibited fairly similar (lower) E/I ratios following 2017 and 2018 spring snowmelt, as well as during the wet 2018 summer when catchments were increasingly hydrologically connected. However, during summer 2017 catchment hydrological connections diminished under drier conditions. With less inflow, the lakes exhibited higher E/I from the strong evaporative influence. YK-15, at the most downstream end of the chain of lakes system, had markedly higher E/I compared to the other lakes as a result of the loss of catchment inflow and strong influence from evaporation on the relatively small lake.

Following the 2017 freshet and snowmelt dilution, E/I ratios were similarly low for this group of lakes, ranging from 0.28 (YK-01) to 0.43 (YK-10). By August 2017, under typical seasonal rainfall conditions, the study lakes were increasingly influenced by evaporation. E/I ratios generally increased moving down the chain-of-lakes system, ranging from 0.60 (YK-16) to 1.20 (YK-15). YK-16, a relatively deeper lake (center depth = 7 m), was influenced the least by evaporation among these lakes, perhaps due to its low surface area relative to overall volume (LA/LD = 2.5%). Following the 2018 freshet, E/I ratios for this group of study lakes were reduced once again, ranging from 0.36 (YK-01) to 0.59 (YK-15), with values slightly greater than during May 2017 given less snowmelt dilution. By August 2018, under pronounced summer rainfall conditions and inflow influence, lake E/I ratios remained similarly low, ranging from 0.32 (YK-01) to 0.55 (YK-16), with YK-15 having an E/I ratio of 0.50.

The pattern of E/I increasing down a chain-of-lakes system during drier conditions (e.g., August 2017) illustrates how lake hydrology is heavily influenced by catchment connectivity ("spill-and-fill" mechanisms) as driven by seasonal rainfall. This confirms previous research findings in the region. Gibson and Reid (2014) found that during periods of low rainfall, lake inflow is likely to decrease (and the evaporative influence increase) as hydrological connectivity from the upper catchment is reduced. This occurs when upstream water body levels do not rise above outlet elevation thresholds (Spence et al., 2019). Lakes further down a chain-of-lakes system, near the terminal end, are likely to be most influenced by evaporation and drawdown during drier conditions when hydrological connectivity diminishes (Spence et al., 2019).

4.4 Large Lake Systems (Prelude Lake and River Lake)

The combined catchments of Prelude Lake (YK-12) and River Lake (YK-08) represent a major drainage network in the region (Figure 4.5). Given the relatively massive size of the

catchment system compared to the other study lakes, it offers a unique opportunity for analysis. These lakes serve as large, deep reservoirs within the landscape. In total, ten study lakes are situated within this greater catchment area, including: YK-02, YK-03, YK-04, YK-05, River Lake (YK-08), Plant Lake (YK-09), YK-11, Prelude Lake (YK-12), YK-13 and YK-14.

In terms of size, Prelude Lake is approximately 3,284 ha and River Lake (hydrologically connected immediately downstream to the west) is approximately 497 ha. Together, their associated catchments drain an area of approximately 7,745 km^2. Prelude Lake was previously assessed by Roberge et al. (1990) and was found to have a mean depth of approximately 18 m and a maximum depth of 53.3 m. A centre depth measurement from River Lake during April 2018 indicated a depth of 23.6 m. Roberge et al. (1990) found that Prelude Lake is thermally stratified in mid-summer, with surface temperatures near 20 °C and a sharp thermocline at approximately 10 m. LA/LD was determined to be 0.4% for Prelude Lake and 0.06% for River Lake.

Prelude Lake (YK-12) and River Lake (YK-08) have notable hydrological drainage inlets and outlets. The lake systems are primarily fed by the Cameron River and its extensive network of headwater tributaries. The Cameron River drains into Prelude Lake to the east, which in turn drains west into River Lake. Discharge from the Cameron River varies depending on the time of year and meteorological conditions. For example, discharge will be relatively high during freshet and following major periods of rain, and low during drier periods (Figure 4.6).

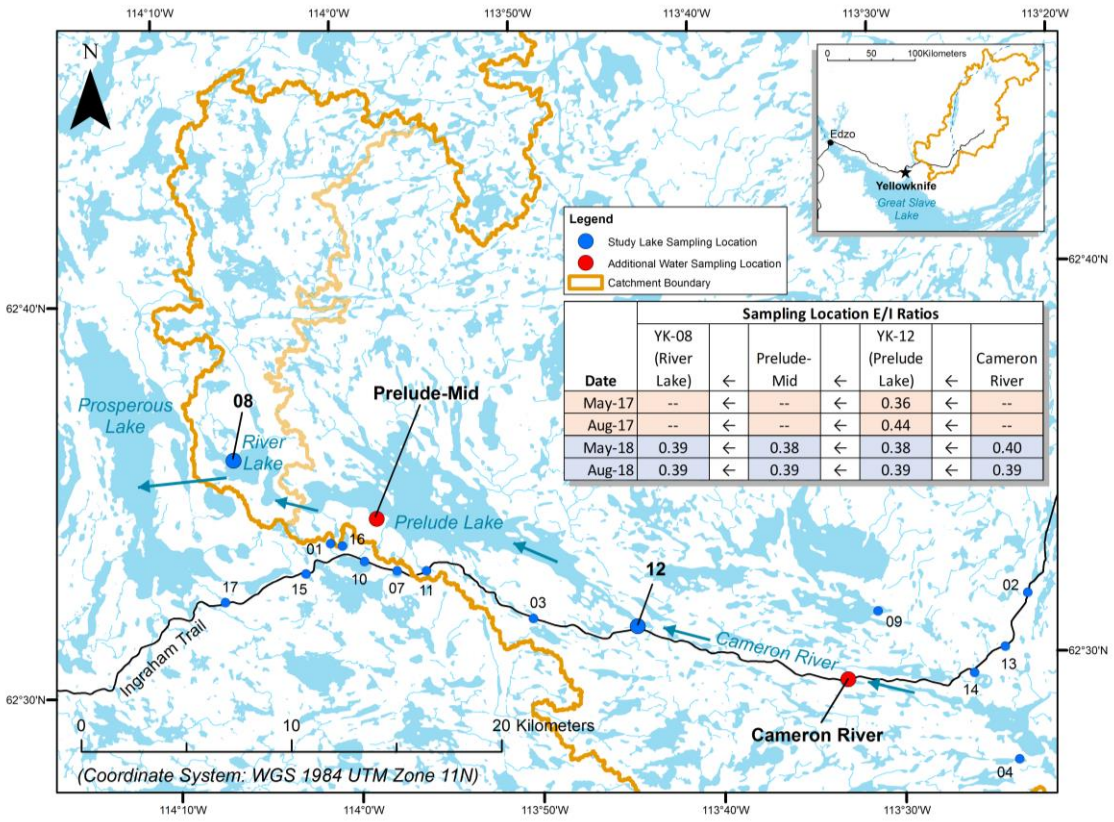

Note:
Study lake names abbreviated.

Figure 4.5 – Map illustrating the hydrology of the Prelude Lake (YK-12) and River Lake (YK-08) system. Available 2017-18 E/I data are provided in the table insert. The data indicate only minor E/I ratio increase from May-August 2017 as found at the lone YK-12 sampling location. During 2018, E/I ratios among the sampling locations remained virtually unchanged through May-August under pronounced summer rainfall conditions. Overall, the data suggest that E/I across the system fluctuates very little, including during both average (2017) and wet (2018) ice-free season conditions. The lack of E/I variability is likely the result of the dilution influence within these large, deep reservoirs.

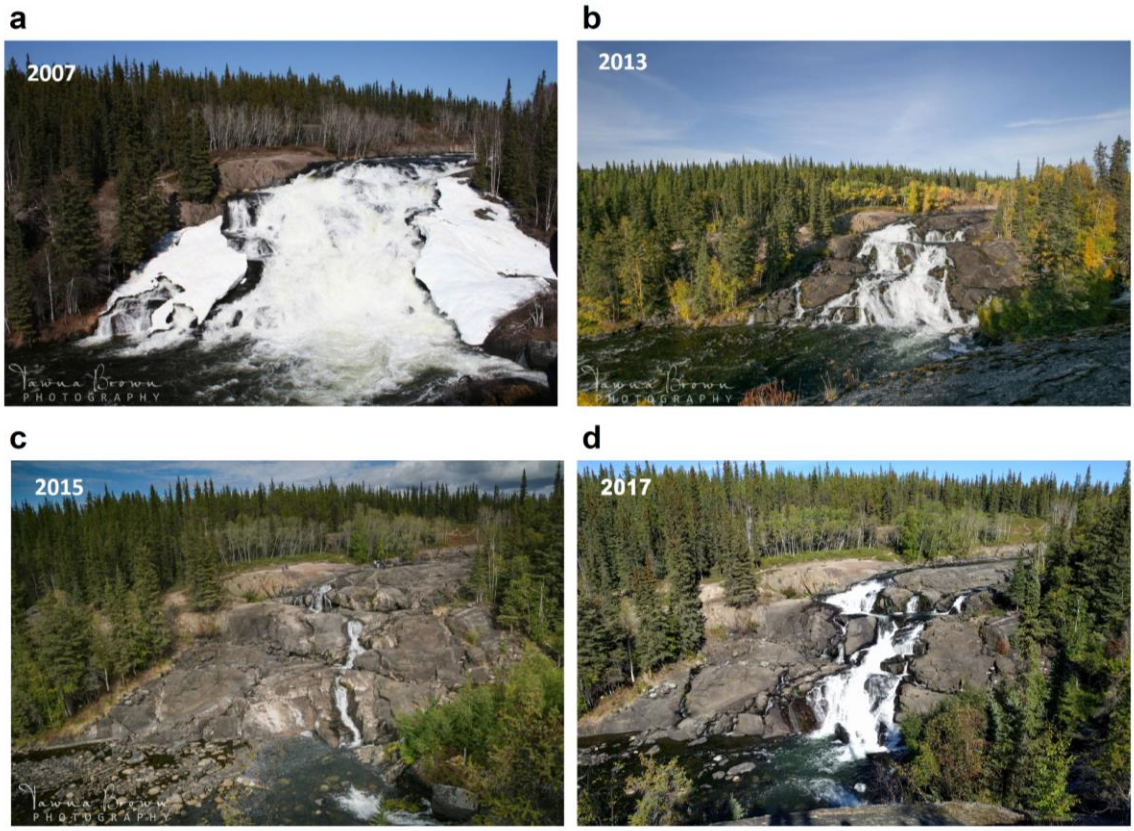

Figure 4.6 – Photographs of Cameron Falls at Prelude Lake (YK-12) showing variable discharge conditions, including (a) high discharge during 2007 (suspected spring freshet period; Tawana Brown Photography, 2018); (b) moderate discharge during 2013 (suspected late summer/fall period; Tawana Brown Photography, 2018); (c) very low discharge during 2015 (suspected early summer period; Tawana Brown Photography, 2018); and (d) low discharge during 29 August 2017 (photograph by J.Viscek).

In addition to sampling locations YK-12 (eastern extent of Prelude Lake) and YK-08 (River Lake), two additional water isotope sampling locations were added during 2018 to more thoroughly investigate the hydrology of the system. These additional sampling locations included the central extent of Prelude Lake ("Prelude-Mid"), as well as the Cameron River main inflow channel ("Cameron River") located 9.5 km upstream (east) of the Prelude Lake discharge point (Figure 4.5). Only data from the YK-12 sampling location were available during 2017, indicating only a minor increase in E/I from May-August (0.36 to 0.44). The 2018 dataset (which includes all four sampling locations) illustrates the broader isotope hydrology of the system under wetter summer conditions. May 2018 E/I ratios were nearly identical across the sampling locations (and

slightly greater than during spring 2017 due to less snowmelt dilution), ranging from 0.38 (YK-12 and Prelude-Mid) to 0.40 (Cameron River). August 2018 E/I ratios were also consistent across the sampling locations, and similar to May results at approximately 0.39. As such, E/I was not found to appreciably fluctuate within these lake systems, likely due to the dilution influence from the large, deep reservoirs. Further, E/I was not found to be as reflective of the seasonal and interannual water level fluctuations experienced by these larger systems compared to the smaller study lakes.

Information presented here showcases how the influence of precipitation on lake hydrological conditions can be highly individual depending on the highly variable catchment properties that exist across the Taiga Shield and Plains regions.

REFERENCES

Gibson, J.J. and Reid, R. 2014. Water balance along a chain of tundra lakes: a 20-year isotopic perspective. *J. Hydrol*. 519, 2148-2164.

Roberge, M.M., J.B. Dunn, M.R. Falk. 1990. Catch, effort and biological data of fish, in particular lake trout (*Salvelinus namaycush*), from Prelude and Prosperous lakes, Northwest Territories, 1973 and 1979. Can. Dat. Rep. Fish. *Aquat. Sci*. 817: v + 52 p.

Spence, C., Ali, G., Oswald, C.J. and Wellen, C. 2019. An application of the T-TEL assessment method to evaluate connectivity in a lake-dominated watershed after drought. *Journal of the American Water Resources Association*. 55(2), 1-16.

Tawna Brown Photography. 2018. Photographs of Cameron Falls: 2007, 2013 and 2015. Provided by Mike Palmer through e-mail correspondence, June 2, 2018.

CHAPTER FIVE

CONCLUSIONS

5.1 Conclusions

Subarctic boreal lakes are prominent features across northern regions which are likely to be impacted from increasing fire and drought with increased climate warming. Here, we build on previous research to characterize the key meteorological and catchment-specific drivers of lake hydrology for 20 lakes within the Taiga Shield and Plains of the North Slave Region. The two-year study provided the opportunity to examine study lakes under relatively average (2017) and wet (2018) ice-free season conditions. Study lakes were selected to represent a range of catchment sizes and physical characteristics, and included several having experienced recent burn during the five-year period prior to study (2012-16). Lake hydrology was evaluated using water isotope tracer data (i.e., δ^2H and $\delta^{18}O$) in conjunction with in-situ lake level monitoring. Lake water isotope data were obtained twice during the ice-free season (May and August) and used to calculate evaporation to inflow (E/I) ratios using conventional methods. Hydrological data were compared to catchment characteristics, including relative size, depth, hydrological connectivity, relative land cover from remote sensing data.

Overall, lake levels decreased under average seasonal rainfall conditions during 2017, as the relative influence of evaporation (E/I) increased. Lake isotope values were relatively high during spring 2018 following drier fall 2017 conditions and lower winter snowfall. During the wet 2018 ice-free season, lake levels largely increased as the strong influence from inflow offset evaporative water loss. Below, we present a summary of interrelated lake hydrological drivers for the North Slave Region (in order of general importance), as determined during the study.

Meteorological Conditions

Precipitation is a major driver of lake hydrology in the Taiga Shield and Plains. Lake E/I values during spring are likely to be lower with greater winter snowfall and subsequent inflow influence following freshet. Rainfall will offset the influence of evaporation during the summer. Under normal rainfall conditions (e.g., 2017), lakes are likely to exhibit high E/I and draw down during the summer from the strong evaporative influence. Conversely, under heavy rainfall conditions (e.g., 2018), lake levels and E/I may remain fairly stable from spring-summer.

Hydrological Connectivity

Hydrological connectivity is an important and complex catchment driver within a chain-of-lakes system that is linked to many factors, including: LA/CA, storage deficit dynamics (fill-and-spill mechanisms), inflow/outflow channels, precipitation, evaporation, topography and land cover. Lakes will be more influenced by inflow (lower E/I) as catchment hydrological connectivity increases, particularly with lower LA/CA. This trend is especially evident following spring freshet when inflows are high. Ice-free season lake E/I change is broadly linked to water level change, and more-so during wet conditions (e.g., 2018) when catchment hydrological connectivity increases. During summer seasons with average to low rainfall (e.g., 2017), flow among catchment water bodies will increasingly diminish. Lakes are more likely to function as isolated systems as a result and will be more influenced by evaporative drawdown, especially further down a chain-of-lakes system.

Lake Surface Area to Catchment Area (LA/CA)

The influence of maximum LA/CA on lake water balance is largely dependent on catchment hydrological connectivity and water body fill-and-spill mechanisms. Lakes with lower LA/CA are likely to be increasingly influenced by inflow (lower E/I) through catchment hydrological connections under wetter conditions (e.g., freshet and summer rainfall). Conversely, lakes with higher LA/CA will receive less water input and be more influenced by evaporation

(higher E/I). Under drier conditions, as catchment connectivity increasingly diminishes, the influence of maximum LA/CA is more unpredictable as catchment lakes will increasingly function as more isolated systems. Future studies should attempt to incorporate dynamic catchment extents for individual lakes, the size of which are dependent on preceding precipitation conditions. This will likely improve our understanding of how multiple landscape variables influence lake hydrological conditions, which are presented in Figure 3.10 (Chapter 3).

Lake Surface Area to Lake Depth (LA/LD)

While findings are based on point depth measurements and somewhat limited, there is evidence that relatively shallower lakes with greater LA/LD are more likely to be influenced by solar heating and draw down from the evaporative influence during the ice-free season. As such, lakes with greater LA/LD may exhibit higher E/I and spring-summer E/I variability. Future studies employing more robust measurement of lake morphology may further confirm these results. Relatively larger and deeper lakes (e.g., Prelude Lake, River Lake) also experience evaporative drawdown during the ice-free season; however, these lakes exhibit very little seasonal E/I fluctuation compared to smaller lakes due to the strong dilution influence within the larger reservoirs.

Catchment Slope

Lakes within catchments that exhibit greater median landscape slope are more likely to be influenced by inflow during the ice-free season (lower E/I). This linkage is particularly relevant for lakes in Shield environments, where topography is typically undulating and variable. Lakes with increasing slope are likely to collect and retain a greater proportion of winter snowfall, with greater spring snowmelt flowing to these lakes during freshet. These lakes may also experience greater runoff drainage efficiency to the basin (less groundwater infiltration and catchment storage) during summer rainfall events compared to lakes with less catchment slope.

Greater catchment slope within a chain-of-lakes system may promote hydrological connectivity between lakes through inflow/outflow channels during snowmelt or rainfall events.

Land Cover

While findings are variable, lakes within catchments comprising greater proportions of open water (which typically have higher LA/CA) are more likely be influenced by evaporation (higher E/I) during the ice-free season. The relationship between catchment mixed vegetation, as well as open terrestrial surface composition and lake E/I was found to be somewhat variable. More abundant catchment vegetation, particularly larger trees and shrubs typically increase snowpack accumulation and subsequent snowmelt input during spring. We detected that recently burned catchments will transmit less snowmelt water to lakes during freshet, resulting in greater influence from evaporation (higher early season E/I). However, our analysis of this relationship was only based on results from one burned lake catchment and two control lake catchments. Overall, catchment burn was found to be less influential in driving lake hydrology compared to other important catchment properties, especially connectivity and LA/CA.

5.2 Future Recommendations

This study demonstrates and integrates analyses of water isotope tracers, lake level changes, local meteorological conditions and remotely sensed data to identify the relative importance of climatic and catchment controls on northern boreal lake hydrology. Future research should increasingly seek to integrate longer term hydrological data from other regional studies, for comparative analyses. For example, further comparison of seasonal water level data, isotopic compositions and/or measured catchment properties may be made to other well-studied systems including Pocket Lake, Baker Creek and Prelude Lake to better understand lake hydrological responses during historical climate fluctuations. Future research programs building on this work should include more study lakes encompassing a variety of catchment conditions

across the North Slave Region to further characterize seasonal isotopic conditions. Adding more frequent isotope sampling intervals (e.g., monthly) may also provide a clearer indication of climate-influenced hydrological changes of lakes during the ice-free season. These analyses may provide a more thorough understanding of multi-year dry/wet cycles in the region, and place the findings from the present study in greater context.

In addition, future work should look to refine and advance remote sensing approaches as part of this research. With respect to land cover classification, the 30-m Landsat imagery used in the current study was suitable to generate only broad land cover classes, which included open water, mixed vegetation and open terrestrial surface. To address some of the limitations/uncertainties associated with this classification method, and to increase the differentiation of more finite land cover classes (e.g., vegetation type) to improve overall accuracy, future studies may consider utilization of higher-resolution data (e.g., Sentinel) or radar data (e.g., Radarsat-2, UAVSAR) where available. As well, the extent of catchments and morphology of lake basins should be refined (using remote sensing technology, wherever possible) and assessed according to their fluctuation in response to preceding precipitation.

Finally, future research should seek to identify long-term lake water isotopic conditions through the evaluation of cellulose-inferred $\delta^{18}O$ from extracted lake sediment cores. As part of a wider, collaborative research effort during 2016-18, sediment cores (Uwitec short-cores) were obtained from several of the present study lakes. An evaluation of the isotope data from these cores may provide insights of climate and lake hydrological fluctuations over the past several hundred years to determine if present conditions fall within the range of natural variability.

5.3 Implications and Practical Applications

The findings presented here serve as a well-rounded benchmark of recent hydrological conditions in the North Slave Region, which may be useful for understanding historical changes as well as anticipating lake hydrological conditions into the future. Furthermore, the relations presented here provide an important reference when interpreting drivers of lake hydrology under fluctuating meteorological conditions, and with increasing wildfire disturbance. The study data show a number of important relationships between meteorological conditions, isotope-derived E/I, lake level change and catchment physical properties derived through remote sensing (e.g., relative catchment size, inferred hydrological connectivity, slope and land cover) and corroborating site observations. Considering practical applications from this work, lake conditions across broader northern boreal regions may be estimated based on monitoring of past and present meteorological data, existing digital shapefiles (e.g., DEMs) and remotely sensed data for land cover classification. At the very least, a preliminary assessment of catchment characteristics will provide the basis for effective site selection for expanded and continued lake hydrological monitoring. Such efforts may elicit savings in research time and costs, and ensure that monitoring lakes represent a spectrum of catchment properties that influence hydrological conditions. Lake hydrology should continue to be monitored across the North Slave Region to further investigate potential impacts under variable climate conditions so that sound land management policies may be developed and employed.

APPENDIX ONE

EQUATIONS AND CALCULATIONS

A1.1 Isotope Framework and E/I Calculations

Measured and modelled parameters were used to develop the LMWL–LEL isotope framework for the Yellowknife study region, utilizing approaches used by Craig and Gordon (1965), Yi et al. (2008) and Turner et al. (2010). Flux-weighted temperature and relative humidity values for the Yellowknife region were calculated using methods developed by Gonfiantini (1986) and Horita and Wesolowski (1994). Mean May-September (ice-free season) temperature and relative humidity data over a five-year window (2014-18), as obtained from the Yellowknife Airport met station records, were incorporated into these flux-weighted calculations (ECCC, 2018a). This five-year window was considered to reasonably reflect recent temperature and humidity conditions. Mean May-September data for total hours of sunshine (also required for the flux-weighted calculations) were obtained from available Yellowknife Airport climate normal records (1981-2010; ECCC, 2018b). The following series of equations/calculations describe how lake E/I ratios were calculated.

Flux-weighted Temperature (T) and Relative Humidity (h)

Average flux-weighted temperature and relative humidity values were calculated for the recent five-year period prior to study (2014-18) during the ice-free season (May-September), using methods described by Gonfiantini (1986).

Monthly Heat Index (li)

$$li = +(T / 5)^{1.5}$$

Where li equals the heat index for the month. *T* equals the average temperature for the month (Yellowknife Airport met station; ECCC, 2018a).

Coefficient (a)

$$a = 0.49 + 0.0179 * li - (7.71 * 10^{-5}) * li^{2} + (6.75 * (10^{-7}) * li^{3}$$

Where *li* equals the average (May-September) monthly heat index.

Monthly Total Potential Evaporation in mm/month (Et)

$Et = (1.6 * (L/3) * (N/N_A) * ((10 * T) / li)^{a}) * 10$

Where *Et* equals the monthly total potential evaporation in mm/month (Et), as calculated using methods developed by Thornthwaite (1948). *L* equals the average monthly day length in hours (total hours of sunshine in the month (Yellowknife Airport Climate Normals, 1981-2010; ECCC, 2018b) divided by number of days in the month), *N* equals the number of days in the month, N_A equals the average (May-September) number of days in a month, *T* equals average monthly temperature in degrees Celsius, *li* equals the average (May-September) monthly heat index, and *a* equals the coefficient.

Yearly Flux-weighted Temperature (Flux T)

*Flux T = [(May T * May Et) + (June T * June Et) + (July T * July Et) + (August T * August Et) (September T * September Et)] / (+May Et + June Et + July Et + August Et + September Et) + 273.15*

Where *T* equals average monthly temperature in degrees Celsius (Yellowknife Airport met station; ECCC, 2018a) and *Et* equals the monthly total potential evaporation in mm/month. Final *Flux T* value will be in Kelvin units.

Yearly Flux-weighted Relative Humidity (Flux h)

*Flux h = [(May h * May Et) + (June h * June Et) + (July h * July Et) + (August h * August Et) (September h * September Et)] / (+May Et + June Et + July Et + August Et + September Et) / 100*

Where *h* equals average monthly relative humidity (%) (Yellowknife Airport met station; ECCC, 2018a) and *Et* equals the monthly total potential evaporation in mm/month. Final *Flux h* value will be in decimal units.

Average Flux-weighted Temperature (Flux T; 2014-2018)

Flux T = (2014 Flux T + 2015 Flux T + 2016 Flux T + 2017 Flux T + 2018 Flux T) / 5

Where *T* equals yearly temperature values in Kelvin (as calculated above). The average value of yearly *Flux T* (2014-2018) in Kelvin, as calculated here, is used as *T* in the following isotope framework calculations.

Average Flux-weighted Relative Humidity (Flux h; 2014-2018)

*Flux h = [(May h * May Et) + (June h * June Et) + (July h * July Et) + (August h * August Et) (September h * September Et)] / (+May Et + June Et + July Et + August Et + September Et)*

Where *h* equals average monthly relative humidity in decimal notation (as calculated above) and *Et* equals the monthly total potential evaporation in mm/month. The average value of yearly *Flux h* (2014-2018) in decimal notation, as calculated here, is used as *h* in the following isotope framework calculations.

Equilibrium Liquid-Vapour Isotopic Fractionation (α^*)

For $\delta^{18}O$:

$$1000ln\alpha^* = -7.685 + 6.7123 (10^3/T) - 1.6664 (10^6/T^2) + 0.35041 (10^9/T^3)$$

For $\delta^{2}H$:

$$1000ln\alpha^* = 1158.8 (T^3/10^9) - 1620.1 (T^2/10^6) + 794.84 (T/10^3) - 161.04 + 2.9992 (10^9/T^3)$$

Where α^* equals the equilibrium liquid-vapour isotopic fractionation, calculated from equations given by Horita and Wesolowski (1994) and *T* equals the interface temperature in Kelvin (average 2014-18 flux-weighted *T*; Gonfiantini, 1986).

Equilibrium Separation (ε^*)

$$\varepsilon^* = (\alpha^* - 1)$$

Where ε^* equals the equilibrium separation, expressed as per mil (‰), between the liquid and vapour phases and α^* equals the equilibrium liquid-vapour isotopic fractionation, calculated from equations given by Horita and Wesolowski (1994).

Kinetic Separation (ε_K)

For $\delta^{18}O$:

$$\varepsilon_K = 0.0142 (1 - h)$$

For $\delta^{2}H$:

$$\varepsilon_K = 0.0125 (1 - h)$$

Where ε_K equals kinetic separation, expressed as per mil (‰), between the liquid and vapour phases and *h* equals relative humidity in decimal notation (average 2014-18 flux-weighted *h*; Gonfiantini, 1986).

Isotopic Composition of Ambient Atmospheric Moisture (δ_{AS})

$$\delta_{AS} = +(\delta_{Ps} - \varepsilon^*) / \alpha^*$$

Where δ_{AS} equals the isotopic composition of ambient atmospheric moisture, calculated for both $\delta^{18}O$ and δ^2H. *The* δ_{Ps} value is the average isotopic composition of summer rainfall (Gibson, 2017). ε^* equals the equilibrium separation, expressed as per mil (‰), between the liquid and vapour phases and α^* equals the equilibrium liquid-vapour isotopic fractionation, calculated from equations given by Horita and Wesolowski (1994).

Steady State Level Isotopic composition (δ_{SSL})

$$\delta_{SSL} = \alpha^* * 1.0142 * (1 - h) * (\delta_P + 1) + \alpha^* * h * (\delta_{AS} + 1) - 1$$

Where δ_{SSL} equals the isotopic composition of a terminal lake basin at steady-state, calculated for both $\delta^{18}O$ and δ^2H. α^* equals the equilibrium liquid-vapour isotopic fractionation, calculated from equations given by Horita and Wesolowski (1994). *h* equals relative humidity in decimal notation (average 2014-18 flux-weighted *h*; Gonfiantini, 1986). δ_P equals the mean annual isotopic composition of precipitation, derived from Canadian Network for Isotopes in Precipitation (CNIP) 1961-1990 average values for Yellowknife (CNIP, 2017). δ_{AS} equals the isotopic composition of ambient atmospheric moisture.

Lake-specific Evaporating Flux Isotopic Composition (δ_E)

$$\delta_E = ((\delta_L - \varepsilon^*) / \alpha^* - h\delta_{AS} - \varepsilon_K) / (1 - h + \varepsilon_K)$$

Where δ_E is the lake-specific isotopic composition of the associated evaporating flux, calculated using the Craig and Gordon (1965) model as formulated by Gonfiantini (1986) in decimal notation. This value is calculated for both $\delta^{18}O$ and δ^2H. δ_L is the measured isotopic composition of lake water. ε^* equals the equilibrium separation, expressed as per mil (‰), between the liquid and vapour phases and α^* equals the equilibrium liquid-vapour isotopic fractionation, calculated from equations given by Horita and Wesolowski (1994). *h* equals relative humidity in decimal notation (average 2014-18 flux-weighted *h*; Gonfiantini, 1986). δ_{AS} equals the isotopic composition of ambient atmospheric moisture. ε_K equals kinetic separation, expressed as per mil (‰), between the liquid and vapour phases.

Lake-specific Input Water Isotopic Composition (δ_I)

$$\delta_I = (b - 10) / (-m + 8)$$

Where *m* equals the slope of the lake evaporation line, calculated using the standard slope equation ($m = (y2 - y1) / (x2 - x1)$), inputting lake-specific δ_L and δ_E coordinates. *b* represents the lake evaporation line intersection with the GMWL, calculated using the above derived slope and lake specific input coordinates through the standard formula $y = mx + b$ (rearranged to solve for *b*). This value is calculated for both $\delta^{18}O$ and δ^2H.

Lake-specific Evaporation-to-Inflow Ratio (E/I)

Evaporation-to-inflow ratio (E/I) calculations are based on isotope mass balance calculations described by:

$E/I = (\delta_I - \delta_L) / (\delta_E - \delta_L)$

Where δ_I is the calculated lake-specific input water isotopic composition, δ_L is the measured isotopic composition of lake water, and δ_E is the isotopic composition of the associated evaporating flux, calculated using the Craig and Gordon (1965) model as formulated by Gonfiantini (1986) in decimal notation.

A1.2 Water Level Sensor Depth Calculation

Lake water level depths were derived from *Onset* HOBO U20 series water level logger data (model numbers: U20-001-04 and/or U20L-04, 13-foot (4-m). HOBO loggers record temperature and pressure data, which are used to calculate water level using a reference logger outside of the lake. Barometric pressure data was provided from the Yellowknife Airport met station; as well as from two HOBO U20 loggers installed to trees (at approximately eye-level height) near regional study locations along the Ingraham Trail (near YK-16) and Mackenzie Bison Sanctuary (near YK-18). Hourly lake level data were calculated through hydraulic/barometric pressure calibration considering the freshwater density factor. Water level data were plotted and screened to correct minor instances of sudden and/or unnatural probe movement. The following equation provided by Onset Computer Corporation (2008) was used to calculate lake depths:

$Sensor\ Depth = 0.3048 * (0.1450377 * 144 * P_{hyd}) / D / 1000{,}000$

Where sensor depth calculated in metres. P_{hyd} equals the hydraulic pressure in kilopascals (kPa) recorded by the lake sensor, 0.3048 represents the feet-to-meters conversion factor, 0.1450377 represents the kPa-to-pounds per square inch (psi) conversion factor, 144 represents the psi-to-pounds per square foot (psf or lb/ft^3) conversion factor, and D / 1000,000 represents the density of water (62.428 lb/ft^3) to grams per cubic metre (g/m^3) conversion factor.

APPENDIX TWO

ISOTOPE DATA

A2.1 Lake Isotope and E/I Results

September 2016				
Lake ID	Sample Collection Date	$\delta_L\,(^{18}O)$	$\delta_L(^{2}H)$	Notes
YK-01	28/09/2016	-12.5	-124	Samples collected during alternate study.
YK-02	28/09/2016	-11.0	-116	Samples collected during alternate study.

(Additional reference data only, not included in E/I analyses)

May 2017										
Lake ID	Sample Collection Date	$\delta_L\,(^{18}O)$	$\delta_L(^{2}H)$	$\delta_E\,(^{18}O)$	$\delta_E\,(^{2}H)$	Lake-specific Evap. Line Slope	Lake-specific Evap. Line-GMWL Intercept	$\delta_I\,(^{18}O)$	$\delta_I\,(^{2}H)$	*E/I*
YK-01	17/05/2017	-16.6	-146	-39.7	-246	4.31	-74.85	-23.0	-174	0.3
YK-02	18/05/2017	-17.4	-150	-41.9	-254	4.27	-75.35	-22.9	-173	0.2
YK-03	18/05/2017	-14.0	-133	-33.0	-215	4.28	-73.39	-22.4	-169	0.4
YK-04	17/05/2017	-13.9	-132	-32.6	-212	4.25	-73.33	-22.2	-168	0.4
YK-05	17/05/2017	-17.1	-149	-41.2	-252	4.28	-75.19	-22.9	-173	0.2
YK-06	17/05/2017	-19.1	-156	-46.2	-269	4.17	-76.29	-22.6	-170	0.1
YK-07	17/05/2017	-13.7	-128	-32.3	-203	4.00	-73.42	-20.9	-157	0.4
YK-08	(No Data)									
YK-09	(No Data)									
YK-10	16/05/2017	-12.9	-124	-30.2	-192	3.93	-73.06	-20.4	-153	0.4
YK-11	16/05/2017	-16.7	-145	-40.0	-242	4.19	-74.95	-22.3	-168	0.2
YK-12	16/05/2017	-13.9	-129	-32.8	-203	3.96	-73.56	-20.7	-155	0.4
YK-13	16/05/2017	-16.1	-145	-38.5	-242	4.35	-74.56	-23.2	-175	0.3
YK-14	16/05/2017	-13.0	-127	-30.4	-200	4.16	-72.92	-21.6	-163	0.5
YK-15	16/05/2017	-15.0	-137	-35.6	-225	4.23	-73.98	-22.3	-168	0.4
YK-16	17/05/2017	-13.3	-126	-31.1	-197	4.00	-73.18	-20.8	-156	0.4
YK-17	17/05/2017	-12.9	-126	-30.1	-197	4.14	-72.86	-21.4	-162	0.5
YK-18	18/05/2017	-14.5	-132	-34.3	-211	3.99	-73.85	-20.9	-157	0.3
YK-19	18/05/2017	-18.4	-154	-44.5	-264	4.23	-75.91	-22.8	-172	0.2
YK-20	(No Data)									
Mean		-15.2	-137.6	-36.1	-225	4.2	-74.2	-22.0	-166	0.3

August 2017										
Lake ID	Sample Collection Date	δ_L (^{18}O)	δ_L (^{2}H)	δ_E (^{18}O)	δ_E (^{2}H)	Lake-specific Evap. Line Slope	Lake-specific Evap. Line-GMWL Intercept	δ_I (^{18}O)	δ_I (^{2}H)	*E/I*
YK-01	28/08/2017	-12.2	-125	-28.2	-195	4.37	-72.26	-22.6	-171	0.7
YK-02	28/08/2017	-10.9	-117	-24.9	-175	4.15	-71.75	-21.2	-160	0.7
YK-03	28/08/2017	-10.9	-118	-24.9	-178	4.25	-71.66	-21.8	-164	0.8
YK-04	25/04/2018	-12.9	-129	-30.1	-204	4.36	-72.69	-22.7	-172	0.6
YK-05	25/04/2018	-14.0	-136	-32.9	-221	4.50	-73.23	-23.8	-180	0.5
YK-06	26/04/2018	-16.5	-144	-39.5	-240	4.18	-74.84	-22.2	-168	0.2
YK-07	28/08/2017	-9.9	-111	-22.2	-162	4.06	-71.29	-20.7	-155	0.9
YK-08	(No Data)									
YK-09	(No Data)									
YK-10	28/08/2017	-10.1	-110	-22.8	-157	3.75	-71.76	-19.3	-144	0.7
YK-11	28/08/2017	-12.4	-124	-28.9	-193	4.16	-72.59	-21.5	-162	0.6
YK-12	28/08/2017	-12.9	-124	-30.2	-192	3.95	-73.03	-20.5	-154	0.4
YK-13	28/08/2017	-10.3	-117	-23.3	-175	4.48	-71.04	-23.0	-174	1.0
YK-14	28/08/2017	-11.1	-117	-25.5	-174	4.01	-72.02	-20.6	-155	0.7
YK-15	28/08/2017	-9.2	-112	-20.5	-162	4.47	-70.42	-22.8	-172	1.2
YK-16	28/08/2017	-11.2	-115	-25.6	-171	3.85	-72.21	-19.8	-148	0.6
YK-17	28/08/2017	-9.4	-110	-21.0	-159	4.21	-70.85	-21.3	-161	1.0
YK-18	28/08/2017	-11.7	-119	-26.9	-179	3.96	-72.36	-20.4	-153	0.6
YK-19	28/08/2017	-11.7	-122	-27.1	-186	4.21	-72.16	-21.7	-163	0.6
YK-20	25/04/2018	-11.4	-120	-26.1	-183	4.24	-71.92	-21.8	-164	0.7
Mean		-11.6	-120.5	-26.7	-184	4.2	-72.1	-21.5	-162	0.7

May 2018										
Lake ID	*Sample Collection Date*	δ_L (^{18}O)	δ_L (^{2}H)	δ_E (^{18}O)	δ_E (^{2}H)	Lake-specific Evap. Line Slope	Lake-specific Evap. Line-GMWL Intercept	δ_I (^{18}O)	δ_I (^{2}H)	*E/I*
YK-01	21/05/2018	-15.9	-145	-38.0	-244	4.46	-74.42	-23.8	-181	0.4
YK-02	21/05/2018	-17.0	-150	-40.8	-255	4.41	-75.07	-23.7	-180	0.3
YK-03	21/05/2018	-13.5	-132	-31.8	-212	4.37	-73.06	-22.9	-173	0.5
YK-04	21/05/2018	-14.0	-134	-33.1	-216	4.32	-73.38	-22.7	-171	0.5
YK-05	21/05/2018	-14.2	-135	-33.4	-220	4.38	-73.43	-23.0	-174	0.5
YK-06	20/05/2018	-17.7	-150	-42.5	-256	4.24	-75.49	-22.7	-172	0.2
YK-07	21/05/2018	-12.7	-126	-29.6	-197	4.21	-72.69	-21.8	-165	0.5
YK-08	21/05/2018	-13.3	-125	-31.2	-194	3.88	-73.28	-20.2	-152	0.4
YK-09	21/05/2018	-12.5	-121	-29.0	-184	3.82	-72.89	-19.8	-149	0.4
YK-10	21/05/2018	-11.6	-118	-26.7	-178	3.96	-72.32	-20.4	-153	0.6
YK-11	21/05/2018	-14.4	-137	-34.0	-222	4.38	-73.55	-23.1	-175	0.4
YK-12	21/05/2018	-13.9	-130	-32.8	-206	4.05	-73.50	-21.1	-159	0.4
YK-13	21/05/2018	-14.4	-138	-34.0	-227	4.51	-73.47	-23.9	-181	0.5
YK-14	21/05/2018	-11.8	-121	-27.2	-184	4.12	-72.27	-21.2	-160	0.6
YK-15	21/05/2018	-12.9	-130	-30.2	-207	4.43	-72.67	-23.2	-175	0.6
YK-16	21/05/2018	-11.7	-118	-26.9	-178	3.93	-72.40	-20.2	-152	0.6
YK-17	21/05/2018	-11.3	-122	-26.0	-186	4.41	-71.72	-22.7	-172	0.8
YK-18	20/05/2018	-14.2	-132	-33.6	-212	4.14	-73.60	-21.6	-163	0.4
YK-19	20/05/2018	-16.9	-148	-40.6	-251	4.32	-75.05	-23.1	-175	0.3
YK-20	21/05/2018	-12.0	-123	-27.8	-191	4.26	-72.27	-22.0	-166	0.6
Prelude Mid	21/05/2018	-13.7	-128	-32.2	-201	3.97	-73.42	-20.7	-156	0.4
Cameron River	21/05/2018	-13.5	-127	-31.6	-199	3.99	-73.29	-20.8	-156	0.4
Mean		-13.8	-131.4	-32.4	-210	4.2	-73.3	-22.0	-166	0.5

August 2018										
Lake ID	Sample Collection Date	$\delta_L(^{18}O)$	$\delta_L(^{2}H)$	$\delta_E(^{18}O)$	$\delta_E(^{2}H)$	Lake-specific Evap. Line Slope	Lake-specific Evap. Line-GMWL Intercept	$\delta_I(^{18}O)$	$\delta_I(^{2}H)$	*E/I*
YK-01	14/08/2018	-14.2	-129	-33.5	-204	3.88	-73.75	-20.3	-152	0.3
YK-02 (avg.)	13/08/2018	-15.4	-134	-36.6	-215	3.85	-74.38	-20.3	-152	0.2
YK-03	13/08/2018	-13.0	-125	-30.3	-195	4.02	-73.00	-20.9	-157	0.5
YK-04	15/08/2018	-13.1	-126	-30.7	-196	4.02	-73.09	-20.9	-157	0.4
YK-05	15/08/2018	-12.7	-123	-29.6	-190	3.96	-72.91	-20.5	-154	0.5
YK-06	15/08/2018	-16.5	-140	-39.6	-231	3.94	-74.94	-20.9	-157	0.2
YK-07	14/08/2018	-11.7	-117	-27.0	-175	3.81	-72.51	-19.7	-148	0.5
YK-08	15/08/2018	-13.1	-124	-30.7	-191	3.84	-73.21	-20.0	-150	0.4
YK-09	15/08/2018	-11.3	-113	-25.8	-165	3.58	-72.53	-18.7	-139	0.5
YK-10	14/08/2018	-11.3	-114	-25.8	-167	3.66	-72.44	-19.0	-142	0.5
YK-11	14/08/2018	-13.8	-128	-32.6	-201	3.91	-73.54	-20.4	-153	0.4
YK-12	13/08/2018	-13.2	-125	-31.0	-193	3.87	-73.26	-20.2	-151	0.4
YK-13 (avg.)	13/08/2018	-13.0	-126	-30.3	-196	4.07	-72.96	-21.1	-159	0.5
YK-14	13/08/2018	-12.2	-121	-28.3	-185	3.96	-72.65	-20.4	-153	0.5
YK-15	14/08/2018	-12.0	-119	-27.7	-179	3.83	-72.64	-19.8	-149	0.5
YK-16	14/08/2018	-11.6	-117	-26.7	-175	3.84	-72.42	-19.8	-149	0.5
YK-17	14/08/2018	-12.0	-119	-27.8	-180	3.88	-72.61	-20.1	-151	0.5
YK-18	17/08/2018	-12.9	-124	-30.2	-193	3.97	-73.01	-20.6	-155	0.4
YK-19	17/08/2018	-13.5	-127	-31.7	-200	3.99	-73.31	-20.8	-156	0.4
YK-20	15/08/2018	-11.9	-121	-27.6	-185	4.08	-72.40	-21.0	-158	0.6
Prelude Mid	14/08/2018	-13.1	-123	-30.6	-190	3.81	-73.22	-19.9	-149	0.4
Cameron River	14/08/2018	-13.1	-124	-30.7	-191	3.85	-73.21	-20.0	-150	0.4
Mean		-12.9	-123.5	-30.2	-191	3.9	-73.1	-20.2	-152	0.4

Overall 2017-18 Lake Results									
	$\delta_L(^{18}O)$	$\delta_L(^{2}H)$	$\delta_E(^{18}O)$	$\delta_E(^{2}H)$	LEL Slope	LEL-GMWL Intercept	$\delta_I(^{18}O)$	$\delta_I(^{2}H)$	*E/I*
Overall 2017-18 Mean	-13.4	-128.2	-31.4	-202	4.1	-73.2	-21.4	-162	0.5

Final 2017-18 E/I Framework Values	
Parameter	Value
h (%)	62.64%
T (°C, K)	14.17, 287.32
α^* (^{18}O, ^{2}H) ‰	1.0103, 1.0915
ε_K (^{18}O, ^{2}H) ‰	0.0053, 0.0047
ε^* (^{18}O, ^{2}H) ‰	0.0103, 0.0195
δ^* (^{18}O, ^{2}H) ‰	-2.21, -76.1
δ_{AS} (^{18}O, ^{2}H) ‰	-26.93, -206.6
δ_{SSL} (^{18}O, ^{2}H) ‰	-9.48, -111.5
δ_{Ps} (^{18}O, ^{2}H) ‰	-16.89, -134.0
δ_P (^{18}O, ^{2}H) ‰	-21.79, -164.3
$\delta_{P\,(CNIP,\,2017)}$ (^{18}O, ^{2}H) ‰	-21.2, -162

A2.2 Precipitation Isotope Results

Snow				
Sample ID	Sample Collection Date	$\delta_L(^{18}O)$	$\delta_L(^{2}H)$	Notes
YK-16 Snow	24/04/2018	-26.3	-208	Sample collected from lake snowpack, composite snow sample from approx. 5-30 cm depth.
YK-05 Snow	25/04/2018	-25.1	-203	Sample collected from lake snowpack, composite snow sample from approx. 5-30 cm depth.
YK-06 Snow	26/04/2018	-27.4	-212	Sample collected from lake snowpack, composite snow sample from approx. 5-30 cm depth.
Mean		-26.3	-208	

Rain				
Sample ID	Sample Collection Date	$\delta^{18}O$	$\delta^{2}H$	Notes
S05	09/06/2016	-16.7	-131	Sample collected from Pocket Lake Rain Gauge (Gibson, 2017)
S09	22/06/2016	-15.1	-118	Sample collected from Pocket Lake Rain Gauge (Gibson, 2017)
S14	12/07/2016	-17.1	-139	Sample collected from Pocket Lake Rain Gauge (Gibson, 2017)
S19	11/08/2016	-15.6	-125	Sample collected from Pocket Lake Rain Gauge (Gibson, 2017)
S24	06/09/2016	-16.5	-133	Sample collected from Pocket Lake Rain Gauge (Gibson, 2017)
S28	28/09/2016	-20.4	-159	Sample collected from Pocket Lake Rain Gauge (Gibson, 2017)
Mean		-16.9	-134	

Rain Source Data:
Isotope-based evaporation and water balance studies at Pocket Lake and Baker Creek, 2016: update on a 26-year assessment. (Gibson, 2017)

APPENDIX THREE

SUPPLEMENTARY TABLES AND FIGURES

Table A3.1 – Regional meteorological station information.

Met Station ID	Coordinates (Decimal Degrees)		Elevation (masl)	Responsible Authority	2017 Rainfall Data	2018 Rainfall Data
	Northing	Easting				
Yellowknife Airport (Station ID 2204100)	62.46	-114.44	205.70	Environment and Climate Change Canada	Yes	Yes
Yellowknife Auto	62.48	-114.46	182.00	GNWT ENR Forest Management Division	Yes	Yes
Pocket Lake	62.51	-114.37	169.58	GNWT ENR Water Resources Division	Yes	Yes
River Lake	62.60	-114.12	148.80	GNWT ENR Water Resources Division	Yes	Yes
Bliss Lake	62.65	-113.73	307.00	GNWT ENR Forest Management Division	Yes	Yes
Tibbitt Muskeg	62.56	-113.34	213.65	GNWT ENR Water Resources Division	Yes	Yes
Cascom Snare Airstrip	63.43	-116.18	191.90	Cascom	Yes	Yes
Snare Rapids	63.51	-116.01	217.50	GNWT ENR Water Resources Division	No	Yes
Chan Lake	61.83	-116.70	75.90	GNWT Department of Infrastructure	No	Yes

Note:
Yellowknife Airport (ECCC, 2018a) – rainfall data range:1/05/17 - 30/09/17 and 1/05/18 - 30/09/18.
Cascom Snare Airstrip (Cascom, 2018) – rainfall data range:1/05/17 - 30/09/17 (station outage: 8/18/17 - 9/21/17) and 1/05/18 - 20/09/18 (station outage 17/08/18 - 23/08/18).
Snare Rapids (GNWT ENR Water Resources Div., 2018a) – rainfall data range: 1/05/18 - 18/09/18.
River Lake (GNWT ENR Water Resources Div., 2018b) – rainfall data range: 1/05/17 - 30/09/17 and 1/05/18 - 29/09/18.
Tibbitt Muskeg (GNWT ENR Water Resources Div., 2018c) – rainfall data range: 1/05/17 - 30/09/17 and 1/05/18 - 30/09/18.
Pocket Lake (GNWT ENR Water Resources Div., 2018d) – rainfall data range: 1/05/17 - 30/09/17 (potential rain gauge malfunction) and 1/05/18 - 30/09/18.
Yellowknife Auto (GNWT ENR Forest Management Div., 2018a) – rainfall data range:1/05/17 - 30/09/17 and 1/05/18 - 30/09/18.
Bliss Lake (GNWT ENR Forest Management Div., 2018b) – rainfall data range:1/05/17 - 30/09/17 and 1/05/18 - 27/09/18.
Chan Lake (GNWT Dept. of Infrastructure, 2018e) – rainfall data range: 1/05/18 - 03/09/18.

Table A3.2 – Water level logger information.

Study Lake/ Logger ID	HOBO Water Level Logger ID	Coordinates (Decimal Degrees)		Logger Activation Date (mm/dd/yyyy)	Barometric Pressure Dataset Used for Water Level Calibration
		Northing	Easting		
YK-01	10860580	62.56144	-114.01993	09/29/2016	Treeville Landlogger/YK Airport
YK-02	10860574	62.52552	-113.37851	09/29/2016	Treeville Landlogger/YK Airport
YK-03	10766050	62.52545	-113.83582	09/29/2016	Treeville Landlogger/YK Airport
YK-04	20081847	62.45475	-113.39454	05/19/2017	Treeville Landlogger/YK Airport
YK-05	20081850	62.61439	-113.38393	05/19/2017	Treeville Landlogger/YK Airport
YK-06	20075768	63.40971	-116.12493	05/19/2017	Treeville Landlogger/YK Airport
YK-07	10766329	62.54850	-113.95967	09/29/2016	Treeville Landlogger/YK Airport
River Lake (YK-08)	10860583	62.59863	-114.10643	09/29/2016	Treeville Landlogger/YK Airport
Plant Lake (YK-09)	10860576	62.52106	-113.51747	09/29/2016	Treeville Landlogger/YK Airport
YK-10	20081846	62.55314	-113.98939	05/19/2017	Treeville Landlogger/YK Airport
YK-11	20081852	62.54795	-113.93246	05/19/2017	Treeville Landlogger/YK Airport
Prelude Lake (YK-12)	20081857	62.51999	-113.73997	05/19/2017	Treeville Landlogger/YK Airport
YK-13	20081848	62.50314	-113.40197	05/19/2017	Treeville Landlogger/YK Airport
YK-14	20081853	62.49262	-113.43156	05/19/2017	Treeville Landlogger/YK Airport
YK-15	20081851	62.54903	-114.04402	05/19/2017	Treeville Landlogger/YK Airport
YK-16	20081858	62.56008	-114.00924	05/19/2017	Treeville Landlogger/YK Airport
YK-17	20081941	62.53825	-114.11970	05/19/2017	Treeville Landlogger/YK Airport
YK-18	20081855	62.10711	-116.29725	05/19/2017	YK-18 Landlogger
YK-19	20081845	62.00099	-116.33416	05/19/2017	YK-18 Landlogger
YK-18 Landlogger	20081854	62.10718	-116.29729	05/19/2017	N/A
Treeville Landlogger	10766028	62.55708	-114.01100	09/29/2016	N/A

Note:
"N/A" – Not Applicable.
"YK Airport" – Yellowknife Airport met station.
"Landlogger" – Indicates water level logger installed on land to collect atmospheric pressure data. Where outlined above, the Treeville Landlogger-provided atmospheric pressure data were used for lake depth calculations from 29 September 2016 – 24 April 2018, until battery exhaustion on 24 April 2018, after which time Yellowknife Airport met station atmospheric pressure data were used for these depth calculations.

Figure A3.1 – Photographs from field work activities in the North Slave Region, NT during 2017 showing water level logger rigging and deployment. Rigging involved tethering a logger to a length of high-strength braided wire, accompanied with an approximate 10-pound anchor weight consisting of bagged gravel. On the shore-bound end, the wire was secured to a mounted steel stake (or boulder), with flagging tape affixed for identification. The loggers were deployed approximately 3 to 6 m into the study lakes (depending on site conditions) and submerged to rest on the lakebed (photographs by J.Viscek).

Table A3.3 – Study lake catchment DEM modelling information.

Study Lake Catchment	DEM Dataset	Spatial Resolution (m)	DEM Modelling Coverage
YK-01	ArcticDEM	5	100%
YK-02	ArcticDEM	5	100%
YK-03	GNWT Centre for Geomatics	10	100%
YK-04	ArcticDEM	5	100%
YK-05	ArcticDEM	5	100%
YK-06	ArcticDEM	5	100%
YK-07	ArcticDEM	5	100%
River Lake	ArcticDEM	5	83%
(YK-08)	GNWT Centre for Geomatics	10	17%
Plant Lake (YK-09)	ArcticDEM	5	100%
YK-10	ArcticDEM	5	100%
YK-11	ArcticDEM	5	92%
	GNWT Centre for Geomatics	10	8%
Prelude Lake	ArcticDEM	5	83%
(YK-12)	GNWT Centre for Geomatics	10	17%
YK-13	ArcticDEM	5	100%
YK-14	ArcticDEM	5	100%
YK-15	ArcticDEM	5	85%
	GNWT Centre for Geomatics	10	15%
YK-16	ArcticDEM	5	100%
YK-17	ArcticDEM	5	100%
YK-18	ArcticDEM	5	66%
	GNWT Centre for Geomatics	10	34%
YK-19	ArcticDEM	5	94%
	GNWT Centre for Geomatics	10	6%
YK-20	ArcticDEM	5	100%

Table A3.4 – Landsat 8 scenes used in the study.

Landsat Scene (Product Identifier)	Study Region	Study Region Coverage	Date (yyyy/mm/dd)	Spatial Resolution (m)	Path	Row	Cloud Cover
LC08_L1TP_046015_20170815_20170825_01_T1	Ingraham Trail	7%	2017/08/15	30	046	015	7.91%
LC08_L1TP_046016_20170831_20170915_01_T1	Ingraham Trail	93%	2017/08/31	30	046	016	3.5%
LC08_L1TP_047017_20180708_20180717_01_T1	Mackenzie Bison Sanctuary	100%	2018/07/08	30	047	017	0.1%
LC08_L1TP_048016_20170829_20170914_01_T1	Snare River Basin	100%	2017/08/29	30	048	016	3.72%

Table A3.5 – Study lake catchment land cover classification modelling information.

Study Region	Area (km^2)	Incorporated Study Lake Catchments	Landsat Scene (Product Identifier)	Land Cover Class (ROI)	Number of ROI Pixels
Ingraham Trail	23,336	YK-01 YK-02 YK-03 YK-04 YK-05 YK-07 River Lake (YK-08) Plant Lake (YK-09) YK-10 YK-11 Prelude Lake (YK-12) YK-13 YK-14 YK-15 YK-16 YK-17 YK-20	LC08_L1TP_046015_ 20170815 _20170825_01_T1 LC08_L1TP_046016_ 20170831 _20170915_01_T1	Open Water Mixed Vegetation Open Terrestrial	46,189 16,655 4,110
Mackenzie Bison Sanctuary	368	YK-18 YK-19	LC08_L1TP_047017_ 20180708 _20180717_01_T1	Open Water Mixed Vegetation Open Terrestrial	8,182 11,849 976
Snare River Basin	112	YK-06	LC08_L1TP_048016_ 20170829 _20170914_01_T1	Open Water Mixed Vegetation Open Terrestrial	3,335 1,417 4,903

Note:
Land cover classification pixel resolution = 30 m.

Table A3.6 – Land cover classification accuracy assessment.

Ingraham Trail							
Land cover class	Open water	Vegetation	Open terrestrial	Commission	Omission	Producer's accuracy	User's accuracy
Open water	197	0	0	0.00	0.50	0.99	1.00
Mixed vegetation	1	190	18	9.09	2.50	0.95	0.91
Open terrestrial	0	5	180	2.70	9.00	0.90	0.97
Overall accuracy: 94.5%; Kappa coefficient: 91.8%							
Snare River Basin							
Land cover class	Open water	Vegetation	Open terrestrial	Commission	Omission	Producer's accuracy	User's accuracy
Open water	44	0	0	0.00	12.00	0.88	1.00
Mixed vegetation	2	48	0	4.00	4.00	0.96	0.96
Open terrestrial	4	2	50	10.71	0.00	1.00	0.89
Overall accuracy: 94.7%; Kappa coefficient: 92.0%							
Mackenzie Bison Sanctuary							
Land cover class	Open water	Vegetation	Open terrestrial	Commission	Omission	Producer's accuracy	User's accuracy
Open water	50	0	0	0.00	0.00	1.00	1.00
Mixed vegetation	0	50	0	0.00	0.00	1.00	1.00
Open terrestrial	0	0	50	0.00	0.00	1.00	1.00
Overall accuracy: 100%; Kappa coefficient: 100%							

Land Cover Classification Limitations/Uncertainties:

While the land cover classification modelling provided a reasonable representation of general landscape conditions, several inherent limitations/uncertainties were acknowledged. These limitations/uncertainties were primarily attributed to a combination of (1) the limits of medium (i.e., 30-m) resolution Landsat imagery, (2) the combination of land cover types into three general classes (3) the relatively small catchment size of a number of study lakes. An observable effect identified from these limitations included potential under-representation of the open water class compared to the mixed vegetation and/or open terrestrial surface land cover class where relatively smaller, shallow water bodies existed. Also, potential under-representation of the mixed vegetation land cover class compared to open terrestrial land cover class where recently burned landscape conditions existed, particularly where a mixture of moderately burned/dead vegetation debris or regenerating vegetation such as grasses and thicket were present.

To address some of these limitations/uncertainties, future studies may consider utilization of higher-resolution data (e.g., Sentinel) or radar data (e.g., Radarsat-2, UAVSAR) where available. Also, of note, manual adjustments of land cover class were made for lakes YK-13 and YK-17. For these relatively smaller study lake catchments (with shallow lake conditions), the modelling largely misclassified the study lake areas as vegetation rather than open water. These study lakes were noted to be the lone water bodies within their respective catchments. As such, for these catchment land cover classifications, LA/CA values (i.e., 7% for YK-13 and 20.6% for YK-17, respectively) were used to represent the open water proportionality. These modified land cover proportions were offset from the over-represented vegetation class in the model.

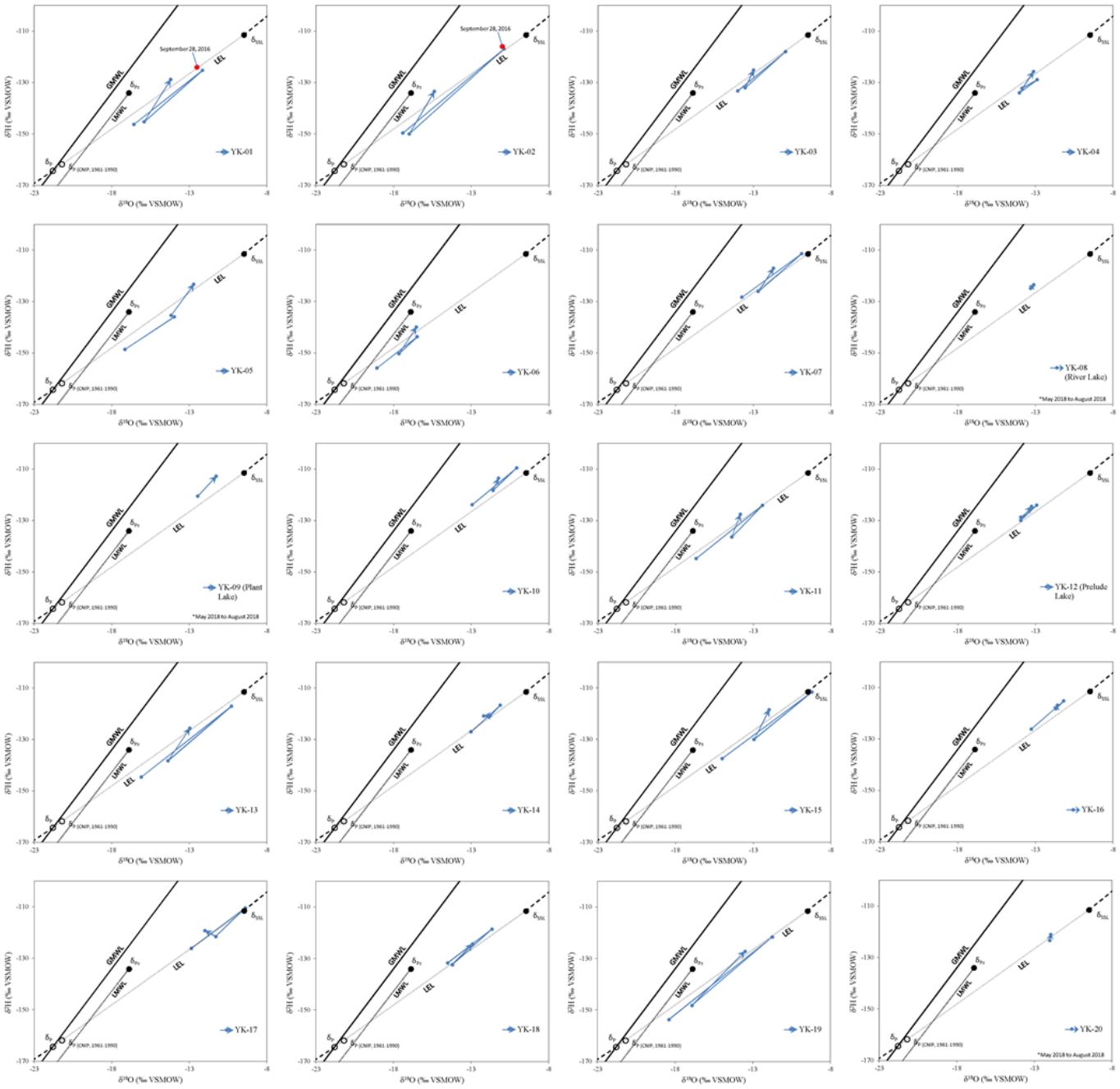

Figure A3.2 – Isotopic evolution of individual study lakes superimposed on the isotopic framework from: May 2017; August 2017; May 2018; and August 2018. Supplementary isotope compositions from samples collected during September 2016 are also shown for YK-01 and YK-02. Overall, the lake isotope plots illustrate the range of hydrological changes as driven by catchment and meteorological conditions.

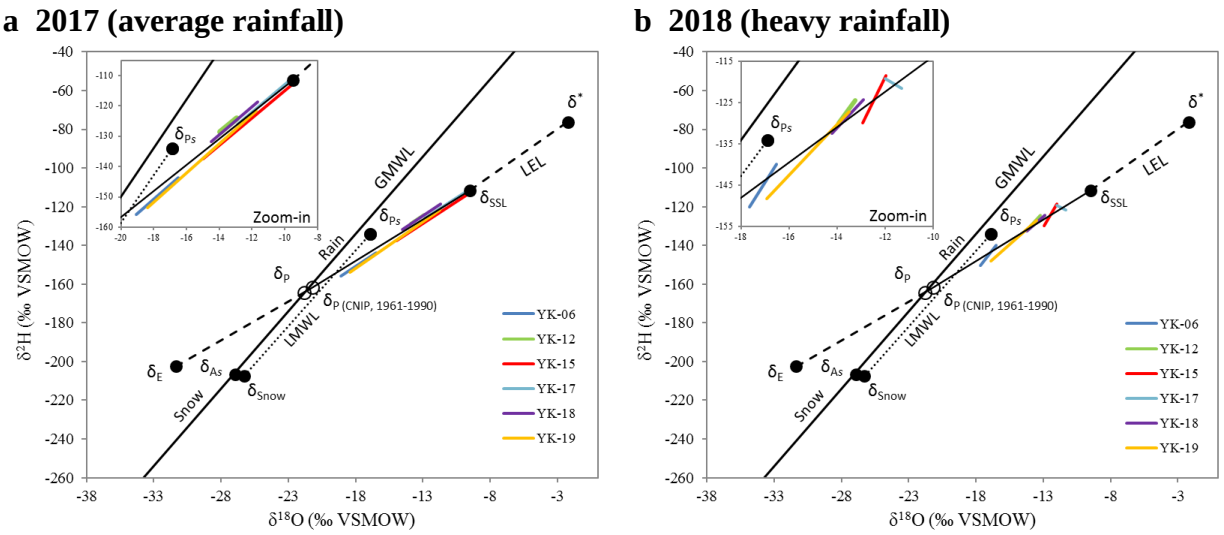

Figure A3.3 – Seasonal isotopic evolution (May to August) of select study lakes representing different hydrological settings and conditions during (a) 2017 and (b) 2018. The lakes can have a variety of isotopic evolution patterns depending on meteorological conditions and catchment characteristics. YK-06 (high catchment slope) is more influenced by snowfall. Prelude Lake (YK-12; large and deep/stratified lake) changes relatively little in seasonal isotope concentration. YK-15 (shallow lake with low LA/CA) is more influenced by evaporation during 2017 (drier year) and more influenced by inflow during 2018 (wetter year) when hydrological connections are active. YK-17 (very shallow lake) shows high spring-summer isotopic variability and is heavily influenced by evaporation during 2017-18. YK-19 (low LA/CA) shows high seasonal isotopic variability due to hydrological connectivity of its larger relative catchment during rainfall and snowmelt. YK-18 (high LA/CA) is less influenced by snowmelt due to its smaller relative catchment. Overall, the greater influence from heavy summer rainfall (δ_{Ps}) is seen in the 2018 plots, with lake isotope concentrations pulling toward this rainfall signal.

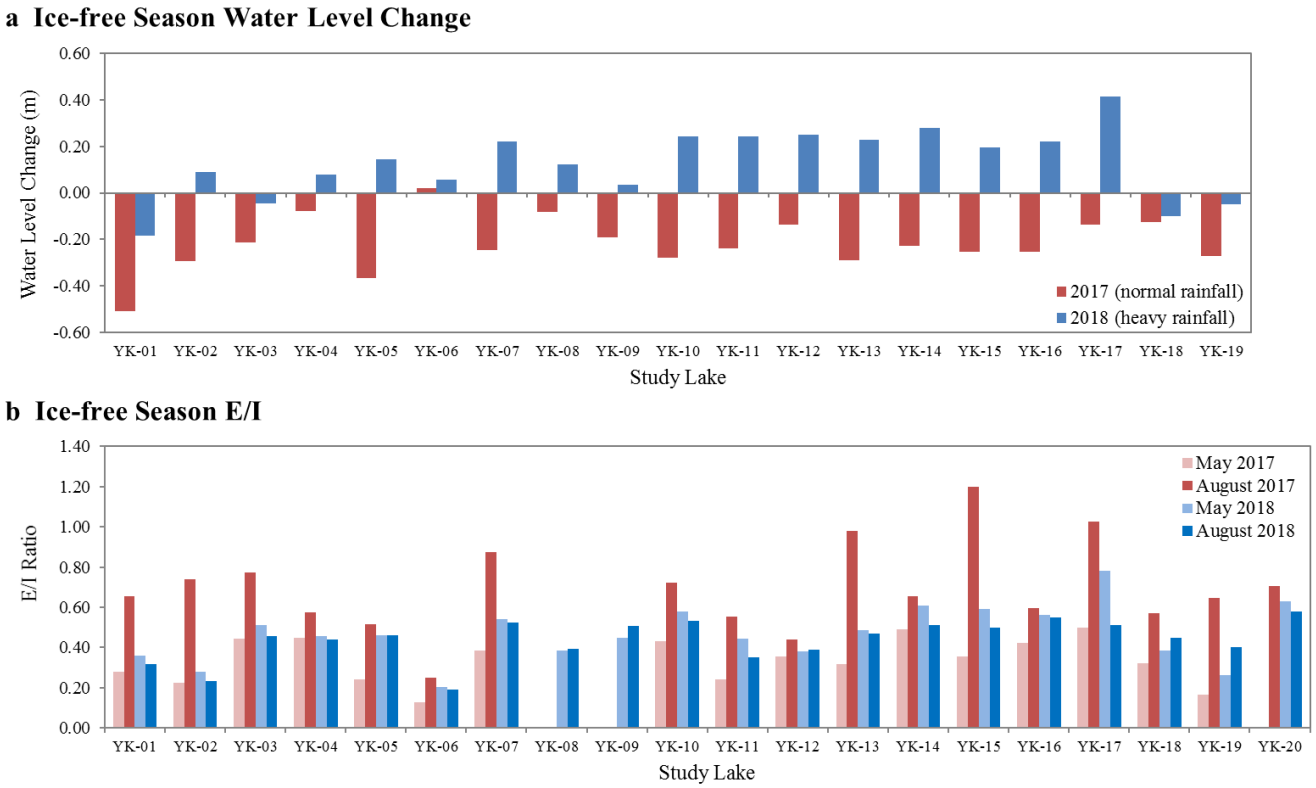

Note:
Water level data ranged from 19 May – 30 September for the 2017 ice-free season; and 19 May – 13 August/15 September for the 2018 ice-free season (refer to Table 3.2 for further details).

Figure A3.4 – (a) Overall ice-free season (May-August/September) water level change for study lakes during 2017 and 2018, respectively. (b) Summary of ice-free season study lake E/I ratios, as calculated for May and August 2017 and 2018, respectively. Lake E/I was relatively greater in August 2017 under drier summer conditions when the influence from evaporation was stronger; while E/I was relatively lower in August 2018 under wetter summer conditions, when the stronger inflow influence offset the evaporative influence. Water level change is linked to E/I, with lakes likely to show higher E/I signatures as lake levels decrease through the influence of evaporation (e.g., August 2017), and lower E/I signatures as lake levels increase from greater inflow offsetting the evaporative influence (e.g., August 2018).

Study Lake ID	E/I (May 2017)	E/I (Aug 2017)	Δ E/I (May-Aug 2017)	E/I (May 2018)	E/I (Aug 2018)	Δ E/I (May-Aug 2018)	Δ Water Level (May-Sep 2017)	Δ Water Level (May-Sep 2018)	Rainfall (2017) (mm)	Lake Area (ha)	LA/CA (%)	Estimated Centre Depth (m)	LA/LD (%)	Median Catchment Slope (°)	Open Water Land Cover (%)	Mixed Vegetation Land Cover (%)	Open Terrestrial Land Cover (%)
YK-06	0.13	0.25	0.12	0.2	0.19	-0.01	0.02	0.07	230	2.1	9.6%	8.3	0.3%	10.27	4.5%	8.2%	87.3%
YK-02	0.22	0.74	0.52	0.28	0.23	-0.05	-0.29	0.09	128.4	7.7	1.1%	NA	NA	2.95	4.8%	33.2%	62.0%
YK-01	0.28	0.65	0.37	0.36	0.32	-0.04	-0.51	-0.17	109.4	1.9	5.2%	NA	NA	4.87	5.7%	39.0%	55.2%
YK-11	0.24	0.55	0.31	0.44	0.35	-0.09	-0.24	0.21	109.4	7.4	8.5%	NA	NA	3.68	1.6%	61.2%	37.2%
YK-12	0.36	0.44	0.08	0.38	0.39	0.01	-0.13	0.25	109.4	3283.8	0.4%	53.3	61.6%	3.07	21.2%	55.0%	23.8%
YK-08	NA	NA	NA	0.39	0.39	0	-0.08	0.13	109.4	496.6	0.1%	23.6	21.0%	3.07	21.0%	55.0%	24.0%
YK-19	0.17	0.65	0.48	0.26	0.4	0.14	-0.28	-0.05	147.1	67.4	1.2%	1.21	55.7%	1.79	16.2%	63.8%	20.0%
YK-04	0.45	0.57	0.12	0.45	0.44	-0.01	-0.08	0.09	128.4	1.6	11.9%	1.38	1.2%	6.95	5.7%	4.5%	89.8%
YK-18	0.32	0.57	0.25	0.38	0.45	0.07	-0.13	-0.09	147.1	45.8	30.8%	1.08	42.4%	2.01	28.7%	58.1%	13.2%
YK-05	0.24	0.52	0.28	0.46	0.46	0	-0.37	0.15	128.4	2.3	1.4%	1.8	1.3%	2.58	0.9%	58.2%	40.9%
YK-03	0.44	0.77	0.33	0.51	0.46	-0.05	-0.21	-0.02	109.4	3	3.3%	NA	NA	4.58	6.5%	45.3%	48.1%
YK-13	0.32	0.98	0.66	0.49	0.47	-0.02	-0.29	0.24	128.4	1.8	6.6%	NA	NA	3.25	6.6%	4.7%	88.7%
YK-15	0.35	1.2	0.85	0.59	0.5	-0.09	-0.25	0.2	109.4	9.3	0.3%	NA	NA	2.57	28.1%	33.8%	38.2%
YK-14	0.49	0.66	0.17	0.61	0.51	-0.1	-0.22	0.28	128.4	48.6	28.1%	NA	NA	3.47	24.0%	23.3%	52.8%
YK-17	0.5	1.03	0.53	0.78	0.51	-0.27	-0.14	0.42	109.4	6.4	20.6%	NA	NA	3.51	20.6%	74.6%	4.8%
YK-09	NA	NA	NA	0.45	0.51	0.06	-0.19	0.04	128.4	540.9	22.6%	10.2	55.8%	3.11	24.0%	54.0%	22.0%
YK-10	0.43	0.72	0.29	0.58	0.53	-0.05	-0.28	0.25	109.4	81.2	19.3%	NA	NA	2.62	22.1%	27.6%	50.3%
YK-07	0.38	0.87	0.49	0.54	0.53	-0.01	-0.25	0.22	109.4	14.1	18.2%	2	7.1%	2.41	16.5%	39.8%	43.7%
YK-16	0.42	0.6	0.18	0.56	0.55	-0.01	-0.25	0.23	109.4	17.3	29.8%	6.97	2.5%	3.15	21.2%	25.6%	53.2%
YK-20	NA	0.71	NA	0.63	0.58	-0.05	NA (Inversed colours)	NA (Inversed colours)	128.4	12.5	16.7%	5.35	2.3%	3.18	12%	30%	59%

LEGEND

Quartile	Colour
Min-Q1	
Q1-Med	
Med-Q3	
Q3-Max	

Note:
Rainfall values estimated based on nearest/most applicable met station to lake.
Water level data presented here covers 19 May – 30 September for the 2017 ice-free season; and 19 May – 13 August/15 September for the 2018 ice-free season (refer to Table 3.2 for further details).

Figure A3.5 – General ranking of key study lake data across quartiles, useful to investigate patterns in the data. Cell shading from light orange/red to dark orange/red reflects quartile, including: minimum to Q1; Q1 to median; median to Q3; and Q3 to maximum. The table is sorted according to August 2018 E/I ratio to highlight the general linkage between E/I and LA/CA during the wet summer of 2018, when catchment hydrological connections were particularly active. As the data illustrate, as LA/CA decreased under wet summer conditions, lake E/I was likely to be lower (greater influence from inflow). This relationship is not observed under average summer rainfall conditions (e.g., 2017), when lake catchments increasingly dried up and were more hydrologically segmented.

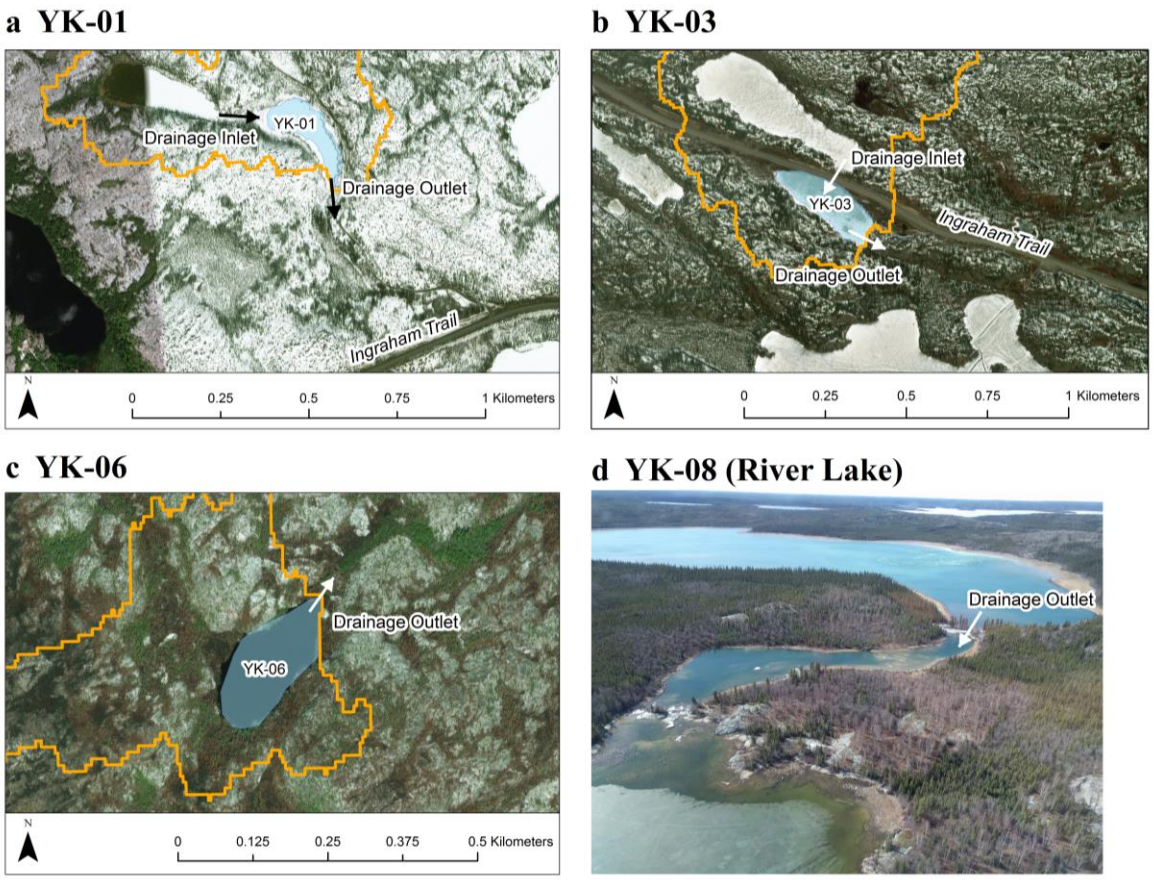

Figure A3.6 – Satellite imagery highlighting study lakes (a) YK-01, (b) YK-03, and (c) YK-06, with notable hydrological drainage inlets/outlets through intermittent channels indicated (lake catchments identified in orange). (d) Photograph (May 2018) of notable drainage outlet west of River Lake (YK-08). Overall, storage capacity thresholds and hydrological connectivity will influence lake water balances. These complex "fill-and-spill" mechanisms are driven by precipitation, and can increase the variability in the relationship between water level and E/I change (DigitalGlobe, 2017; GeoEye, 2017; photograph by J.Viscek).